
Genetic analysis of M94 of murine cytomegalovirus

Silke Maninger



München 2010

Genetic analysis of M94 of murine cytomegalovirus

Silke Maninger

Dissertation zur Erlangung des Doktorgrades
der Fakultät für Chemie und Pharmazie
der Ludwig-Maximilians-Universität
München

vorgelegt von
Silke Maninger
aus Wiesbaden-Sonnenberg

München 2010

Erklärung

Diese Dissertation wurde im Sinne von §13 Absatz 4 der Promotionsordnung vom 29. Januar 1998 von Herrn Prof. Koszinowski betreut und von Herrn Prof. Beckmann vor der Fakultät für Chemie und Pharmazie vertreten.

Ehrenwörtliche Versicherung

Diese Dissertation wurde selbständig, ohne unerlaubte Hilfe erarbeitet.

München, am 15.04.2010

.....

(Unterschrift des Autors)

Dissertation eingereicht am : 15.04.2010
Erstgutachter : Herr Prof. Koszinowski
Zweitgutachter : Herr Prof. Beckmann
Tag der mündlichen Prüfung : 29.06.2010

Contents

Summary	xv
Zusammenfassung	xvii
1 Introduction	1
1.1 <i>Herpesviridae</i>	1
1.1.1 Clinical relevance of human cytomegalovirus	2
1.1.2 The murine cytomegalovirus model of HCMV	3
1.1.3 Structure of cytomegaloviruses	4
1.1.4 The genome of cytomegaloviruses	4
1.1.5 Replication of cytomegaloviruses	5
1.2 Genetics of herpesviruses	8
1.2.1 Forward Genetics	8
1.2.2 Reverse Genetics	8
1.2.3 Mutagenesis of bacterial artificial chromosomes	9
1.2.4 Random mutagenesis	9
1.2.5 Dominant negative mutants	11
1.3 The M94 gene of murine cytomegalovirus	12
1.4 Aims of this study	12
2 Materials and Methods	14
2.1 Material	14

2.1.1	Devices	14
2.1.2	Consumables	15
2.1.3	Reagents	16
2.1.4	Commercially kits	17
2.1.5	Bacteria	18
2.1.6	Cells	18
2.1.6.1	Cell culture reagents	18
2.1.7	Plasmids and bacterial artificial chromosomes	19
2.1.7.1	Commercial available plasmids	19
2.1.7.2	Available plasmids in the lab	20
2.1.7.3	Cloned plasmids	21
2.1.8	Oligonucleotides	22
2.1.9	Viruses	23
2.1.10	Antibodies	24
2.2	Methods	24
2.2.1	Bacterial cell culture	24
2.2.1.1	Preparation of chemocompetent bacteria	25
2.2.1.2	Transformation of chemocompetent bacteria	26
2.2.1.3	Preparation of electrocompetent bacteria	26
2.2.1.4	Transformation of electrocompetent bacteria	26
2.2.1.5	Preparation of glycerol stocks	27
2.2.2	Isolation and purification of DNA	27
2.2.2.1	Small scale isolation of plasmid DNA	27
2.2.2.2	Large scale isolation of plasmid DNA	27
2.2.2.3	Small scale isolation of BAC DNA	27
2.2.2.4	Large scale isolation of BAC DNA	28
2.2.2.5	Concentration of DNA by ethanol precipitation	28
2.2.2.6	Isolation of DNA from cell culture	29
2.2.2.7	Determination of DNA concentration	29

2.2.3	Analysis and cloning of DNA	29
2.2.3.1	Polymerase chain reaction	29
2.2.3.2	Buffer change of PCR products	31
2.2.3.3	Restriction enzyme digest of DNA	31
2.2.3.4	Dephosphorylation of DNA	31
2.2.3.5	Blunting of DNA fragments by DNA polymerase	31
2.2.3.6	Agarose gel electrophoresis	32
2.2.3.7	Isolation of DNA fragments from agarose gels	32
2.2.3.8	Ligation of DNA fragments	32
2.2.3.9	Sequencing of DNA	32
2.2.4	Transposon mutagenesis	33
2.2.5	Mutagenesis of BACs	35
2.2.5.1	Generation of recombinant BACs	35
2.2.5.2	Insertion of genes by Flp recombinase	36
2.2.6	Cell culture	37
2.2.6.1	Cultivation of mammalian cells	37
2.2.6.2	Freezing of cells	37
2.2.6.3	Thawing of cells	38
2.2.6.4	Determination of cell numbers	38
2.2.6.5	Transfection of cells using Superfect	38
2.2.6.6	Transfection of cells using CaPO ₄ precipitation	39
2.2.6.7	Application of additional cell culture reagents	39
2.2.7	Virological methods	39
2.2.7.1	Virus reconstitution from BAC DNA	39
2.2.7.2	Infection of cells with MCMV	40
2.2.7.3	Preparation of MCMV stock	40
2.2.7.4	Determination of MCMV titre by standard plaque assay	41
2.2.7.5	Determination of MCMV titre by TCID ₅₀	41
2.2.7.6	Growth kinetics of MCMV	42

2.2.8	Packaging assay	42
2.2.8.1	Southern blot analysis	43
2.2.8.2	Quantification of Southern blot analysis	44
2.2.9	Protein analysis	44
2.2.9.1	Protein extraction from eukaryotic cells	44
2.2.9.2	SDS-PAGE	45
2.2.9.3	Western Blot analysis	45
3	Results	47
3.1	M94 is essential in MCMV	47
3.2	Transposon mutagenesis	49
3.3	Cloning of M94	51
3.4	Transposon mutagenesis of M94	53
3.5	Analysis of the M94 library	59
3.6	Analysis of M94 mutants in the viral context	62
3.7	Identification of inhibitory mutants	68
3.8	Verification of the dominant negative mutants	71
3.9	Protein analysis of the DN mutant	77
3.9.1	Characterisation of anti-M94 serum	77
3.9.2	Analysis of the expression of M94 alleles	79
3.9.3	M94 is expressed by true late kinetics	80
3.10	M94 plays an essential role in secondary envelopment	82
3.11	Spread deficiency of MCMV lacking M94	85
3.12	M94 is not essential for viral cleavage-packaging	87
3.12.1	Packaging assay	88
4	Discussion	93
4.1	Generation of mutant libraries	93
4.2	Analysis of M94 mutants by <i>cis</i> -complementation	96

Contents	viii
4.3 Identification and analysis of DN mutants	97
4.4 Comparative analysis of the M94 deletion and DN mutant	98
4.5 M94 is a key player in secondary envelopment of <i>β-Herpesvirinae</i>	100
Bibliography	105
Acknowledgements	116
Curriculum vitae	117

List of Figures

1.1	Herpesvirus virion	4
1.2	Herpesvirus conserved gene blocks	5
1.3	Herpesvirus life cycle	7
1.4	Mutagenesis strategies	10
2.1	Generation of recombinant BACs	36
2.2	Insertions of genes into BACs	37
3.1	Growth kinetics of M94 deletion mutant and rescues	48
3.2	Overview of GPS [®] -LS Linker Scanning system	50
3.3	Strand transfer reaction	51
3.4	Generation of 5 amino acid insertion	52
3.5	Restriction analysis of Litmus28-HAM94	52
3.6	Transposon mutagenesis	53
3.7	Analysis of transprimer insertions	55
3.8	Analysis for transprimer insertions in M94	56
3.9	Analysis for the position of mutations in M94	58
3.10	Selected mutants in the M94-ORF	61
3.11	Loss-of-function screen	63
3.12	Analysis for double insertions in the loss-of-function screen	64
3.13	Restriction analysis of the BAC mutants in the loss-of-function screen	66
3.14	Result of the loss-of-function screen	67

3.15	Inhibitory screen	69
3.16	Result of the inhibitory screen	70
3.17	Conditional expression cassette	71
3.18	Growth kinetics of inhibitory mutants	75
3.19	Growth kinetics of DN mutant M94i13	76
3.20	Sera test for M94 recognition	78
3.21	Analysis of gene expression of the DN mutant	79
3.22	Analysis of gene expression in presence of PAA	81
3.23	Electron microscopy analysis of infected cells	83
3.24	Electron microscopy analysis of primary envelopment	84
3.25	Electron microscopy analysis of secondary envelopment	85
3.26	Spread assay	86
3.27	Cleavage-packaging of viral genomes	88
3.28	Southern probe position	89
3.29	Packaging assay	90
3.30	Quantification of the packaging assay	92
4.1	Comparison of library coverage	95
4.2	Models for nuclear egress	101
4.3	Model for secondary envelopment	103

List of Tables

2.7	Standard media for cell culture	38
3.1	Transposition reaction	54
3.2	Conditional expression constructs	73
3.3	Values of the quantified packaging assay	91
4.1	Comparison of transposon mutageneses	94

Nomenclature

aa	amino acid
Amp	ampicillin
APS	ammonium persulfate
BAC	bacterial artificial chromosome
bp	base pairs
Cam	chloramphenicol
DMEM	Dulbeccos Modified Eagle Medium
DMSO	dimethyl sulfoxide
DN	dominant negative
DNA	desoxy ribonucleic acid
Dox	doxycyclin
DPBS	Dulbeccos Phosphate Buffered Saline
dpi	days post infection
ds	double stranded
<i>E. coli</i>	<i>Escherichia coli</i>
EBV	Epstein-Barr virus
EDTA	ethylenediaminetetraacetic acid
EM	electron microscopy
ER	endoplasmic reticulum
EtBr	ethidium bromide
FBS	Foetal Bovine Serum

FRT	Flp recombinase target
HCMV	human cytomegalovirus
hpi	hours post infection
HRP	horseradish peroxidase
HSV	Herpes simplex virus
IE	immediate early
INM	inner nuclear membrane
Kan	kanamycin
kbp	1000 base pairs
MCMV	murine cytomegalovirus
MEM	Minimal Essential Medium
MOI	multiplicity of infection
NCS	Newborn Calf Serum
NEAA	Non-Essential Amino Acids
NEB	New England Biolabs
OD	optical density
OD ₆₀₀	optical density at 600 nm
ONM	outer nuclear membrane
ORF	open reading frame
PAA	phosphono acetic acid
PCR	polymerase chain reaction
pi	post infection
pM94	protein of gene M94
Q	L-glutamine
rpm	rounds per minute
RPMI	Roswell Park Memorial Institute
RT	room temperature
SDS	sodium dodecyl sulfate
ss	single stranded

TCID ₅₀	tissue culture infective dose 50
TEMED	N,N,N',N'-Tetramethylethylenediamine
<i>tet</i> O ₂	<i>tet</i> -operator
TetR	repressor protein
<i>tet</i> R	<i>tet</i> -repressor
TGN	trans-Golgi network
TRE	tetracycline-response element
tTA	tetracycline-controlled transactivator
VZV	Varicella-zoster virus
wt	wild type
Zeo	zeocin

Summary

The M94 gene of murine cytomegalovirus (MCMV) is one of the about 40 core genes of the subfamily of β -*Herpesvirinae* with unknown function. MCMV is utilised as an *in vivo* model for studying human cytomegalovirus (HCMV) due to the strict species specificity of HCMV and major homologies to MCMV. HCMV is an important human pathogen with worldwide distribution. Although infection of the immune competent host is usually clinically silent, infection of the foetus and the newborn causes severe organ damage and infection of immunocompromised patients induces life-threatening disease.

M94 has not been studied intensely as a single gene before, but studies on its homologues in other *Herpesviridae* demonstrated expression as true late gene, presence in the virion, interaction of UL94 and UL99 in HCMV and capsid binding in α -*Herpesvirinae*. While UL94 in HCMV is essential, M94 homologues in α -*Herpesvirinae* are not essential, indicating an essential function of M94 conserved in β -*Herpesvirinae* but lost in α -*Herpesvirinae*. For the identification of this essential function, a library of random mutants was generated by a modified Tn7 transposon mutagenesis. The modifications in the transposon mutagenesis produced a library of high diversity and wide coverage containing 32,000 primary clones including stop and insertion mutants. The analysis of 613 clones by sequencing resulted in 399 unique mutants containing a correct 15 base pair (bp) insertion in M94. 116 stop and insertion mutants were individually reinserted into the viral genome and studied in the viral context. The primary analysis showed the ability of certain mutants to complement the M94 deletion, thereby identifying the essential regions in the M94 protein. Secondly, the M94 mutants were re-inserted as second gene and analysed for their inhibitory capacity

of the M94 wild type (wt) functions to identify dominant negative (DN) mutants. The inhibitory mutants found were then verified as DN mutants by regulated expression in the virus context and by analysis of their specific phenotype induced by overexpression.

Further analysis of the DN mutant in comparison to a M94 deletion mutant revealed no effect of M94 in viral cleavage-packaging, despite previous publications. Additional analysis showed a block in secondary envelopment for both the DN mutant and the deletion mutant and the determination of the spread deficient phenotype of the M94 deletion virus. Altogether these results constitute a new model for secondary envelopment in *β -Herpesvirinae*.

Zusammenfassung

Das M94 Gen des murinen Cytomegalovirus (MCMV) ist eines der ungefähr 40 Kerngene aus der Unterfamilie der β -*Herpesvirinae* mit unbekannter Funktion. MCMV dient als *in vivo* Modell zum Studium des humanen Cytomegalovirus (HCMV), da HCMV eine strikte Spezies-Spezifität aufweist und große Homologien zu MCMV bestehen. HCMV ist ein wichtiges humanes Pathogen mit weltweiter Verbreitung. Obwohl die Infektion immunkompetenter Wirte normalerweise klinisch unauffällig verläuft, verursacht die Infektion von Föten und Neugeborenen schwere Organschäden und die Infektion immunsupprimierter Patienten ruft lebensbedrohliche Krankheiten hervor.

M94 als Einzelgen wurde zuvor nicht intensiv studiert, aber Studien über seine Homologe zeigten seine späte Expressionskinetik und seine Existenz als Teil des Virions. Es wurde eine Interaktion von UL94 mit UL99 in HCMV entdeckt und in α -*Herpesvirinae* eine Bindung der M94 Homologen an Capside. Während UL94 in HCMV essentiell ist, sind M94 Homologe in α -*Herpesvirinae* nicht essentiell. Dies lässt auf eine essentielle Funktion von M94 schließen, die in β -*Herpesvirinae* konserviert ist, aber nicht in α -*Herpesvirinae*. Zur Identifikation dieser essentiellen Funktion wurde durch eine modifizierte Tn7 Transposon-Mutagenese eine Bibliothek von zufälligen Mutanten erstellt. Durch die Modifikationen in der Transposon-Mutagenese wurde eine Bibliothek erzielt, welche hohe Diversität und große Abdeckung mit 32.000 primäre Klone mit Stopp- und Insertionsmutanten aufwies. Die Analyse von 613 Klonen durch Sequenzierung resultierte in 399 individuellen Mutanten mit einer korrekten 15 Basenpaar Insertion in M94. 116 Stopp- und Insertionsmutanten wurden einzeln in das virale Genom inseriert und im viralen Kontext geprüft. Die primäre

Analyse offenbarte die Fähigkeit der Mutanten die M94 Deletion zu komplettieren, dabei wurden die essentiellen Regionen im M94 Protein identifiziert. Zweitens wurden die Mutanten auf ihre inhibitorische Kapazität in Anwesenheit des M94 Wildtyp Allels analysiert, um dominant negative (DN) Mutanten zu identifizieren. Die identifizierten inhibitorischen Mutanten wurden als DN Mutanten durch regulierte Expression im Viruskontext und Analyse ihres spezifischen Phänotyps während der Überexpression verifiziert.

Die weitere Analyse der DN Mutante im Vergleich zu einer M94 Deletionsmutante offenbarte keinen Effekt auf virales Cleavage-Packaging, trotz früherer Publikationen. Zusätzliche Analysen zeigten eine Blockierung der zweiten Umhüllung sowohl für die DN Mutante als auch für die Deletionsmutante und den ausbreitungsdefiziente Phänotyps des M94 Deletionsvirus. Zusammen zeigen diese Resultate eine wichtige Funktion von M94 bei der zweiten Umhüllungsphase der *β-Herpesvirinae* auf.

Chapter 1

Introduction

1.1 *Herpesviridae*

Herpesviruses are large double stranded DNA viruses causing latent and lytic infections in animals including humans. The order of the *Herpesvirales* consists of three families, the *Alloherpesviridae* including herpesviruses of fish and amphibians, the *Malacoherpesviridae* containing herpesviruses of the bivalves and the *Herpesviridae* with herpesviruses of mammals, birds and reptiles [51]. The latter virus family developed from a common ancestor around 400 million years ago [50] and separated into three subfamilies, the α -*Herpesvirinae*, the β -*Herpesvirinae* and the γ -*Herpesvirinae*. This classification was based on biological properties in the 1970s and is proved by sequence analysis of *Herpesviridae* genomes today [76].

The α -*Herpesvirinae* are characterised by a wide host range, a short replication cycle, fast dissemination in cell culture, viral host shut-off, efficient lysis of infected cells and establishment of latency predominantly in neurons. In contrast, β -*Herpesvirinae* have a more restricted host range and a longer replication cycle. They spread slower in cell culture with milder cytopathic effects and latency can be established in different cell types. Similar to the β -*Herpesvirinae* the γ -*Herpesvirinae* exhibit a restricted host range and replicate slowly if at all in cell culture. In contrast to the α -*Herpesvirinae*, which can lytically in-

fect almost all cell types, the γ -*Herpesvirinae* are lymphotropic and also establish latency in lymphoblasts [66]. The well known Epstein-Barr virus (EBV), which causes infectious mononucleosis, also known as kissing disease, is a member of the γ -*Herpesvirinae*. The most prominent members of the α -*Herpesvirinae* are the herpes simplex virus (HSV) and Varicella-zoster virus (VZV), whereas the β -*Herpesvirinae* are represented by HCMV and MCMV.

Traditionally the lytic infection cycle of *Herpesviridae* is investigated in α -*Herpesvirinae* due to their short replication cycle. Additionally, HSV was the first isolated herpesvirus [34]. In the majority of cases, new details on the lytic cycle are detected in α -*Herpesvirinae* and subsequent confirmed in β -*Herpesvirinae*, whereas immunological studies are performed mainly in β -*Herpesvirinae* due to established MCMV model in mice for HCMV. The research in γ -*Herpesvirinae* examines transformation of cells, unique among the *Herpesviridae*.

The protein M94 investigated in this study is involved in the lytic cycle of MCMV. This study represents a case of a functional analysis of a herpes viral protein involved in the lytic cycle primarily in β -*Herpesvirinae*.

1.1.1 Clinical relevance of human cytomegalovirus

Human cytomegalovirus shows a worldwide distribution within humans as its exclusive host. Depending on the socio-economic status 50-100 % of the adult population is seropositive, where lower socio economic status correlates with higher infection rate [11,62]. HCMV infection in the immune competent host is usually clinically silent. Spread of HCMV occurs via horizontal transmission as well as vertical transmission.

The most common transmission route is vertically from mother to child either prenatal, perinatal or via breast feeding. Prenatal infection through the placenta and perinatal infection by virus shedding during birth in the maternal genital tract [74] can cause organ threatening disease. Although the most common route for vertical transmission is breast feeding [26], infection usually proceeds clinically silent and congenital infection is the clin-

ically most relevant form. Infection of the foetus can occur as a result of recurrence from latency as well as from primary infection of the mother [87] and leads to severe damage of the foetal organs or central nervous system [78]. Congenital HCMV infection therefore has been estimated to be the leading cause for sensorineural deafness and brain damage in children [65].

Horizontal transmission requires direct contact of a susceptible person with infectious body fluid such as urine, saliva, tears, semen, and cervical secretions, where it can be detected for month to years after initial infection [59]. Therefore, horizontal transmission of HCMV correlates with contact to young children and sexual activity [2, 12]. Horizontal transmission also occurs through blood transfusion [1] or solid organ [37, 75] and bone marrow transplantation [32].

Additionally, HCMV is one of the most common and difficult opportunistic pathogens that complicates the care of immunocompromised patients, such as AIDS and transplant patients [29, 86], inducing esophagitis, gastroenteritis, retinitis, pneumonia and mononucleosis like illness [16, 44]. At the moment there is no vaccine available. Thus, a potential HCMV vaccine was identified as one of the most cost effective and efficient ways to enhance life quality [90].

1.1.2 The murine cytomegalovirus model of HCMV

As a result of its strict species specificity, studies on HCMV *in vivo* are restricted by the guidelines on experiments involving humans. Therefore, as they show a high homology in genome sequence [70] and similar infection biology [39], MCMV was established as a model for CMV infection *in vivo*. With this reactivation from latency as well as viral immune evasion strategies can be studied in detail as well as dissemination of virions in the organism and establishment of latency. Although resulting findings cannot be directly transferred to HCMV, there are established mouse models to mimic certain clinical situations such as bone marrow transplantation [67] and human leukocyte antigen transgenic mouse models proved to be useful for HCMV epitope identification and preclinical vaccination studies [69].

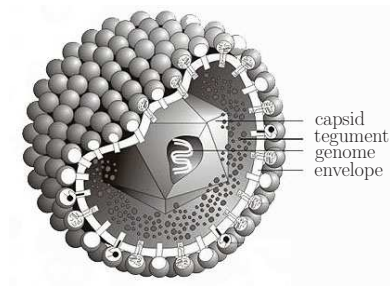


Figure 1.1: Schematic representation of the HCMV virion (adapted from [73]). The major virion components are indicated.

1.1.3 Structure of cytomegaloviruses

The composition of cytomegalovirus infectious particles is similar to other herpesviruses (Fig. 1.1). The mature virion has a diameter of 200-300 nm containing the viral capsid surrounded by tegument [31], an amorphous, proteinaceous layer [14] that is sequentially acquired during virus maturation [56]. The envelope is derived from the Golgi/trans-Golgi compartment and contains several virus encoded glycoproteins [28]. The icosahedral capsid has a diameter of 130 nm and contains the viral DNA. As every herpesvirus capsid, it is composed of 162 capsomers out of 150 hexons and 12 pentons. The five proteins constituting the hexons and pentons are conserved among the *Herpesviridae* [8]. The capsid protects the viral DNA against external influences. The viral genome is discussed in more detail in the next section.

1.1.4 The genome of cytomegaloviruses

The genomes of HCMV and MCMV consist of approximately 230 kbp of double stranded (ds) DNA and are together with the pox viruses the largest among vertebrate viruses. The genome of MCMV is a single unique sequence with short direct repeats at either end [27], whereas the genome of HCMV is separated by internal repeats into a unique long and a unique short region [13]. Additionally, the genome is flanked by terminal repeats, including multiple copies of *a*-sequences. These contain several repeats and two unique sequences which generate the *pac1* and the *pac2* signal, which determine the sites for viral DNA cleavage and packaging [17].

The *Herpesviridae* share common genome architecture. The conserved genes are located in

the middle of the genome, flanked by subfamily specific genes and surrounded by species specific genes at both ends of the genome (Fig. 1.2). The core genes are arranged in 7 gene blocks. In one cluster the gene order and polarity are conserved, whereas the order of the gene blocks varies between the subfamilies (Fig. 1.2).

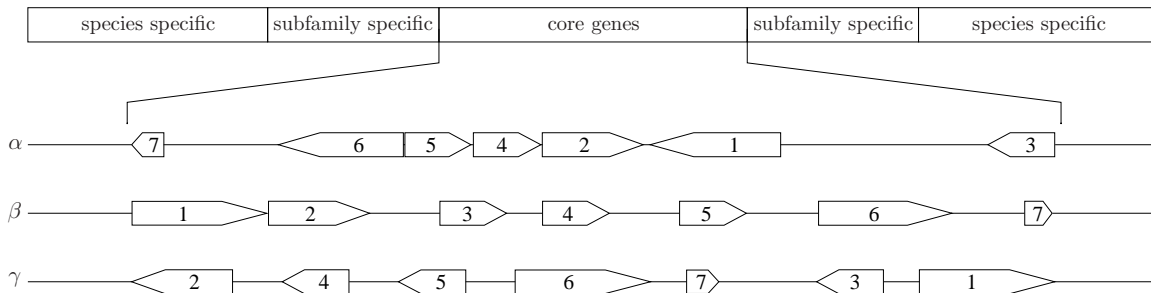


Figure 1.2: Schematic diagram of herpesvirus genome organisation for all 3 subfamilies (modified from [59]). The herpesvirus genomes consist of species specific genes located at both end, with subfamily specific genes within. The inner part is composed of the core genes with the 7 conserved gene blocks. These are enlarged for every subfamily in the next lines. The gene order and orientation is conserved within the subfamily, whereas the order of conserved gene blocks varies between the subfamilies.

1.1.5 Replication of cytomegaloviruses

As discussed previously the models for lytic infection are predominantly based on HSV and are devolved on CMV. An overview of the herpesvirus life cycle is illustrated in Fig. 1.3. The virus enters the cell by binding to specific cell surface receptors and fusion of the viral envelope with the cellular membrane. For example, heparan sulphate proteoglycans are among the receptors for HCMV [20]. The capsid is then delivered into the cytoplasm and transported to the nucleus via microtubuli where the viral DNA is released [84]. After circularisation of the DNA in the nucleus, gene expression is initiated.

Gene expression in the lytic cycle is strictly regulated and executed in a cascade manner [38], starting with expression of immediate early (IE) genes. The IE proteins induce the transcription of most other viral genes and also affect the host cell [94]. Thereby, innate immune response and apoptosis are inhibited and the cell is prepared for viral replication. The genes expressed upon IE induction are called early genes and their expression proceeds 6 to 24 h post infection (pi) [94]. Most of these gene products are involved in viral DNA replication and also in modulation of host immune response.

The replication of viral DNA, which starts 14-16 hpi leads to the expression of late genes. It is still unclear whether the expression of late proteins starts with the viral DNA replication or increases to detectable limits by this stage of infection. These proteins are involved in capsid maturation as well as DNA encapsidation and egress, processes that lead to production of infectious viral particles. Only a few genes are dependent on DNA replication for their expression, these are called true late genes.

The viral genome replication produces head-to-tail concatemers, which are cleaved into unit length genomes simultaneously to insertion into the capsid [52]. The capsid assembly itself also takes place in the nucleus. It is composed of 5 conserved proteins, arranged into a procapsid, which matures to the final capsid by protease cleavage and DNA insertion [55]. The capsid leaves the nucleus by budding into the perinuclear space, so called primary envelopment, and is transported from there by fusion of the primary envelope with the outer nuclear membrane into the cytoplasm [30]. On the way to the plasma membrane via the secretory pathway the tegument is added and the final or secondary envelopment occurs at the trans Golgi network (TGN) [79]. The mature virion is then transported to the cell surface and secreted into the extracellular space.

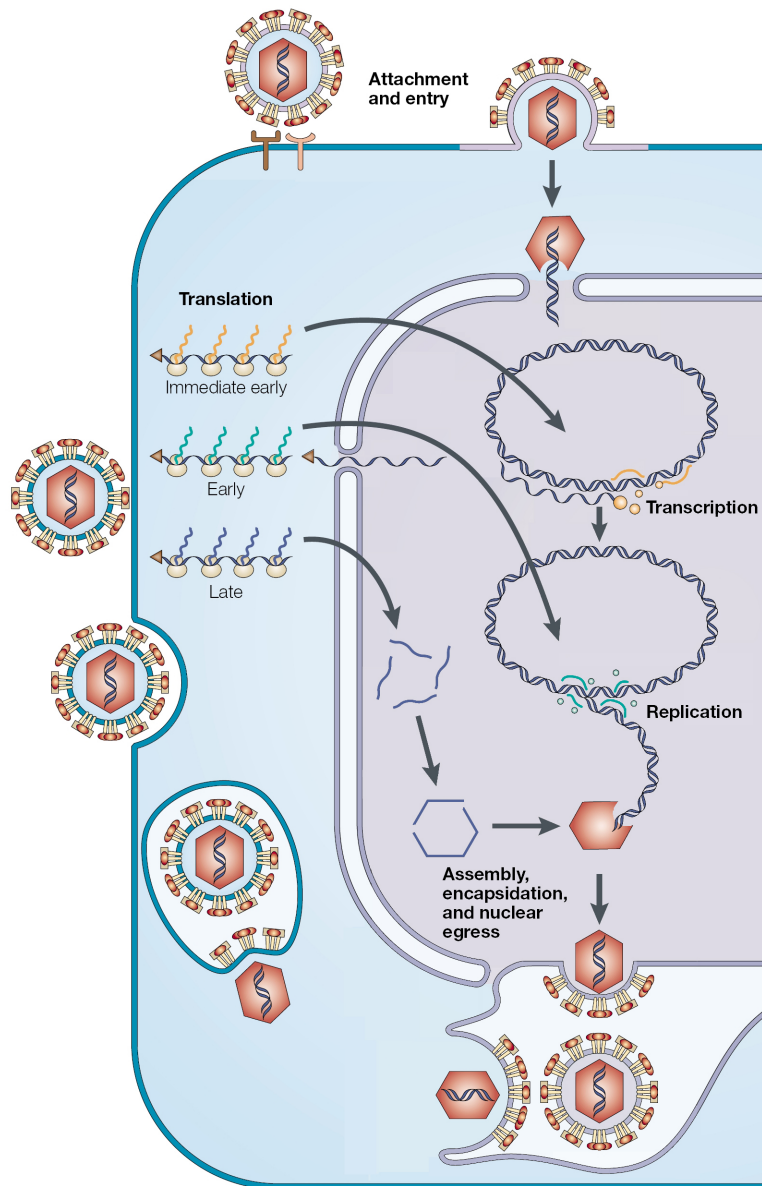


Figure 1.3: Diagram of the herpesvirus life cycle (adapted from [19]). The virion enters the cell by fusion with the plasma membrane after attachment via glycoproteins. This leads to release of the viral capsid into the cytoplasm. The capsid is then transported to the nucleus, where the viral genome is inserted into the nucleus through nuclear pore and circularises. Transcription is separated into 3 phases. Starting with the transcription of immediate early genes (orange), which activates the transcription of early genes (green). The translated early genes induce the replication of the viral genome and also the expression of the late genes (blue). These are mainly structural proteins and provide the components for virus capsid assembly. The viral DNA is then encapsidated into preformed capsids. These leave the nucleus by budding in an enveloping- and de-enveloping event and traverse the cytoplasm to the trans-Golgi-network while virion maturation proceeds. The mature virion is finally exocytosed into the extracellular space.

1.2 Genetics of herpesviruses

Since analysis by molecular cloning, the mutation of genes served as a powerful tool to analyse their function. Accordingly a mutagenesis was utilised for functional analysis in this study, the basic mutagenesis strategies will be explained. Mutagenesis of a defined gene and investigation of the resulting phenotype (reverse genetics) is thus distinguished from investigation of the genetic background of a known phenotype (forward genetics).

1.2.1 Forward Genetics

Early mutagenesis strategies were dependent on chemical agents or UV radiation for enhancement of the mutation rate during replication [40]. Interesting phenotypes were then investigated for their genetic background. Originally, temperature sensitive mutants were preferred as these mutants replicate like wt at permissive temperature and demonstrate the mutant phenotype only at the non-permissive temperature, facilitating the production of mutant virus and investigation of its phenotype [80].

The mutation causing the phenotype was identified using cross-complementation and marker rescue. Therefore a genome sector next to a marker was inserted into infected eukaryotic cells. Recombination events due to homologies with the viral genome were selected by the marker. The absence or presence of the mutant phenotype in the recombined viruses led to localisation of the mutation. This procedure was time-consuming and work-intensive.

1.2.2 Reverse Genetics

After identification of the mutation in the forward genetics, it remained unclear whether the phenotype arose from a single or multiple mutations. The discovery of molecular cloning and the publication of the MCMV genome opened the route for specific mutageneses of viral genes by homologous recombination [58]. Viral genes could be mutated and propagated in *Escherichia coli* (*E. coli*) and inserted into infected eukaryotic cells (Fig. 1.4). By homologous recombination at flanking homologies the viral gene could be substituted by

the mutated gene and a selectable marker in infected cells [85]. Due to the selectable marker the mutated genome could be separated from wt genomes. The mutation was established by this procedure and the resulting phenotypes could be analysed.

1.2.3 Mutagenesis of bacterial artificial chromosomes

The homologous recombination in eukaryotic cells produced low amounts of mutant virus which needed to be purified from wt virus. By cloning the MCMV genome as bacterial artificial chromosome (BAC) [54] the mutagenesis and genome propagation was carried out in *E. coli*. The resulting genome was pure from wt contamination and only the mutated virus was reconstituted from the mutant BAC (Fig. 1.4). The homologous recombination occurs in *E. coli* by ET recombination [97] and this was adapted by our lab for the CMV mutagenesis using linear DNA fragments [92]. Subsequently cells are transfected with the mutant BAC and the mutant virus was reconstituted. Hence, every conceivable mutation can be introduced into the virus.

1.2.4 Random mutagenesis

Structural knowledge of a protein permits the application of reverse genetics as specific sequences can be targeted by a selected mutation. Without structural information of the protein a random mutagenesis procedure is required. There are several techniques for random mutageneses established such as application of a mutator *E. coli* strain [33] or error-prone polymerase chain reaction (PCR) [42]. For this study the transposon mutagenesis was chosen, as it almost guarantees a single mutation in the gene of interest and next to insertion mutants stop mutants are also generated.

Transposons are mobile genetic elements which can insert into DNA sequences. The corresponding reaction is named transposition and different mechanisms are known. The relevant one in this study is the class II transposon. In this reaction a transposon is excised or copied from a donor position by the respective enzyme, the transposase, and

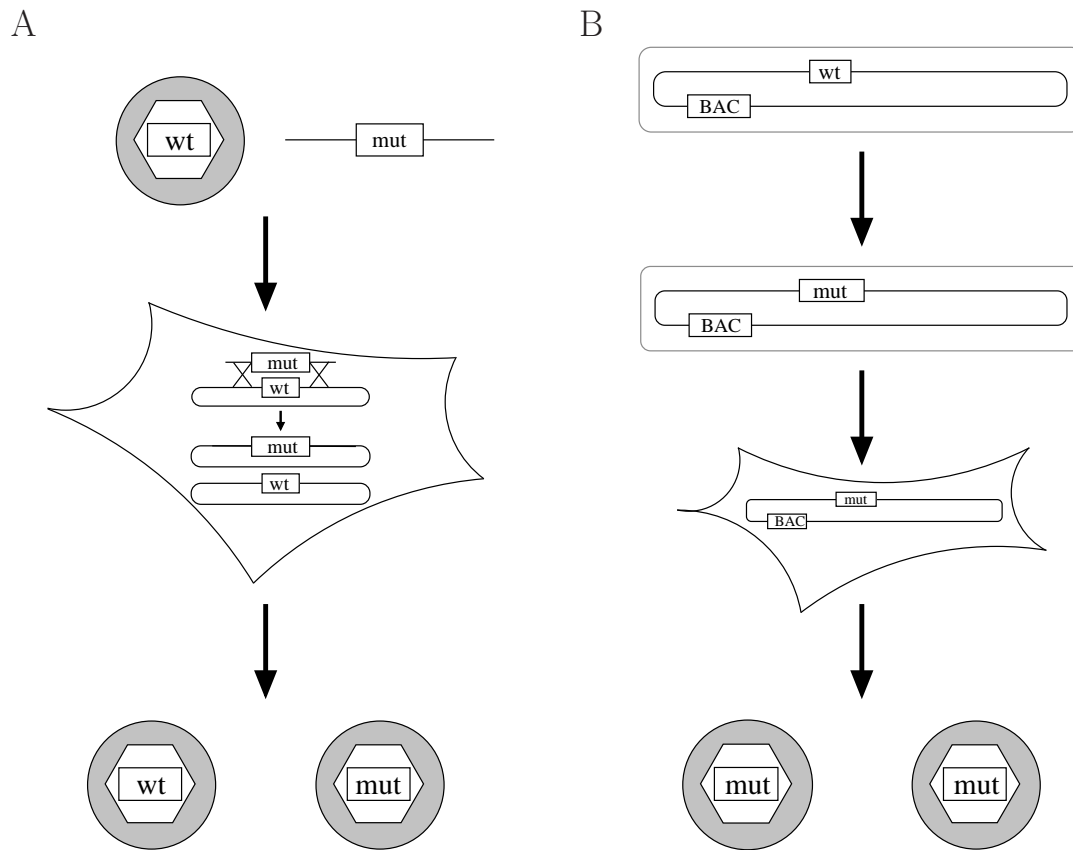


Figure 1.4: Strategies for mutagenesis in reverse genetics. Mutagenesis of a gene in *E. coli* and subsequent homologous recombination in eukaryotic cell with the viral genome, resulting in mutated and wt viral particles, is depicted in A, whereas B illustrates the mutagenesis of BAC in *E. coli* and reconstitution of the mutant BAC in eukaryotic cells.

inserted into a non-homologous target site. The first transposon was discovered in 1948 in maize [49], but the transposon Tn7 utilised in this study originates from bacteria [5] and permits a random insertion of the transposon into the target vector [6].

Mutagenesis of the BAC by transposon insertion is comparable to chemically induced mutagenesis, but only a single mutation is introduced by the transposon. Consequently essential and non-essential viral genes can easily be identified as essential genes destroyed by insertional mutagenesis prevent viral reconstitution from the BAC [9]. For the mutagenesis of a single viral gene, the gene is subcloned into a vector and the mutagenesis occurs on the plasmid. Mutants are subsequently inserted into the BAC deleted in that gene. The reconstitution of virus reveals the influence of the mutation on the protein function.

This method was utilised in this study.

1.2.5 Dominant negative mutants

The term antimorphic mutation, which was later renamed as dominant negative mutation, was introduced by Hermann Joseph Muller on the Sixth International Congress of Genetics in 1932 [60]. A DN mutation is defined as mutation leading to mutant protein that disrupts the activity of the wild type gene when overexpressed [36]. Therefore a DN protein must fulfil at least two functions. One function will remain intact as in the parental wild type protein, but another function is disrupted either by deletion of this protein domain or by its mutation to non-functionality.

For example, the DNA-binding domain of a transcription factor remains intact, but the activation domain is mutated. The DN mutant protein thereby blocks the wt protein from binding to the DNA by occupying the binding site itself, but does not continue in gene activation, thereby inhibiting wt function. Another example would be a DN mutant in a multimeric complex. The mutant would allow complex formation but not the execution of its downstream functions. Hence, DN mutants affect interactions either of proteins and DNA or among proteins.

An expressed DN mutant can result in the same phenotype as a deletion mutant. However the investigation of a deletion mutant demands a trans-complementing cell line. This obstacle can be avoided by the conditional expression of a DN mutant. Thereby the mutant virus can be produced regularly and the mutant phenotype is induced by expression of the DN mutant when needed. So, comparable to the temperature sensitive mutants the DN mutant can be generated and investigated using one construct. This principle was utilised for investigation of the function of M94.

1.3 The M94 gene of murine cytomegalovirus

M94 belongs to the 43 core genes of MCMV [23] and is located in gene block 6 (Fig. 1.2), consequently it is conserved in all *Herpesviridae*. Studies on M94 itself are highly limited, only one study identified M94 as virion associated [41].

Despite the sparse publications on M94, there have been several studies on its homologues UL94 in HCMV and UL16 in HSV, revealing several similarities. Both homologues have been identified as virion components and as true late genes, thus depending on viral genome replication [63, 95]. The overall sequence similarity in the homologues is low, but 7 cysteines are highly conserved in all *Herpesviridae* [64]. The exact function of these cysteines is unknown, but they seem to be involved in different binding activities.

The interaction between pUL16 and pUL11 has been already shown in 2003 [45] and recently the same interaction has been demonstrated for the pUL94 with pUL99, the homologue of pUL11 in HCMV [43]. Despite deletions of multiple parts of UL16/UL94, a discrete binding site for pUL11/pUL99 could not be identified [43, 96], although Yeh et al. could show that the interaction takes place in absence of viral or cellular partners [96]. However, blocking of the cysteines in pUL16 inhibits the binding to pUL11 [96]. Also two studies identified the cysteines as necessary for transient capsid binding of pUL16 [53, 96]. The main difference is the fact, that UL16 and homologues of α -*Herpesvirinae* are dispensable for virus replication in cell culture [3], whereas UL94 and homologues, as M94 itself, are essential in β -*Herpesvirinae* [25]. Consequently in this study an essential viral function of β -*Herpesvirinae* was investigated, which is absent in α -*Herpesvirinae*.

1.4 Aims of this study

As mentioned before, M94 is conserved in all *Herpesviridae*. The study of the conserved genes is of special interest as the analysis of a single gene provides information not only on this single gene but also on its homologues in the different *Herpesviridae*. The M94 gene of MCMV presents a unique factor in this setting as the function of most core genes

is already known [24]. The fact that M94 is essential in β -*Herpesvirinae* but not in α -*Herpesvirinae* makes this gene an interesting candidate for analysis. Thus, a detailed study of a β -*Herpesvirinae* member might identify the essential function in β -*Herpesvirinae* and thereby also contribute information to its function in α -*Herpesvirinae*.

The investigation of a deletion mutant typically results in a complex phenotype as most viral proteins are multifunctional. Analysis of a DN mutant phenotype is more subtle as this maintains at least one protein function intact namely to interact with at least some of its partner proteins. Other functions are lost and define the DN phenotype.

Therefore, the aim of this study was, next to the investigation of the deletion mutant, the identification of a DN mutant of M94 for analysis of its function in the MCMV life cycle. In order to do this, a random mutant library was constructed by Tn7-transposon insertion covering M94. The library was analysed by introduction into the virus context. This defined essential regions in M94 and also essential regions, which by insertin mutagenesis gave rise to DN mutants. The parallel investigation of deletion mutants and DN mutants provided insight into the function of M94.

Chapter 2

Materials and Methods

2.1 Material

2.1.1 Devices

Bacterial shaker ISF-1-W	Kühner, Adolf AG, Birsfelden, CH
Bacterial shaker Certomat [®] BS-1	Sartorius, Göttingen, D
Biofuge pico	Heraeus, Hanau, D
Bio-Photometer	Eppendorf, Hamburg, D
CASY [®] cell counter	Schärfe System, Reutlingen, D
Centrifuge Avanti [™] J-20 XP	Beckman Coulter, Krefeld, D
Centrifuge Evolution RC	Sorvall, Waltham, MA, USA
Crosslinker BLX-254	MS Laborgeräte, Wiesloch, D
Developing machine Optimax TR	MS Laborgeräte, Wiesloch, D
Econo-Submarine Electrophoresis System	C.B.S., Del Mar, CA, USA
Electrophoresis Power Supply EPS 1001	Amersham Pharmacia Biotech, Freiburg, D
Electrophoresis Power Supply EPS 200	Pharmacia Biotech, Freiburg, D
GeneAmp [®] PCR System 9700	Applied Biosystems, Foster City, CA, USA
Gene Pulser [™]	Bio-Rad, München, D
Hybridisation Oven 612	UniEquip, Martinsried, D
Incubater B5050E	Heraeus, Hanau, D
Incubator BB16CU	Heraeus, Hanau, D
Light microscope Axiovert 25	Carl Zeiss, Jena, D
Mini-PROTEAN [®] 3 Cell	Bio-Rad, München, D

Multifuge 3 S-R	Heraeus, Hanau, D
NanoDrop TM ND-1000 Spectrophotometer	Peqlab, Erlangen, D
Optima TM L-80 XP Ultracentrifuge	Beckman Coulter, Krefeld, D
PCR machine TGradient	Biometra, Göttingen, D
pH meter 430	Corning, Miami, FL, USA
Photo documentation apparatus (Eagle Eye)	Bio-Rad, München, D
Roller mixer SRT1	Stuart, Staffordshire, UK
Shaker Swip	Edmund Bühler, Hechingen, D
Thermomixer 5436	Eppendorf, Hamburg, D
Tissue cell culture lamina flow	BDK, Sonnenbühl-Genkingen, D
Trans-Blot TM SD Semi-Dry Eletrophoretic Transfer cell	Bio-Rad, München, D
Typhoon 9400	Amersham Bioscience, Freiburg, D
Vortex Mixer	Bender/Hobein, Bruchsal, D
Water Bath F10	Julabo, Seelbach, D
Water Bath GFL 1002	GLF, Burgwedel, D

2.1.2 Consumables

Cell culture dishes (15 cm, 10 cm, 6 cm)	Becton Dickinson, Heidelberg, D
Cell culture well plates (6-, 12-, 24-, 48-, 96-well)	Becton Dickinson, Heidelberg, D
Cell scrapers (25 cm, 39 cm)	Sarstedt, Nümbrecht, D
Chemiluminescence Hyperfilm TM ECL	Amersham Bioscience, Freiburg, D
Combitips plus (2.5 ml, 5 ml, 10 ml)	Eppendorf, Hamburg, D
CryoTube TM Vials	nunc, Langenselbold, D
Cuvettes	Brand, Wertheim, D
Dishes	Greiner Bio-one, Kremsmünster, A
Electroporation cuvettes	Bio-Rad, München, D
Falcons conical tubes (15 ml, 50 ml)	Becton Dickinson, Heidelberg, D
Inoculation loops	nunc, Langenselbold, D
Medical X-Ray screen film	CEA, Hamburg, D
PCR Softstrips	Biozym, Oldendorf, D
Pipettes (2 ml, 5 ml, 10 ml, 25 ml)	Sarstedt, Nümbrecht, D
Reaction tubes (0.5 ml, 1.5 ml, 2 ml)	Eppendorf, Hamburg, D
SafeSeal-Tips [®]	Biozym, Oldendorf, D
Ultracentrifugation tubes	Beckman Coulter, Krefeld, D

2.1.3 Reagents

Agarose	Invitrogen, Karlsruhe, D
Ammonium persulfate (APS)	Sigma-Aldrich, Taufkirchen, D
Ampicillin (Amp)	Sigma-Aldrich, Taufkirchen, D
Bacto TM Agar	Becton Dickinson, Heidelberg, D
Bacto TM Tryptone	Becton Dickinson, Heidelberg, D
Bacto TM Yeast Extract	Becton Dickinson, Heidelberg, D
BenchMark TM Prestained Protein Ladder	Invitrogen, Karlsruhe, D
Boric acid	Roth, Karlsruhe, D
Bromphenolblue	Sigma-Aldrich, Taufkirchen, D
Calcium chloride	Sigma-Aldrich, Taufkirchen, D
Carboxymethylcellulose, sodium salt 400-800 cps	Sigma-Aldrich, Taufkirchen, D
Chloramphenicol (Cam)	Sigma-Aldrich, Taufkirchen, D
Crystal violet	Merck, Darmstadt, D
Dimethyl sulfoxide (DMSO)	Merck, Darmstadt, D
DNA ladder (100 bp, 1 kbp)	NEB, Ipswich, MA, USA
Doxycycline (Dox) hydrochloride	Sigma-Aldrich, Taufkirchen, D
Ethanol	Merck, Darmstadt, D
Ethidium bromide (EtBr)	Roth, Karlsruhe, D
Ethylenediaminetetraacetic acid (EDTA)	VWR, Darmstadt, D
Ficoll 400	Pharmacia Fine Chemicals, Uppsala, S
Formaldehyde	Merck, Darmstadt, D
Glucose	Merck, Darmstadt, D
Glycerol	Roth, Karlsruhe, D
Glycine	Roth, Karlsruhe, D
HEPES	Fluka, Taufkirchen, D
Hydrochloric acid	Roth, Karlsruhe, D
Isopropanol (2-propanol)	Merck, Darmstadt, D
Kanamycin (Kan)	Sigma-Aldrich, Taufkirchen, D
L-Arabinose	Sigma-Aldrich, Taufkirchen, D
Maleic acid	Sigma-Aldrich, Taufkirchen, D
Manganese chloride	Sigma-Aldrich, Taufkirchen, D
β -Mercaptoethanol	Sigma-Aldrich, Taufkirchen, D
Methanol	Merck, Darmstadt, D
MOPS	Roth, Karlsruhe, D

N,N,N',N'-Tetramethylethylenediamine (TEMED)	Roth, Karlsruhe, D
Orange G	Sigma-Aldrich, Taufkirchen, D
Phenol red	Merck, Darmstadt, D
Phosphono acetic acid (PAA)	Sigma-Aldrich, Taufkirchen, D
Potassium acetate	Merck, Darmstadt, D
Potassium chloride	Merck, Darmstadt, D
Potassium hydrogenphosphate	Merck, Darmstadt, D
RNase	Sigma-Aldrich, Taufkirchen, D
Roti [®] -Phenol/C/I (Phenol/Chloroform/Isoamylalcohol 25/24/1)	Roth, Karlsruhe, D
Rotiphorese [®] Gel 30 (Acrylamid-bis-acrylamid 37.5:1)	Roth, Karlsruhe, D
Rubidium chloride	Sigma-Aldrich, Taufkirchen, D
D(+)-Saccharose	Roth, Karlsruhe, D
Skim milk powder	Merck, Darmstadt, D
Sodium acetate	Merck, Darmstadt, D
Sodium chloride	Merck, Darmstadt, D
Sodium citrate	Roth, Karlsruhe, D
Sodium dodecyl sulfate (SDS)	Roth, Karlsruhe, D
Sodium hydroxide	Fluka, Taufkirchen, D
SuperFect [®]	Qiagen, Hilden, D
Tris	Roth, Karlsruhe, D
Tween20	Sigma-Aldrich, Taufkirchen, D
Urea	Fluka, Taufkirchen, D
Zeocin (Zeo)	Sigma-Aldrich, Taufkirchen, D

2.1.4 Commercially kits

DIG Easy Hyb Granules	Roche, Mannheim, D
DIG Luminescent Detection Kit	Roche, Mannheim, D
DNeasy [™] Blood & Tissue Kit	Qiagen, Hilden, D
ECL Plus Western Blotting Detection Reagents	GE Healthcare, Freiburg, D
Expand High Fidelity PCR System	Roche, Mannheim, D
GPS [®] -LS Linker scanning system	NEB, Ipswich, MA, USA
GFX PCR DNA and Gel Band Purification Kit	GE Healthcare, Freiburg, D
GFX <i>Micro</i> Plasmid Prep Kit	Amersham Bioscience, Freiburg, D

NucleoBond TM Xtra Midi Kit	Macherey-Nagel, Düren, D
NucleoBond TM PC100	Macherey-Nagle, Düren, D
PCR DIG Probe Synthesis Kit	Roche, Mannheim, D
QIAEX II DNA Extraction from Agarose Gels	Qiagen, Hilden, D

2.1.5 Bacteria

<i>E. coli</i> strain	Genotype
DH10B	F ⁻ <i>mcrA</i> Δ (<i>mrr-hsdRMS-mcrBC</i>) ϕ 80 <i>lacZ</i> Δ M15 Δ <i>lacX74</i> <i>recA1</i> <i>endA1</i> <i>araD139</i> Δ (<i>ara, leu</i>)7697 <i>galU</i> <i>galK</i> λ ⁻ <i>rpsL</i> <i>nupG</i> (Invitrogen, Karlsruhe, D)
PIR1	F ⁻ Δ <i>lac169</i> <i>rpoS</i> (Am) <i>robA1</i> <i>creC510</i> <i>hsdR514</i> <i>endA</i> <i>recA1</i> <i>uidA</i> (Δ <i>MluI</i>):: <i>pir</i> -116 (Invitrogen, Karlsruhe, D)
Xl1-blue	<i>endA1</i> <i>supE44</i> <i>thi-1</i> <i>hsdR17</i> <i>gyrA96</i> <i>relA1</i> <i>lac</i> [F' <i>proAB</i> <i>lacI</i> ^q Z Δ M15 Tn10 (Tet ^r)] (Stratagene, La Jolla, CA, USA)

2.1.6 Cells

Cell type	Description
293	human embryonic kidney cells transformed with adenovirus 5, ATCC [®] number: CRL-1573
M2-10B4	bone marrow stromal cells from (C57BL/6J X C3H/HeJ)F1 mouse, ATCC [®] number: CRL-1972
MEF	murine embryonal fibroblast of BALB/c-mouse [81]
NIH3T3	mouse embryonic fibroblast cell line from NIH Swiss mouse, ATCC [®] number: CRL-1658
NTM94	NIH3T3 cells mutated by Tet-Off TM -System (Clontech) as transcomplementing cell line for M94 deletion mutant

2.1.6.1 Cell culture reagents

All reagents were received from Invitrogen.

DMEM (Dulbeccos Modified Eagle Medium)	+4.5 g/l glucose, +L-glutamine, -pyruvate
RPMI (Roswell Park Memorial Institute)	+L-glutamine
DPBS (Dulbeccos Phosphate Buffered Saline)	-CaCl ₂ , -MgCl ₂
FBS (Foetal Bovine Serum)	
Hygromycin B	50 mg/ml in PBS
L-Glutamine (Q)	100x
MEM (Minimal Essential Medium)	+Earles, -L-glutamine, -NaHCO ₃
NEAA (Non-Essential Amino Acids)	100x
NCS (Newborn Calf Serum)	
Penicillin Streptomycin (P/S)	10000 units/ml penicillin, 10000 µg/ml streptomycin
Sodium pyruvate (NaHCO ₃)	100 mM
Trypsin-EDTA	0.25 % Trypsin-EDTA

2.1.7 Plasmids and bacterial artificial chromosomes

The following tables summarise the plasmids and BACs used in this study and give a short introduction in their function.

2.1.7.1 Commercial available plasmids

Name	Replication ability, temperature, antibiotic resistance	Description
Litmus28	DH10B, 37°C, Amp	Cloning vector from NEB
pGPS4	PIR1, 37°C, Cam	Donor vector in transposon mutagenesis (GPS [®] -LS Linker scanning system)

2.1.7.2 Available plasmids in the lab

Name	Replication ability, temperature, antibiotic resistance	Description
pSM3fr-FRT	DH10B, 37°C, Cam	complete MCMV genome as BAC including FRT site between genes m16 and m17 ([10])
pKD46	DH10B, 30°C, Amp	expresses recombinases α , β , and γ from λ phage for BAC ET-cloning ([22])
pCP20	DH10B, 30°C, Amp, Cam	expresses Flp recombinase for BAC mutagenesis ([15])
pGPS1.1	PIR1, 37°C, Kan	template vector for PCR for BAC mutagenesis
pOriR6K-ie	PIR1, 37°C, Zeo	expression vector for subcloning in transposon mutagenesis containing FRT site for ectopic insertion into BACs (GenBank: AY700021.1)
pOriR6K-ie-HAM94	PIR1, 37°C, Zeo	HA-tagged M94 under control of HCMV immediate early promoter enhancer in pOriR6K-ie
pSM3fr Δ M94	DH10B, 37°C, Cam, Kan	MCMV genome deleted in M94 replaced by kanamycin resistance
pSM3fr Δ M94-EPM94	DH10B, 37°C, Cam, Kan, Zeo	rescue of pSM3fr Δ M94 by ectopic insertion of M94 under control of its endogenous promoter
pO6CMV	PIR1, 37°C, Zeo	conditional expression cassette including HCMV immediate early promoter enhancer for expression of mutants in pOriR6K-ie vector ([77])
pO6SVT	PIR1, 37°C, Zeo	conditional expression cassette including SVT40 early enhancer for expression of mutants in pOriR6K-ie vector ([77])
pSM3fr-FRT- Δ 1-16	DH10B, 37°C, Cam	MCMV genome deleted in genes m01 to m16 including FRT site between genes m16 and m17

2.1.7.3 Cloned plasmids

Name	Replication ability, temperature, antibiotic resistance	Description
Litmus28-HAM94	DH10B, 37°C, Amp	HA-M94 subcloned from pOriR6K-ie-HAM94 into Litmus 28 (section 3.3)
pSM3fr Δ M94-EHAM94	DH10B, 37°C, Cam, Kan, Zeo	rescue of pSM3fr Δ M94 by ectopic insertion of HA-M94 (pOriR6K-ie-HAM94) under control of HCMV immediate early promoter enhancer
pOriR6K-ie-mLM94i7	PIR1, 37°C, Zeo	DN mutant M94i7 resulting from transposon mutagenesis and subsequent subcloning under control of HCMV immediate early promoter enhancer in pOriR6K-ie
pOriR6K-ie-mLM94i13	PIR1, 37°C, Zeo	DN mutant M94i13 resulting from transposon mutagenesis and subsequent subcloning under control of HCMV immediate early promoter enhancer in pOriR6K-ie
pO6CMV-M94i7	PIR1, 37°C, Zeo	DN mutant M94i7 subcloned from pOriR6K-ie-mLM94i7 by PCR using primers M94-Mlu1-for and M94-Pvu2-rev and subsequent restriction with <i>MluI</i> and <i>PvuII</i> into pO6CMV digested with <i>AscI</i> and <i>HpaI</i> for conditional expression
pO6CMV-M94i13	PIR1, 37°C, Zeo	DN mutant M94i13 subcloned as described for pO6CMV-M94i7
pO6SVT-M94i7	PIR1, 37°C, Zeo	DN mutant M94i7 subcloned from pOriR6K-ie-mLM94i7 by PCR using primers M94-Mlu1-for and M94-Pvu2-rev and subsequent restriction with <i>MluI</i> and <i>PvuII</i> into pO6SVT digested with <i>AscI</i> and <i>HpaI</i> for conditional expression
pO6SVT-M94i13	PIR1, 37°C, Zeo	DN mutant M94i13 subcloned as described for pO6SVT-M94i7
pSM3frCMV-RM94i7	DH10B, 37°C, Cam, Zeo	pO6CMV-M94i7 ectopically inserted via Flp-FRT system into pSM3fr-FRT
pSM3frCMV-RM94i13	DH10B, 37°C, Cam, Zeo	pO6CMV-M94i13 ectopically inserted via Flp-FRT system into pSM3fr-FRT

pSM3frSVT-RM94i7	DH10B, 37°C, Cam, Zeo	pO6SVT-M94i7 ectopically inserted via Flp-FRT system into pSM3fr-FRT
pSM3frSVT-RM94i13	DH10B, 37°C, Cam, Zeo	pO6SVT-M94i13 ectopically inserted via Flp-FRT system into pSM3fr-FRT
pSM3fr Δ 1-16CMV-RM94i7	DH10B, 37°C, Cam, Zeo	pO6CMV-M94i7 ectopically inserted via Flp-FRT system into pSM3fr-FRT- Δ 1-16
pSM3fr Δ 1-16CMV-RM94i13	DH10B, 37°C, Cam, Zeo	pO6CMV-M94i13 ectopically inserted via Flp-FRT system into pSM3fr-FRT- Δ 1-16
pSM3fr Δ 1-16SVT-RM94i7	DH10B, 37°C, Cam, Zeo	pO6SVT-M94i7 ectopically inserted via Flp-FRT system into pSM3fr-FRT- Δ 1-16
pSM3fr Δ 1-16SVT-RM94i13	DH10B, 37°C, Cam, Zeo	pO6SVT-M94i13 ectopically inserted via Flp-FRT system into pSM3fr-FRT- Δ 1-16
pSM3fr Δ 1-16-EHAM94	DH10B, 37°C, Cam, Zeo	HA-M94 (pOriR6K-ie-HAM94) under control of HCMV immediate early promoter enhancer ectopically inserted into pSM3fr-FRT- Δ 1-16 as overexpressing control in Southern blot analysis
pO6SVT-HAM94	PIR1, 37°C, Zeo	HAM94 subcloned from pOriR6K-ie-HAM94 by PCR using primers HAM94-Asc-for and HAM94-Sma-rev and subsequent restriction with <i>AscI</i> and <i>SmaI</i> into pO6SVT digested with <i>AscI</i> and <i>HpaI</i> for conditional expression
pSM3fr Δ 1-16SVT-RHAM94	DH10B, 37°C, Cam, Zeo	HA-M94 (pO6SVT-HAM94) under control of inducible SVT40 early enhancer ectopically inserted into pSM3fr-FRT- Δ 1-16 as overexpressing control in western blot analysis

2.1.8 Oligonucleotides

Oligonucleotides were synthesised by Metabion, whereas primers for sequencing were provided by GATC Biotech.

Name	Sequence (5' → 3')	Comment
M94-Mlu1-for	GTGTACGCGTACCATGTACCCC TACGACGTGCCC	forward primer for subcloning of M94i7 and M94i13 into pO6CMV and pO6SVT
M94-Pvu2-rev	ACACCAGCTGTCTGACTTCACAT GTGCTCGAGAAC	reverse primer for subcloning of M94i7 and M94i13 into pO6CMV and pO6SVT
HAM94-Asc-for	GGTGGCGCGCCTCACTATAGGG AGACCCAAGCT	forward primer for subcloning of HAM94 into pO6SVT
HAM94-Sma-rev	GTGGCCCGGGAGAGTCTGACTTC ACATGTGCTC	reverse primer for subcloning of HAM94 into pO6SVT
Apa2-for	ATCGGGTCACAGTCCTCACGCC	forward primer for generation of Southern probe for Southern blot analysis on MCMV Δ 1-16
Apa2-rev	CAACATCCGTGGGTCTGACACC	reverse primer for generation of Southern probe for Southern blot analysis on MCMV Δ 1-16
CMV-F	CGCAAATGGGCGGTAGGCGTG	sequencing primer for pOriR6K, pO6CMV and pO6SVT constructs
BGH-Reverse	TAGAAGGCACAGTCGAGG	sequencing primer for pOriR6K constructs
pEGFP-FP	TTTAGTGAACCGTCAGATC	sequencing primer for pO6CMV and pO6SVT constructs

2.1.9 Viruses

Viruses used in this study were recovered from BACs mentioned in section 2.1.7 by reconstitution (section 2.2.7.1) and labelled according to the BAC names by exchanging "pSM3fr" with MCMV.

The virus MCMV Δ M94tTA was kindly provided by Christian Mohr. The corresponding BAC pSM3fr Δ m157 Δ M94tTA includes the MCMV genome deleted in m157 and M94. The non-essential gene m157 was replaced by a floxed OVA-cassette as the virus was originally created for *in vivo* experiments. M94 was replaced by a tetracycline-controlled transactivator (tTA) from the Tet-OffTM Gene Expression System (Clontech). The corresponding tetracycline-response element (TRE) was provided by pTRE2hyg. M94 was subcloned into this vector under control of TRE. This vector was transformed into NIH3T3 cells and se-

lected for the inherent plasmid by hygromycin selection (section 2.2.6.1). Infection of these cells with MCMV Δ M94tTA resulted in binding of tTA from the virus to TRE in the cells, consequently the expression of M94 in the cells was activated and provided the essential component for viral progeny, but remained the virus genetically deleted in M94. So the virus MCMV Δ M94tTA was produced on this complementing cell line.

2.1.10 Antibodies

CROMA101 (α -pp89)	mouse monoclonal antibody	provided by S. Jonjic, University of Rijeka, Rijeka, Croatia
α -M50	rabbit polyclonal serum	published in [61]
α -M94 A and B	rabbit polyclonal sera	produced by metabion against peptides CMLVNKSARYREFRAV and CRDS-GRHVDPTGRFV
α -HA-Peroxidase High Affinity	rat monoclonal antibody conjugated to peroxidase	purchased by Roche

Secondary antibodies were coupled to horseradish peroxidase (HRP) and purchased from Dianova.

anti-mouse IgG (H+L)	HRP coupled
anti-rabbit IgG (H+L)	HRP coupled
anti-rat IgG (H+L)	HRP coupled

2.2 Methods

2.2.1 Bacterial cell culture

The bacterial strains DH10B and PIR1 (section 2.1.5) were grown in LB media either in liquid culture or on LB agar plates at 37°C or 30°C depending on the comprising plasmid. The bacterial strain XL1blue (section 2.1.5) was cultured in SOC media at 37°C. Plasmid maintenance was guaranteed by maximal selection pressure through addition of antibiotics,

except the combination of Cam and Zeo, which was not applied in liquid culture as this combination inhibited bacterial growth unspecifically. Cell density was determined by measurement of the optical density (OD) of a liquid culture at OD₆₀₀.

LB medium

10 g BactoTM Tryptone
5 g BactoTM Yeast Extract
4 g sodium chloride
add 1 l

SOC medium

20 g BactoTM Tryptone
5 g BactoTM Yeast Extract
0.5 g sodium chloride
20 mM glucose
add 1 l

LB Agar

7.5 BactoTM Agar
add 500 ml LB medium

Antibiotics (stock/final concentration)

Amp	100 mg/ml	100 µg/ml
Kan	100 mg/ml	50 µg/ml
Cam	25mg/ml	25 µg/ml
Zeo	100mg/ml	30 µg/ml

2.2.1.1 Preparation of chemocompetent bacteria

All steps were performed at 4°C or on ice using pre-cooled pipettes, flasks and solutions. 50 ml LB media containing antibiotics were inoculated with 1 ml overnight culture and grown at either 30°C or 37°C up to an OD₆₀₀ of 0.5. The culture was chilled on ice for 5 min and bacteria collected by centrifugation (2,600 g, 15 min, 4°C). The supernatant was discarded, the pellet resuspended in 10 ml TfBI-buffer and incubated on ice for 50 min. After centrifugation of the bacteria (2,600 g, 15 min, 4°C), the pellet was resuspended in 1 ml TfBII-buffer and aliquots of 100 µl were snap frozen in liquid nitrogen before transferred to -80°C storage.

TfBI-buffer

100 mM RbCl₂
50 mM MnCl₂
30 mM KAc
10 mM CaCl₂
pH 5.8

TfBII-buffer

10 mM MOPS pH 7.0
10 mM RbCl₂
75 mM CaCl₂
15 % glycerol
pH 7.0

2.2.1.2 Transformation of chemocompetent bacteria

For transformation of chemocompetent bacteria, aliquots were thawed on ice and 10 ng of plasmid DNA was added. This reaction was incubated on ice for 30 min and subsequently heat shocked for 45 sec at 42°C, before chilled on ice for 2 min. 1 ml LB media without antibiotics was added and the culture incubated for 1 h at the appropriate temperature. About 100 μ l of the culture were plated on LB agar plates containing the corresponding antibiotics.

2.2.1.3 Preparation of electrocompetent bacteria

The preparation of electrocompetent bacteria was performed on ice using pre-cooled pipettes, flasks and solutions. 400 ml LB media containing antibiotics were inoculated with 1.5 ml overnight culture and grown at 37°C up to OD₆₀₀ of 0.5. The culture was incubated on ice for 30 min and bacteria were pelleted by centrifugation (5,500 g, 10 min, 4°C). After discarding the supernatant, the pellet was resuspended in 200 ml water. Centrifugation was repeated and the bacteria resuspended in 5 % glycerol. This step was repeated once, followed by an additional washing in 10 % glycerol. The pellet was then resuspended in 2 ml 10 % glycerol and aliquots of 50 μ l were snap frozen in liquid nitrogen and stored at -80°C.

2.2.1.4 Transformation of electrocompetent bacteria

For transformation of electrocompetent bacteria, aliquots were thawed on ice, 10-50 ng of plasmid DNA were added and this mixture was transferred into a pre-cooled electroporation cuvette (diameter 2 mm). The electroporation was performed at a 2.5 kV, resistance of 200 Ω , and a capacitance of 25 μ F. The bacteria were immediately transferred into 1 ml LB media without antibiotics and grown for 1 h at 37°C. Subsequently 100 μ l were plated on antibiotic containing LB agar plates.

2.2.1.5 Preparation of glycerol stocks

Bacteria containing cloned plasmids or BACs were stored as glycerol stocks at -80°C . To this end $600\ \mu\text{l}$ of overnight culture were mixed with $400\ \mu\text{l}$ of 50 % glycerol and transferred to -80°C .

2.2.2 Isolation and purification of DNA

Isolated DNA was dissolved in Tris-HCl buffer (T-buffer) and stored at -20°C . Centrifugations including volumes up to 2 ml were performed in Heraeus Biofuge pico, whereas cultures up to 50 ml were collected in Heraeus Multifuge 3 and larger volumes were processed in Sorvall Evolution RC. All steps were accomplished at room temperature (RT) except as noted otherwise.

T-buffer: 10 mM Tris/HCl pH 8.0

2.2.2.1 Small scale isolation of plasmid DNA

Small scale isolation of high and low copy plasmid DNA was performed using GFX *Micro* Plasmid Prep Kit from Amersham Bioscience. An overnight culture of 2 ml was treated according to manufacturers purification from 1-1.5 ml culture protocol.

2.2.2.2 Large scale isolation of plasmid DNA

Large scale isolation of plasmid DNA was accomplished by NucleoBondTM Xtra Midi Kit from Macherey-Nagel. Commonly 150 ml of overnight culture grown in LB media containing antibiotics were treated according to manual for high copy plasmid purification. Purified DNA was dissolved in 200-500 μl T-buffer.

2.2.2.3 Small scale isolation of BAC DNA

A 10 ml overnight culture was collected by centrifugation (2,600 g, 15 min, RT), the pellet resuspended in 300 μl Resuspension buffer, and transferred to 2 ml reaction tubes. 300 μl

Lysis buffer were added and samples inverted several times. Next 300 μl of Neutralisation buffer were added and samples inverted several times again. The lysates were then incubated 10 min on ice and cleared by centrifugation (20,000 g, 5 min, RT). The supernatant was transferred into a new reaction tube and 1 ml Roti[®]-Phenol/C/I (Roth) was added. The samples were incubated on roller shaker for at least 10 min for protein extraction. The aqueous phase was regained by centrifugation (20,000 g, 5 min, RT) and transferred into a new reaction tube. 1 ml isopropanol was added for DNA precipitation. After proper mixing, the DNA was collected by centrifugation (20,000 g, 30 min, RT). After discarding the supernatant, the DNA pellet was washed by adding 1 ml 70 % ethanol and centrifugation (20,000 g, 10 min, RT). The DNA pellet was dried at 45°C for 5-15 min and resuspended in 50 μl T-buffer including 100 $\mu\text{g}/\text{ml}$ RNase. This procedure yielded material for a single restriction analysis.

<u>Resuspension buffer</u>	<u>Lysis buffer</u>	<u>Neutralisation buffer</u>
50 mM Tris/HCl, pH 8.0	200 mM NaOH	3 M KAc, pH 4.8
10 mM EDTA	1 % (w/v) SDS	
100 $\mu\text{g}/\text{ml}$ RNase		

2.2.2.4 Large scale isolation of BAC DNA

For large scale isolation of BAC DNA NucleoBond[™] Xtra Midi Kit from Macherey-Nagel was utilised. The protocol for low-copy plasmid purification provided by manufacturers was modified by using 10 ml of buffers RES, LYS and NEU instead of 16 ml. Otherwise the protocol was performed as described. The DNA pellet was dissolved in 100 μl T-buffer. For handling of BAC DNA solution pipette tips with extended cut were used.

2.2.2.5 Concentration of DNA by ethanol precipitation

The solution containing the DNA was drugged with $\frac{1}{10}$ (v/v) 3 M sodium acetate and threefold volume of pure ethanol. The reaction was incubated at -80°C for 20 min and the precipitated DNA collected by centrifugation (20,000 g, 5 min, 4°C). The pellet was

washed by adding 200 μl of 70 % ethanol and centrifugation (20,000 g, 5 min, 4°C). After air drying of the pellet, it was resuspended in 10 μl T-buffer.

2.2.2.6 Isolation of DNA from cell culture

DNA was isolated from cells by using DNeasyTM Blood & Tissue Kit from Qiagen. The procedure "Purification of Total DNA from Animal Blood or Cells (Spin-Column Protocol)" was complied according to the manual.

2.2.2.7 Determination of DNA concentration

The concentration of isolated DNA was determined by spectral measurement with NanoDropTM micro spectrophotometer by the manufacturers standard protocol given.

2.2.3 Analysis and cloning of DNA

2.2.3.1 Polymerase chain reaction

For the *in vitro* amplification of DNA the PCR was utilised. As the PCR was required for several experiments, the composition and conditions are listed below separately. The reactions were setup on ice in the indicated order.

PCR for cloning				
H ₂ O	add 50 μl	94°C	5 min	
10x buffer no.2	1x	94°C	30 sec	20 cycles
dNTP mix (10 mM)	200 μM	62-52°C	30 sec	20 cycles
for primer (10 μM)	300 nM	72°C	1 min/1000 bp	20 cycles
rev primer (10 μM)	300 nM	94°C	30 sec	20 cycles
template (10 ng/ μl)	1 ng/ μl	50°C	30 sec	20 cycles
High Fidelity polymerase	1 unit	72°C	1 min/ 1000 bp	20 cycles
		72°C	3 min	
		4°C	∞	

Reagents for cloning PCR were purchased from Expand High Fidelity PCR system from Roche. In this touch down PCR the annealing temperature dropped 0.5°C in every cycle

automatically due to the setting of the TGradient PCR machine from Biometra.

PCR for BAC mutagenesis				
H ₂ O	add 100 μ l	95°C	5 min	
10x buffer no.2	1x	95°C	30 sec	17 cycles
dNTP mix (10 mM)	200 μ M	62-45°C	30 sec	17 cycles
for primer (10 μ M)	300 nM	72°C	1 min/1000 bp	17 cycles
rev primer (10 μ M)	300 nM	95°C	30 sec	18 cycles
template (10 ng/ μ l)	1 ng/ μ l	45°C	30 sec	18 cycles
High Fidelity polymerase	1 unit	72°C	1 min/ 1000 bp	18 cycles
		72°C	5 min	
		4°C	∞	

For the BAC mutagenesis PCR the reagents from the Expand High Fidelity PCR system from Roche were used. The temperature in this touch down PCR dropped by 1°C each cycle by using the same PCR machine as in the cloning PCR.

PCR for generation of Southern probe				
H ₂ O	add 50 μ l	94°C	5 min	
10x buffer vial 3	1x	94°C	30 sec	20 cycles
dNTP mix (10 mM) vial 2/4	200 μ M	65-45°C	30 sec	20 cycles
for primer (10 μ M)	300 nM	72°C	1 min/1000 bp	20 cycles
rev primer (10 μ M)	300 nM	94°C	30 sec	28 cycles
template (10 ng/ μ l)	1 ng/ μ l	45°C	30 sec	28 cycles
High Fidelity polymerase	1 unit	72°C	1 min/ 1000 bp	28 cycles
		72°C	7 min	
		4°C	∞	

For the generation of the Southern probe the reagents contained in the PCR DIG Probe Synthesis Kit from Roche were applied. The control PCR without Dig labelling contained dNTP mix vial 4, whereas the PCR with Dig labelling included vial 2 containing Dig labelled NTPs. In this touch down PCR the temperature dropped 1°C in each cycle, using the GeneAmpTM PCR System 9700 from Applied Biosystems.

2.2.3.2 Buffer change of PCR products

Digested DNA were prepared for ligation by buffer change using GFX PCR DNA and Gel Band Purification Kit from GE Healthcare according to manufacturers protocol for purification of DNA from solutions. DNA was eluted by two sequential applications of 20 μ l of T-buffer.

2.2.3.3 Restriction enzyme digest of DNA

Restriction enzymes from New England Biolabs (NEB) or Fermentas were used according to manual with 10 units of enzyme for each digest, supplemented with 1x buffer, and $\frac{1}{100}$ volume of BSA as needed. For digestion with two enzymes either a buffer permitting 100 % restriction efficiency for both enzymes was selected from the companies buffer set or a sequel digest was applied.

Analytic digestion of plasmid DNA was performed in 20 μ l final volume including 5 μ l of the small scale preparation for 1 h at the appropriate temperature. Whereas for preparative digestion were carried out in up to 80 μ l final volume and at least 3 h at the appropriate temperature. Analytic digestion of BAC DNA was performed in 60 μ l final volume for small scale preparations including the entire isolate and in 40 μ l for large scale isolates containing 1.5 μ g DNA for 2-3 h at the appropriate temperature.

2.2.3.4 Dephosphorylation of DNA

Digested DNA was dephosphorylated by Antarctic Phosphatase from NEB following the manual.

2.2.3.5 Blunting of DNA fragments by DNA polymerase

DNA overhangs were either filled (5'overhangs) or removed (3'overhangs) via DNA Polymerase Large (Klenow) Fragment from NEB. Conditions were used according to manufacturers protocol.

2.2.3.6 Agarose gel electrophoresis

Digested DNA was supplemented with $\frac{1}{5}$ volume of loading buffer and separated on non denaturing agarose gels of 1 % (w/v) for plasmid DNA and 0.8 % (w/v) for BAC DNA. Ethidium bromide was added to final concentration of 1 $\mu\text{g}/\text{ml}$ to the gels and for analysis of BACs ethidium bromide was also added to the buffer. The agarose gels for analysis of plasmids were prepared with and separated in TAE buffer, whereas TBE buffer was used for analysis of BACs. Agarose gel electrophoresis was performed at constant voltage of 5 V/cm for up to 1 h in case of plasmids and at 80 V for 16-24 h for BACs. The resulting banding pattern were then visualised by UV light on Eagle Eye imager from Bio-Rad.

<u>TAE (50x)</u>	<u>TBE (10x)</u>	<u>Loading buffer (6x)</u>
2 M Tris	900 mM Tris	15 % (w/v) Ficoll
250 mM sodium acetate	900 mM boric acid	0.25 % (w/v) Orange G
50 mM EDTA	10 mM EDTA	
pH 7.3	pH 8.0	

2.2.3.7 Isolation of DNA fragments from agarose gels

DNA fragments were isolated from agarose gels by using "QIAEX II DNA Extraction from Agarose Gels" Kit from Qiagen according manufacturers instructions.

2.2.3.8 Ligation of DNA fragments

The vector, containing the origin of replication and the antibiotic resistance, and the subcloned fragment, the insert were ligated by mixing 100 ng vector with threefold molar ratio of insert and 20 units T4 DNA Ligase (NEB) and corresponding buffer in a final volume of 20 μl and incubated at 16°C overnight. Bacteria were transformed with $\frac{1}{10}$ of this reaction.

2.2.3.9 Sequencing of DNA

Successful cloning of DNA constructs was verified by sequencing. Plasmid DNA was sequenced by GATC Biotech (Konstanz, D) and BAC DNA by Sequiserve (Vaterstetten, D).

The resulting sequences were aligned and compared using Vector NTI Advance[™] Software.

2.2.4 Transposon mutagenesis

The HA-tagged M94 was subcloned from pOriR6K-ie-HAM94 (section 2.1.7) into Litmus28, as this contained no *PmeI* restriction site and no chloramphenicol resistance and could replicate in bacteria other than PIR1. The detailed cloning is described in section 3.3.

The transposon reaction was performed *in vitro* using the GPS[®]-LS Linker Scanning system (NEB) according to the manual (Tab. 4.1). XL1-blue bacteria, supplied by Stratagene with warranty of sufficient transformation efficiency, were transformed with 2 μ l of this reaction according to the manufacturers instructions. The transformants were incubated in 1 ml SOC medium without antibiotics for 1 h at 37°C and 100 μ l of a 1:10 dilution of this culture was plated on LB agar plates containing Amp and Cam.

The size of the library was estimated by the number of streaked colonies and 20 clones were analysed to shown the efficiency of transprimer insertions into Litmus28-HAM94 by restriction with *Acc65I* and *NsiI*, cleaving HA-M94 and potential insertion from the vector. As this demonstrated adequate results, the complete transformation was plated onto LB agar plates (diameter 15 cm) in volume corresponding to the plate size and the colony number on the trial streak. The colonies were then scraped in LB media and collected by centrifugation (6000 g, 15 min, 4°C). The DNA of this pool was isolated by using the NucleoBond[™] PC100 Kit from Macherey-Nagel. The protocol was slightly modified and as follows.

The bacterial pellet was resuspended in 8 ml buffer S1 on ice and 8 ml of buffer S2 were added. The solution was inverted 5 times and then incubated on ice for 5 min. Subsequently 8 ml of buffer S3 were added, the solution inverted 15 times, and again incubated on ice for 5 min. The supernatant was cleared by centrifugation (17,000 g, 30 min, 4°C), before transferred via filter paper onto the column, which was pre-equilibrated with 2.5 ml of buffer N2. The column flow through was harvested and transferred onto the column

again. The column was then washed 3 times with 5 ml buffer N3. The DNA was eluted by addition of twice 2.5 ml of 50°C heated buffer N5. The solution was covered with 3.5 ml isopropanol and mixed right before centrifugation (27,000 g, 30 min, 4°C). The supernatant was discarded immediately and 5 ml of ice-cold 70 % ethanol were added and centrifuged (27,000 g, 10 min 4°C). Again the supernatant was discarded immediately and the pellet was air dried. The DNA was then resuspended in 50 μ l T-buffer overnight at 4°C.

The isolated DNA was digested by *Acc65I* and *NsiI*. Thereby HA-M94 encoding fragments were cleaved out from the vector. The HA-M94 fragments containing a transprimer insertion could be selectively isolated due to their increased size after agarose gel electrophoresis and were purified as described (section 2.2.3.7).

The expression vector pOriR6K-ie was digested with *Acc65I* and *NsiI* and dephosphorylated. The transprimer marked HA-M94 encoding fragments, which were isolated from the library, were ligated to this vector. In this ligation the vector was added in threefold higher molar concentration compared to the library derived fragments. This increased the chance for each individual fragment for ligation with a vector molecule. Since both fragments contained an antibiotic resistance, remaining vector fragments could be removed after transformation by double selection.

$\frac{1}{10}$ of this ligation was electroporated into highly competent PIR1 bacteria and 100 μ l of a 1:10 dilution were plated on LB agar plates containing Cam and Zeo. By this trial plate out, the library size was estimated and 20 clones were analysed. If this was positive, the entire transformation was plated completely, the colonies were collected, and library DNA isolated as described previously.

This pool of plasmids was digested with *PmeI* to remove the transprimer. The remaining vector fragment was separated from the transprimer by agarose gel electrophoresis and isolated and purified as described earlier. The isolated vector fragment was then religated by standard ligation protocol. Again PIR1 were electroporated with a fraction of $\frac{1}{10}$ of the ligation and 100 μ l of a 1:10 dilution were plated on LB agar plates containing Zeo. The final size of the library was estimated. Single clones were picked and removal of the transprimer was analysed by identification of loss of chloramphenicol resistance. The po-

sition of the transposon insertion in HA-M94 derived from restriction analysis and finally the mutant open reading frame (ORF) was sequenced.

2.2.5 Mutagenesis of BACs

The cloning of the MCMV genome as bacterial artificial chromosome [54] increased its accessibility for mutagenesis strategies. However, here classical cloning methods are not applicable due to high frequency of restriction sites and the large size of the construct. Our laboratory adapted homologous recombination by ET cloning for mutagenesis of BACs [92]. In this process a linear DNA fragment, produced by PCR, is inserted into bacteria containing the BAC and a plasmid pKD46 [22] expressing the recombinases α , β , and γ from λ phage. By double crossing-over with flanking homologies between the PCR fragment and the target BAC the mutation is introduced into the MCMV BAC as illustrated in figure 2.1.

In this study, in order to verify the phenotype of a gene deletion, a rescue by reinsertion of the deleted gene is applied. Therefore the MCMV BAC utilised in this study contained a Flp recombinase target (FRT) site. The Flp recombinase from the 2 μ m plasmid of yeast recognises the FRT sites and mediates a specific recombination between two of these. Consequently a plasmid containing the gene of interest and a FRT site is introduced ectopically into the BAC at the position of its FRT site.

2.2.5.1 Generation of recombinant BACs

The PCR for generation of the linear DNA fragment was already specified in section 2.2.3.1 and performed using pGPS1.1 as template. After analysis of the PCR product by agarose gel electrophoresis, the DNA was purified by buffer change (section 2.2.3.2) and subsequently digested with *DpnI* to disintegrate the template DNA. The PCR product was then precipitated (section 2.2.2.5).

Bacteria containing the BAC for mutagenesis were prepared as chemical competent (section 2.2.1.1) and transformed with 10 ng pKD46 (section 2.2.1.2). These bacteria were

then utilised for preparation of electrocompetent bacteria (section 2.2.1.3) in presence of 0.1 % (w/v) L-Arabinose at 30°C and transformed with 0.5-1.5 μg of the precipitated linear fragment at 37°C. The resulting clones contained the mutated BACs and lost pKD46 due to its temperature sensitive origin of replication preventing a replication at 37°C and selection for both antibiotics. They were analysed by restriction digest.

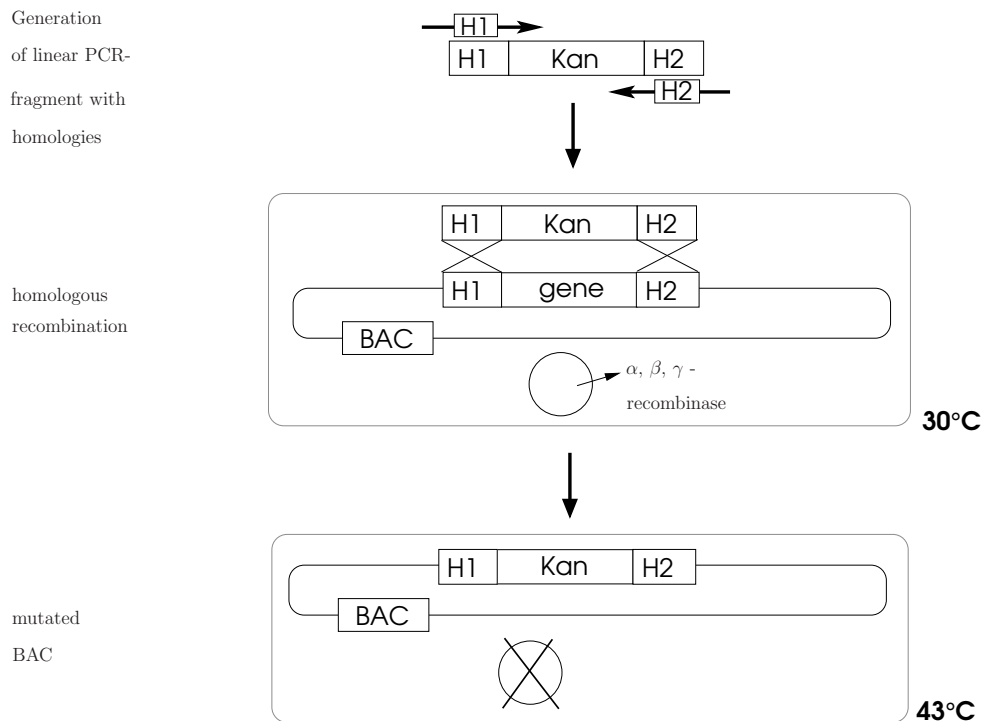


Figure 2.1: For the generation of recombinant BACs the linear DNA fragment containing the homologies (H1 and H2) is generated by PCR. The fragment is transformed into bacteria containing the BAC and pKD46, the plasmid expressing the recombinases, which is subsequently lost due to its temperature sensitive origin of replication.

2.2.5.2 Insertion of genes by Flp recombinase

The plasmid pCP20 was inserted into bacteria containing the BAC with the target FRT site for insertion by chemical transformation. The resulting bacteria were then prepared to be electrocompetent and transformed with 10-50 ng of a pOriR6K construct containing a FRT site and the gene of interest at 30°C. The culture was selectively plated on LB agar plates containing Cam and Zeo and incubated at 43°C overnight to remove pCP20 containing a temperature sensitive origin of replication. The resulting constructs were

analysed by restriction digest for insertion of the pOriR6K construct. Occuring multiple insertions of the vector, called double insertions, were also separated by this restriction analysis.

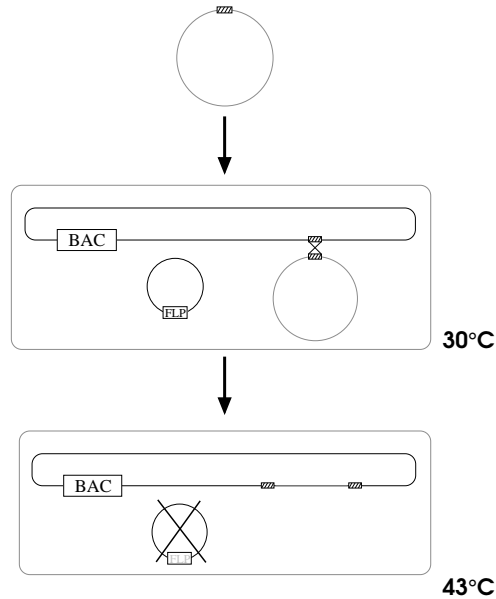


Figure 2.2: For the insertion of genes by Flp recombinase, the pOriR6K construct including an FRT site is transformed into bacteria containing the BAC and pCP20 expressing the Flp recombinase, which is subsequently lost due to its temperature sensitive origin of replication.

2.2.6 Cell culture

2.2.6.1 Cultivation of mammalian cells

All cells were cultivated at 37°C in presence of 5 % CO₂ and 95 % humidity. Cells were splitted in ration and frequency according to table 2.7. In order to subculture cells, they were washed with DPBS and detached from the cell culture dish by trypsin-EDTA treatment. Detached cells were resuspended in appropriated media and distributed on fresh cell culture dishes.

2.2.6.2 Freezing of cells

For storage of cells they were frozen in media containing DMSO and stored in liquid nitrogen. Confluent cells were detached by trypsin-EDTA treatment and collected by

Table 2.7: Standard media for cell culture

Cell line	Basic medium	Additives	Split/interval
293	DMEM	10 % FBS, P/S, Q	1:5/2-3 days
M2-10B4	RPMI	10 % FBS, P/S	1:6/2-3 days
MEF	DMEM	10 % FBS, P/S	1:4/3-4 days
NIH3T3	DMEM	5 % NCS, P/S	1:6/2-3 days
NTM94	DMEM	5 % NCS, P/S, 50 μ g/ml hygromycin	1:6/2 days

centrifugation (310 g, 5 min, RT). The cell pellet was resuspended in freezing media and aliquoted by 1 ml in 1.8 ml freezing vials. These were transferred in boxes containing isopropanol into -80°C for 24 h and subsequently transferred into liquid nitrogen.

Freezing media

10 % DMSO

25 % FBS

65 % basic medium (Tab. 2.7)

2.2.6.3 Thawing of cells

Cells were thawed at 37°C in water bath and immediately transferred into their standard medium. To remove DMSO, cells were collected by centrifugation (310 g, 5 min, RT) and resuspended in fresh medium, before applied on cell culture dish.

2.2.6.4 Determination of cell numbers

Numbers of detached viable cells were determined by measurement with CASY[®] cell counter from Schärfe System. The cell suspension was diluted 1:100 in CASY[®]-Ton and analysed according to manufacturers instructions.

2.2.6.5 Transfection of cells using Superfect

Confluent 10 cm dish of MEF cells was splitted onto 6 of 6 cm dishes 1 day prior transfection with SuperFect[®] Transfection Reagent from Qiagen. About 1.5 μ g of BAC DNA was transferred in reaction tubes and filled by basic medium to 150 μ l final volume. 10 μ l

of ice-cold SuperFect[®] Transfection Reagent was added and the reaction incubated for 10-15 min after mixing. Then 1 ml standard medium was added to the DNA/SuperFect[®] mixture and this solution was transferred onto cells. After 3 h the solution was exchanged to medium.

2.2.6.6 Transfection of cells using CaPO₄ precipitation

Confluent 10 cm dish of 293 cells was splitted onto 4 of 6 cm dishes 1 day prior the transfection. All solutions were sterile filtered and stored on ice. To 7 µg of DNA, 250 µl of 250 mM calcium chloride were added. While mixing the solution, 250 µl of HEBS buffer were added slowly. The reaction was incubated for 15 min and then transferred onto cells. These were harvested after 24 h.

HEBS buffer

16 g/l NaCl

0.72 g/l KCl

0.25 g/l Na₂HPO₄·2H₂O

10 g/l HEPES

2 g/l glucose

adjust pH 7.5 by NaOH

2.2.6.7 Application of additional cell culture reagents

Dox was prepared as 10 mg/ml stock solution in DPBS and stored at -80°C. PAA was prepared as 300 mg/ml stock solution in water and stored at -20°C. Both reagents were added 1 hpi to the cells. Dox was applied in 1 µg/ml final concentration, whereas PAA was used in 300 µg/ml final concentration.

2.2.7 Virological methods

2.2.7.1 Virus reconstitution from BAC DNA

MEF cells were transfected with BAC DNA using SuperFect[®] Transfection Reagent (section 2.2.6.5). After 24 h cells were splitted 1:3 on 10 cm cell culture dishes.

For production of viral inoculum, cells were subcultured again once they showed plaque formation.

In case of analytical virus reconstitution, cell were not subcultured after plaque formation, but time points of first plaque formation and lysis were observed. If plaque formation was absent, cells were splitted 1:2 every second week for 6 weeks. Cultures without plaque formation after 6 weeks were dismissed.

2.2.7.2 Infection of cells with MCMV

Cells numbers were determined (section 2.2.6.4) and appropriate cell numbers were provided in 15 ml tubes. Viral inoculum was added corresponding to the intended multiplicity of infection (MOI) together with Dox if necessary. The infected cells were then distributed on cell culture dishes.

2.2.7.3 Preparation of MCMV stock

M2-10B4 cells from three 15 cm cell culture dishes were harvested, infected with 10 ml viral inoculum and distributed on 20 of 15 cm cell culture dishes. Upon 2 days after 100 % cytopathic effect cells were scraped from plates in their own media and collected by centrifugation (5,500 g, 15 min, 4°C). The supernatant was collected and stored on ice, whereas the pellet was resuspended in media and homogenised by douncer. Thereby cell associated virus was released and remaining cells were removed by centrifugation (17,000 g, 10 min, 4°C). This supernatant was combined with the supernatant from the previous centrifugation and viral particels were collected by centrifugation (20,000 g, 3 h, 4°C). The pellet was resuspended in 4 ml own media and transferred onto a 15 % sucrose cushion. The virus particles were purified by pelleting them through a sucrose cushion (20000 rpm, 90 min, 4°C, SW 32 Ti) and the pellet resuspended in virus stock buffer overnight at 4°C. After solubilising the pellet, aliquots were stored at -80°C.

<u>Virus stock buffer</u>	<u>Virus stock buffer with 15 % sucrose</u>
50 mM Tris/HCl	75 g D(+) saccharose
12 mM KCl	add 500 ml virus stock buffer
5 mM EDTA	
adjust pH 7.8 by HCl	

2.2.7.4 Determination of MCMV titre by standard plaque assay

The viral titre was determined by applying of a dilution series onto MEF cells and counting of plaques 4 days pi. Therefore MEF cells were distributed on 48 well plates 24 h ahead the assay. The virus samples were serially diluted (10^{-1} to 10^{-6}) in DMEM on 48 well plates and 200 μ l of each dilution were transferred onto the plates with MEFs. After 1 h incubation the media were removed and 500 μ l of methylcellulose-media were added to each well. Numbers of plaques were determined at 4 days pi and viral titre calculated from plaques quantity and dilution factor [71].

$$\text{Virus titre (PFU/ml)} = \text{counted plaques} \cdot \frac{\text{dilution factor}}{\text{volume of virus dilution}}$$

Methylcellulose-media
 3.75 g Carboxymethyl-cellulose (400-800 cps)
 388 ml H₂O, autoclaved
 25 ml FBS
 50 ml 10x MEM
 5 ml Q
 2.5 ml NEAA
 5 ml P/S
 24.7 ml NaHCO₃

2.2.7.5 Determination of MCMV titre by TCID₅₀

As the viral growth of MCMV Δ M94tTA was dependent on the complementing cell line NTM94 and this cell line did not exhibit contact inhibition, the determination of viral titre by plaque quantification was not applicable. Therefore viral titres were defined by tissue culture infective dose 50 (TCID₅₀) [35]. NTM94 cell were splitted 1:12 onto a 96 well plate by 100 μ l each well. After 4 h of cell growth, the virus was diluted 1:100 and

serial diluted in media on 96 well plates in 1:10 dilution steps. From this plates 100 μ l of each well were transferred to the corresponding wells of the plate with. In doing so the residual medium of the cells was not removed and the cells were incubated for 4 days and stained with crystal violet. Plaques positive wells were counted and viral titre calculated according to Reed and Munch method [72].

10x Crystal violet
10 % formaldehyde in DPBS
1 % (w/v) crystal violet

2.2.7.6 Growth kinetics of MCMV

Each virus was analysed in duplicates and if necessary in absence and presence of Dox in viral growth analysis. MEF cells were splitted 1:5 on 2 of 12 well plates and the cell number of three wells was determined after 24 h. Cells were infected with MOI of 0.1 by addition of diluted virus stock in 1 ml final volume of standard media in absence of Dox. After incubation for 1 h, the supernatants of 4 wells, 2 for each duplicate were harvested and all wells were washed 3 times with DPBS, before addition of fresh medium to one plate and fresh medium including Dox to the second plate. Supernatants were harvested every day up to 5 days pi. They were stored at -80°C and the number of released infectious particles for each time point were determined by standard plaques assay.

2.2.8 Packaging assay

The packaging assay was based on the different genome forms occurring during the MCMV replication (section 3.12), primarily concatemers and cleaved genomes. These forms were distinguished by different fragments recognised by a probe in a Southern blot analysis.

The generation of the probe for the Southern blot analysis was described in section 2.2.3.1.

The DNA was isolated from infected cells (section 2.2.2.6) harvested 48 hpi.

2.2.8.1 Southern blot analysis

The probe was generated by PCR using the primers Apa2-for and Apa2-rev (section 2.1.8) on pSM3fr-FRT as template. The PCR product was purified by GFX PCR DNA and Gel Band Purification Kit (section 2.2.3.2). M210B4 cells were infected with MOI 0.1 to 0.5 and total cellular DNA was isolated 48 hpi. From these 1 μ g DNA of infected cells was digested by 40 units of *Apa*LI in a final volume of 40 μ l overnight at 37°C. The DNA was then applied to agarose gel electrophoresis at 80 V for 24 h. The gel size was reduced to minimal size for detection of required bands and size marker was documented by photography of the gel next to a ruler. To mobilise the DNA in the gel, it was incubated in 250 mM HCl twice for 10 min and subsequently for 45 min in denaturation buffer. Afterwards the gel was incubated for 30 min, followed by additional 10 min, in neutralisation buffer.

The DNA was then transferred by capillary force to a membrane (Amersham HybondTM-N⁺, GE Healthcare). For this, blotting paper (Macherey-Nagel) in gel width was placed in an agarose gel electrophoresis chamber with both ends dunked in 20x SSC buffer. The gel was placed onto the paper and the membrane in gel size on top of the gel. The capillary force was established by 2 gel size blotting papers soaked in 20x SSC and 2 additional dry ones, followed by a tower of tissue papers. This was fixed by weight and balanced. Blotting was performed overnight.

The papers were removed the next day and the DNA on the membrane was cross-linked by 0.125 Joule UV-light. The gel was investigated for remaining DNA by UV illumination. The membrane was then transferred into 20 ml hybridisation buffer (DIG Easy Hyb Granules from Roche) and incubated at 60°C for 4-5 h in a hybridisation oven. The probe was boiled for 10 min at 95°C to separate double strand DNA, before added to the hybridisation buffer. The incubation was continued at 60°C overnight.

The next day the membrane was washed twice for 5 min with washing buffer I at RT and twice for 15 min with washing buffer II at 60°C. DIG labeled probes were detected using the DIG Luminescent Detection Kit from Roche according to manufacturers instructions and exposure to chemiluminescence film.

<u>Denaturation buffer</u>	<u>Neutralisation buffer</u>	<u>20x SSC</u>
1.5 M NaCl	1 M Tris	3 M NaCl
0.5 M NaOH	1.5 M NaCl	0.3 M sodium citrate
	pH 7.4	
<u>Washing buffer I</u>	<u>Washing buffer II</u>	
2 % SSC	0.5 % SSC	
1 % SDS	1 % SDS	

2.2.8.2 Quantification of Southern blot analysis

For quantification of Southern blots, the signal was illuminated by fresh CSPD from the DIG Luminescent Detection Kit and chemiluminescence signal was quantitatively detected using a typhoon scanner. The resulting image was evaluated by Image Quant software and the values compared to each other.

2.2.9 Protein analysis

2.2.9.1 Protein extraction from eukaryotic cells

NIH3T3 cells were infected with MOI 0.1 to 0.5 and additives (Dox, PAA) were added 1 hpi if needed. Cells were harvested 24 hpi by scraping cells in DPBS on ice and collecting by centrifugation (6,800 g, 3 min, 4°C). The pellet was washed by resuspending in 1 ml DPBS and centrifugation (6,800 g, 3 min, 4°C). Cell pellets from 6 cm cell culture dish were resuspended in 150 μ l total lysis buffer and cell pellets from 10 cm dishes in 250 μ l total lysis buffer. 1 μ l benzonase for each 50 μ l total lysis buffer was added and incubated on ice for 90 min, before snap frozen in liquid nitrogen and transferred to -80°C storage.

Total lysis buffer
 62.5 mM Tris/HCl pH 6.8
 2 % (v/v) SDS
 10 % (v/v) glycerol
 6 M urea
 5 % (v/v) β -mercaptoethanol
 0.01 % (w/v) bromphenolblue
 0.01 % (w/v) phenolred

2.2.9.2 SDS-PAGE

SDS-PAGE were prepared according to following table. Samples were incubated at 95°C

	Stacking gel (4 %)	Resolving gel (12 %)
Rotiphorese® Gel 30	4 ml	2.5 ml
Gel buffer	2.5 ml	3.75 ml
H ₂ O	3.4 ml	9.75 ml
10 % APS	100 μ l	100 μ l
TEMED	3.3 μ l	20 μ l

for 10 min prior to loading on the gel. Proteins were separated by 160 V for 1-2 h in Laemmli buffer.

<u>Stacking gel buffer</u>	<u>Resolving gel buffer</u>	<u>10x Laemmli</u>
0.5 M Tris	1.5 M Tris	250 mM Tris
0.4 % (w/v) SDS	0.4 % (w/v) SDS	2 M glycine
pH 6.8	pH 8.8	1 % (w/v) SDS

2.2.9.3 Western Blot analysis

For western blot analysis the proteins separated by SDS-PAGE were transferred onto a PVDF membrane (Amersham Hybond™-P, GE Healthcare) by semi dry blotting using Trans-Blot™ SD Semi-Dry Electrophoretic Transfer cell from Bio-Rad according to manufacturers instructions.

The membrane was blocked with 5 % (w/v) skimmed milk powder in TBST overnight at 4°C. Subsequently the membrane was washed 3 times with water and twice with TBST, before incubated with the first antibody in 5 ml TBST for 2 h at 4°C. The membrane was then washed with TBST for 10 min to 2 h depending on the first antibody. Incubation with the second antibody was performed in 5 ml TBST for 1 h at RT and membrane was washed with TBST again for 10 min to 2 h.

Signals were detected by using ECL Plus (GE Healthcare) according to the manual and exposure to chemiluminescence films.

First antibody (dilution)	Second antibody (dilution)	Washing time
α -pp89 (1:3000)	α -mouse (1:8000)	2 h
α -M50 (1:3000)	α -rabbit (1:8000)	30 min
α -M94 (1:2500)	α -rabbit (1:8000)	2 h
α -HA-Pox (1:1500)	—	10 min

Blotting buffer

24 mM Tris
192 mM glycine
20 % (v/v) methanol

TBST

150 mM NaCl
10 mM Tris/HCl pH 8.0
0.05 % Tween20

Chapter 3

Results

3.1 M94 is essential in MCMV

UL94, the homologue of M94 in HCMV was proven to be essential [25]. This indicated that M94 will also be essential for virus growth in cell culture. This property was also crucial in this study. Here, the analysis of mutants in the viral context was based on their capacity to rescue viral productivity. Only mutations affecting an essential gene and hence affecting the MCMV life cycle could be detected. Therefore the essentiality of M94 was inspected.

Figure 3.1 shows for verification of the essentiality the growth analysis of wt MCMV-FRT, an M94 deletion mutant, and two M94 ectopic revertants. A schematic representation of the mutant genomes is included. The rescue strategy was based on *cis*-complementation. In this case the phenotype of no viral growth of the deletion mutant which requires *trans*-complementation of the protein is compensated by introduction of the deleted gene in *cis*, so on the identical DNA, but at a different position in the genome to exclude polar effects. The deleted gene is complemented by the expression of the ectopically inserted gene. By restoration of the wt phenotype the gene is identified as exclusive factor for the deletion phenotype.

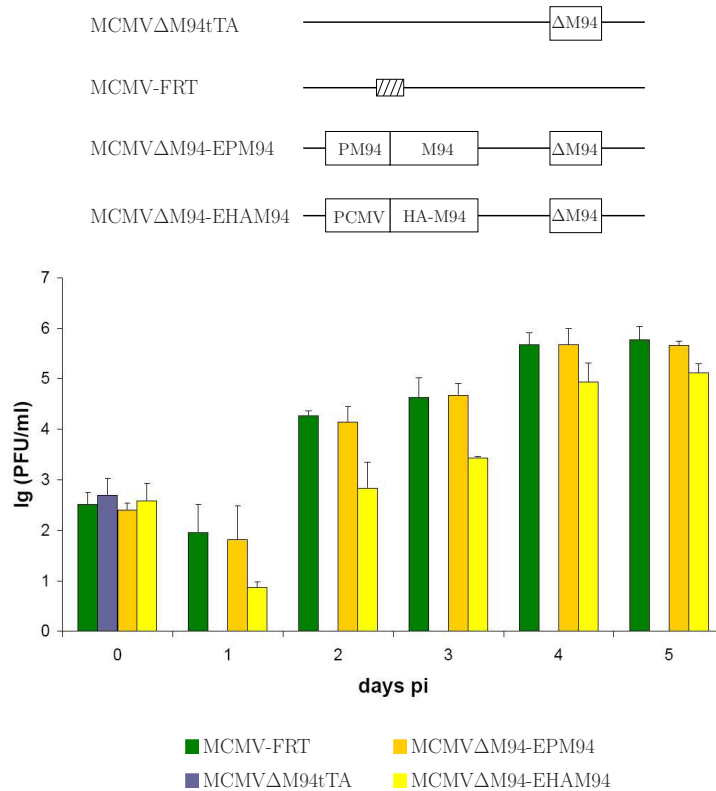


Figure 3.1: Schematic representation of the mutant genomes and their growth kinetics of wt (MCMV-FRT, green), M94 deletion mutant (MCMVΔM94tTA, violet), rescue under control of endogenous M94 promoter (MCMVΔM94-EPM94, gold) and rescue under control of the CMV promoter (MCMVΔM94-EHAM94, yellow), the latter with HA-tagged M94.

Growth analysis on MEF was initiated at MOI of 0.1 with inoculi generated from transfected BACs (section 2.2.7.1) for all viruses and the titre drop on day 1 indicated stringent washing. Wild type virus MCMV-FRT contained the complete MCMV genome and demonstrated standard growth kinetics up to 10^6 PFU/ml at 5 dpi. The deletion virus MCMVΔM94tTA (section 2.1.9) was deleted in M94 replaced by tTA and in m157 replaced by a floxed OVA-cassette and produced on a complementing cell line. After infection with the same MOI no production of any viral progeny was detected. This phenotype was rescued by Flp-FRT mediated ectopic insertion of M94 either under control of endogenous M94 promoter (MCMVΔM94-EPM94) or under control of HCMV immediate early promoter enhancer, further called CMV promoter (MCMVΔM94-EHAM94) into the M94 deleted MCMV genome. Both rescues showed titres comparable to wild type. Hence, the essentiality of M94 was proven for MCMV.

The analysis of MCMV Δ M94-EHAM94 also demonstrated that the M94-ORF itself is sufficient for the rescue of the null phenotype of the deletion and there is no polar effect of the deletion and the expression under control of a different promoter was functional. Finally the analysis showed the fitness of the HA-tagged protein in MCMV Δ M94-EHAM94. The virus titres were comparable to wt, demonstrating that the HA-tag has no influence on viral fitness.

3.2 Transposon mutagenesis

For the analysis of the essential M94 function, the genetic approach of random mutagenesis was chosen. As described in section 1.2.4 the random mutagenesis was achieved by a transposon mutagenesis. In order to explain the individual steps of the mutagenesis and the differences between the modified mutagenesis and the original one, the transposon mutagenesis will now be detailed, followed by a report on the actual experiment.

The GPS[®]-LS Linker scanning system was used for the *in vitro* transposition reaction. To this end the donor vector and the target vector are combined with the transposase enzyme (Fig. 3.2) in a transposition reaction. The applied transposase TnsABC* is a mutated Tn7 bacterial enzyme [88]. The original form consists of 4 subunits and insertion of the transposon either at a specific site or randomly depends on the subunit composition [21]. The mutated form lacks the subunit determining the integration manner and thus the sequence dependency is decreased. Besides, the target immunity of Tn7 prevents a second insertion [89] of a transposon into a Tn7 containing DNA up 100 kbp *in vitro* and 1 Mbp *in vivo* [21].

The transposon utilised in this study, called transprimer, consists of the Tn7-ends with *Pme*I-restriction sites and a chloramphenicol-resistance for selection [6]. Due to its origin of replication, the donor vector pGPS4 containing the transprimer can only be propagated in PIR1 bacteria as these bacteria express the replication protein II, which is required for replication of plasmids containing the R6K γ origin of replication [57]. pGPS4 is therefore

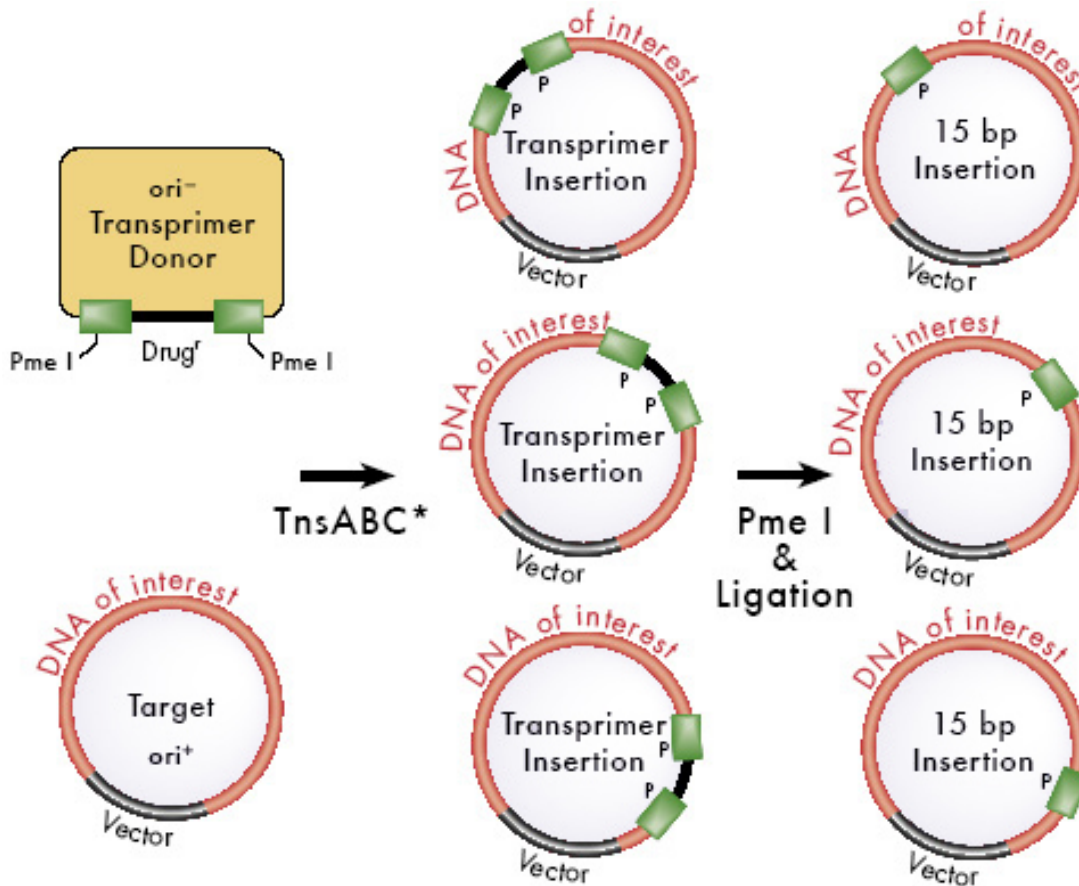


Figure 3.2: Overview of GPS[®]-LS Linker Scanning system [7]. The transprimer of the donor vector is randomly inserted into the target vector by the transposase (*TnsABC*^{*}). The majority of the transprimer is removed by *Pme*I restriction and religation, resulting in a 15 bp insertion including a *Pme*I restriction site.

lost in further reaction steps carried out in DH10B.

The random insertion by the transposase does not facilitate generation of compatible ends in the target vector. After the donor change, the transprimer is therefore connected to the plasmid at overhangs of the DNA backbone and the remaining gaps are filled during plasmid replication *in vivo*. This results in the repetition of 5 bp at both ends of the transprimer (Fig. 3.3), forming part of the mutation.

By excision of the transprimer by *Pme*I digest one *Pme*I restriction site of 8 bp resides along with 2 bp remaining from the transprimer. Subsequent to the religation of the vector, these 10 bp along with the duplicated 5 bp result in the insertion of 15 bp. Depending on

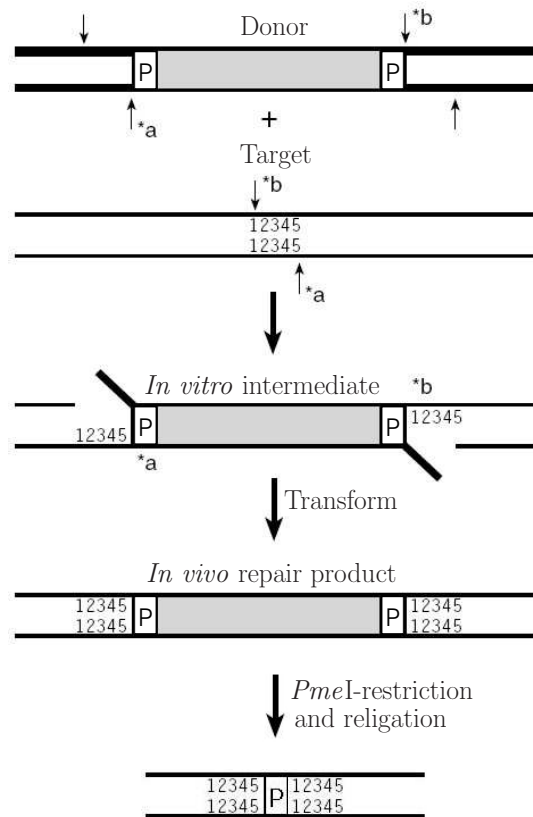


Figure 3.3: Strand transfer reaction in the transposition [7]. The restriction of the donor vector by the transposase enzyme (slight arrows) produces 3' overhangs, whereas the target vector is generated with 5' overhangs. The random insertion produces incompatible ends and therefore the resulting construct is repaired *in vivo*, in this process 5 bp are duplicated. The *PmeI* digest removes the transposon and generates the insertion.

the frame of the insertion this produces in $\frac{2}{3}$ of all mutations an insertion of 5 amino acids (aa) or in $\frac{1}{3}$ of the cases a stop codon (Fig. 3.4).

3.3 Cloning of M94

A target vector in the GPS[®]-LS Linker Scanning system has to meet several requirements. First a *PmeI* restriction site is not allowed in the target construct. Second, the vector must be sensitive to chloramphenicol, and finally the vector must be able to replicate in bacterial strains other than PIR1. Also, the target vector should not contain Tn7 ends to prevent target immunity. The sequence size ratio between the gene of interest and

<u>Top Strand</u>		<u>Bottom Strand</u>	
Frame 1	CCA TGT TTA AAC AGC Pro Cys Leu Asn Ser	Frame 4	GGC TGT TTA AAC ATA Gly Cys Leu Asn Thr
Frame 2	CAT GTT TAA ACA GCC His Val STOP	Frame 5	GCT GTT TAA ACA TGG Ala Val STOP
Frame 3	ATG TTT AAA CAG CCC Met Phe Lys Aln Pro	Frame 6	CTG TTT AAA CAT GGG Leu Phe Lys His Asn

Figure 3.4: Generation of 5 aa insertion. The total insertion of 15 bp is illustrated with the duplicated base pairs shown in black, the *PmeI* restriction site in red, and the one base pair remaining from the transprimer in blue. The insertion can take place into the three frames and in both orientations. This results in 6 options with 2 of them representing stop codons and the other 4 resulting in 5 aa insertions [7].

the vector backbone is relevant as the transprimer insertions occur both into the gene of interest as well as into the backbone. Therefore M94 was subcloned into Litmus28.

The vector pOriR6K-ie-HAM94 (section 2.1.7) was utilised for one rescue in the previous growth analysis (section 3.1). It contains the M94-ORF with an N-terminal HA-tag. Using *KpnI* and *SalI*, HA-M94 was excised from pOriR6K-ie-HAM94 and ligated into Litmus28 opened with *KpnI* and *XhoI*. The resulting vector, Litmus28-HAM94, was analysed by restriction using several enzymes (Fig. 3.5). This vector Litmus28-HAM94 was utilised in the transposon mutagenesis.

3.4 Transposon mutagenesis of M94

In order to separate insertions into M94 from insertions into the vector backbone, the transposon mutagenesis was modified. Figure 3.6 illustrates the modified mutagenesis. The transposition (A) reaction was performed according to the GPS[®]-LS Linker Scanning manual.

The transposition reactions are recorded in table 4.1 and conditions were selected according to the manual [7]. The negative control, control 1, contained no transposase enzyme, whereas control 2 served to spot influences of HA-M94 on the reaction, as it contained Litmus28 vector solely. Subsequently electrocompetent *E. coli* XL1 blue bacteria from

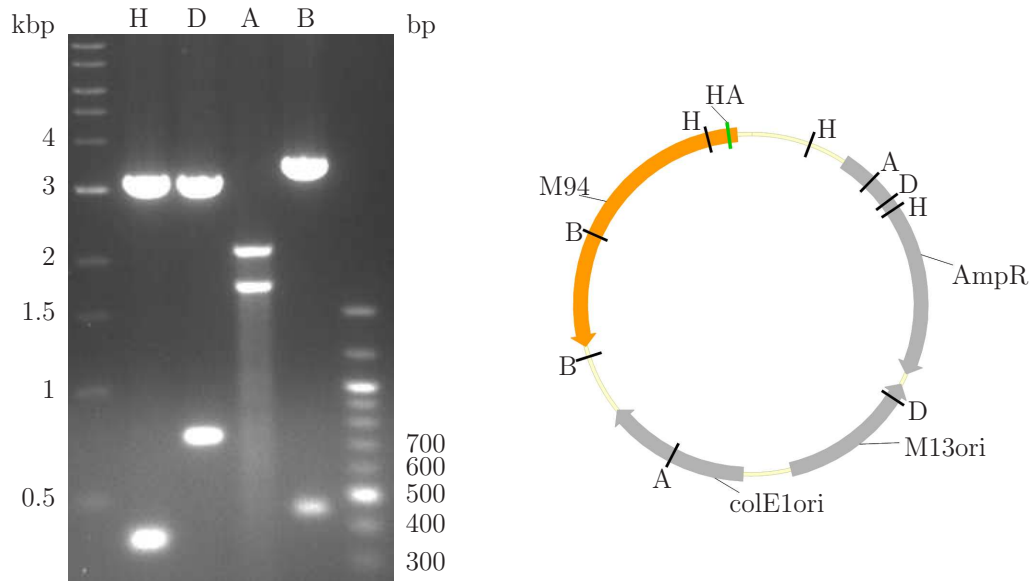


Figure 3.5: Restriction analysis of Litmus28-HAM94 by *HincII* (H), *DraI* (D), *ApaLI* (A), and *BglII* (B) digest. The *HincII* digest resulted in a 3,077 bp fragment and two additional fragments with 385 bp and 363 bp, represented by a thick band. The restriction using *DraI* produced two bands with 3,075 bp and 750 bp. Also the digest by *ApaLI* and *BglII* resulted in two bands respectively. These were 2,088 bp and 1,737 bp for *ApaLI* and 3,370 bp and 446 bp for *BglII* in size.

Table 3.1: The transposition reaction was composed according to the manual with additional controls for reaction efficiency [7].

	control 1	control 2	reaction
Litmus28 (20 ng/ μ L)	4 μ L	4 μ L	–
Litmus28-HAM94 (20 ng/ μ L)	–	–	4 μ L
10xGPS buffer	2 μ L	2 μ L	2 μ L
pGPS4 (20 ng/ μ L)	1 μ L	1 μ L	1 μ L
H ₂ O	12 μ L	11 μ L	11 μ L
Transposase	–	1 μ L	1 μ L

Stratagene were transformed with $\frac{1}{10}$ of controls and reaction. Transformations were plated on ampicillin-chloramphenicol-agar plates. The result showed no colonies for control 1 and comparable colony numbers for control 2 and the reaction.

The size of this library pool (Fig. 3.6B) was calculated as 5.99×10^5 clones from the trial plating. For first analysis, 20 clones out of this pool were analysed for their transprimer insertion (Fig. 3.7).

M94 including the transprimer has a size of 2,488 bp, leaving a 2,723 bp fragment of the vector. These two bands were present in lane 4, 10, 13, 19 and 20. The additional band

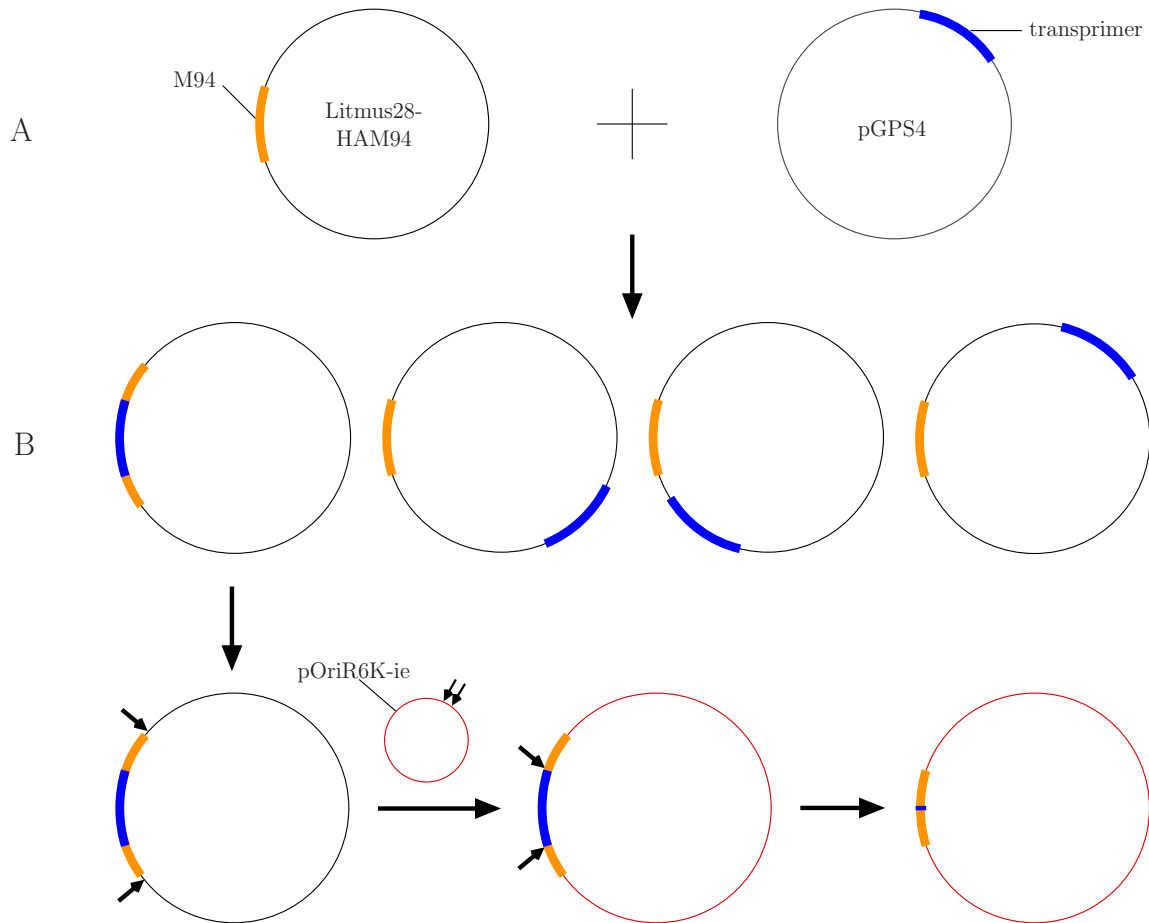


Figure 3.6: Overview of the modified transposon mutagenesis. The transprimer (blue) was excised from the donor vector pGPS4 and randomly inserted into the target vector Litmus28-HAM94, containing HA-tagged M94 (orange). Out of the mutant pool with random transprimer insertions (B), mutants containing insertions in HA-M94 were subcloned into the expression vector pOriR6K-ie. Restriction using *PmeI* and religation of the vector resulted in a 15 bp insertion.

in lane 13 and 19 referred to vector backbone including transposon from a second clone isolated in the same sample. As HA-M94 comprises about a quarter of the total target plasmid sequence, the same proportion of the isolated clones was expected to acquire a transprimer insertion in HA-M94, disregarding non viable mutants containing transprimer insertions in the origin of replication or the ampicillin resistance. With the 5 clones positive for transprimer insertion in M94, this expectation was met, indicating that the mutagenesis was indeed random.

To reject mutations outside the HA-M94 sequence, the M94-ORF containing the transprimer was subcloned into the expression vector pOriR6K-ie. To do so, a portion of the library

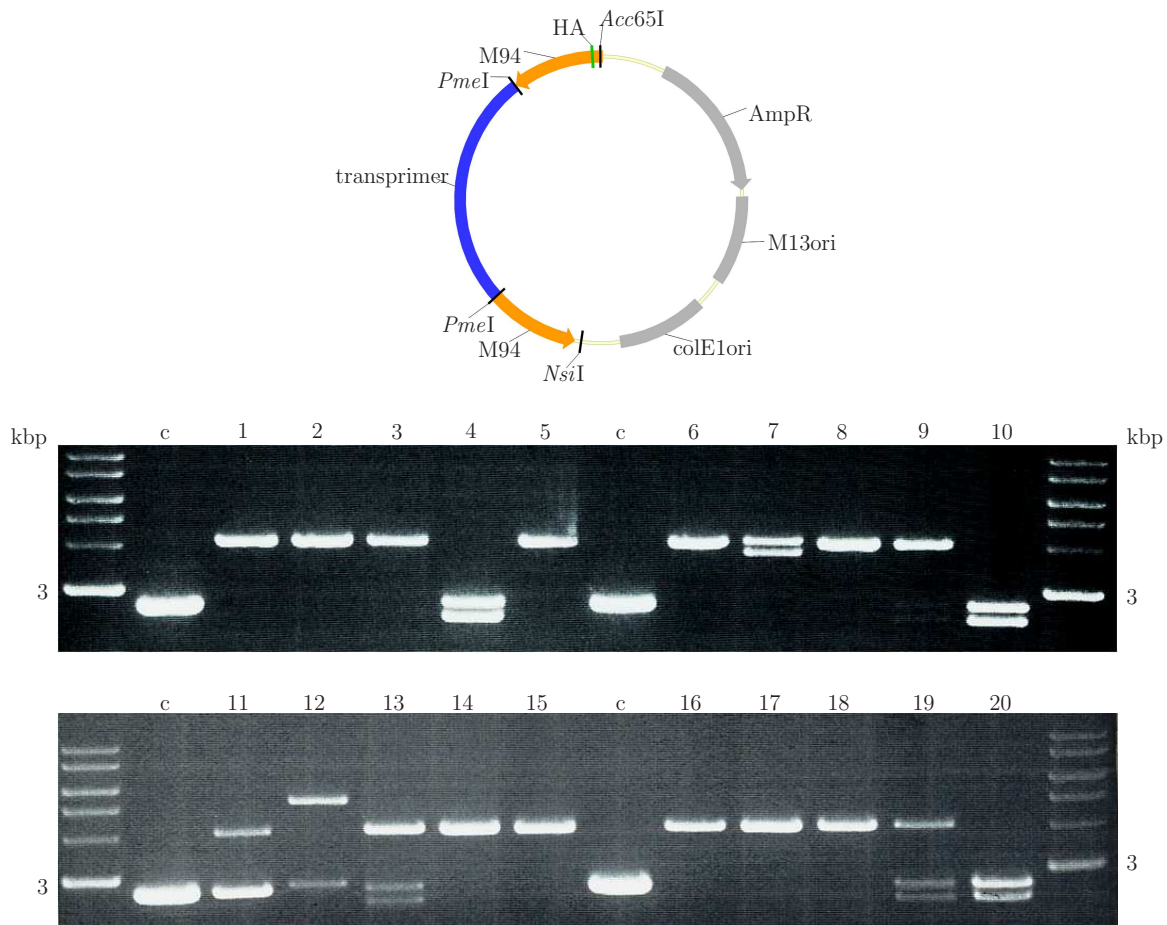


Figure 3.7: Restriction analysis of the transprimer insertions into Litmus28-HAM94. The DNA of 20 mutants was isolated and digested using *Acc65I* and *NsiI*, numbered 1 to 20 in the figure. Litmus28 was also digested as control (c). By this restriction the HA-M94 was excised from the vector, with a size of 1,102 bp, leaving a vector fragment of 4,101 bp. HA-M94 including the transprimer was 2,488 bp in size, leaving a 2,723 bp vector fragment. These desired two bands were present in the mutants no. 4, 10, 13, 19 and 20.

was plated. This portion contained enough clones to statistically allow one mutation per base pair of HA-M94 for at least 150 times (59,900 clones). All colonies were harvested, the DNA of the pool was isolated, and restricted using *Acc65I* and *NsiI*, the same restriction as for the analysis (Fig. 3.7). By this procedure the DNA fragment HA-M94 containing the transprimer was excised from the vector, isolated and subsequently ligated into the *Acc65I/NsiI* opened expression vector pOriR6K-ie. At this stage the library contained 1.2×10^7 clones. As the library size did not decrease compared to the earlier step, the diversity of the library was kept during the subcloning. In order to verify the enrichment of insertions in M94 in the library pool, 20 clones were analysed for their transprimer in-

sertion in HA-M94 (Fig. 3.8).

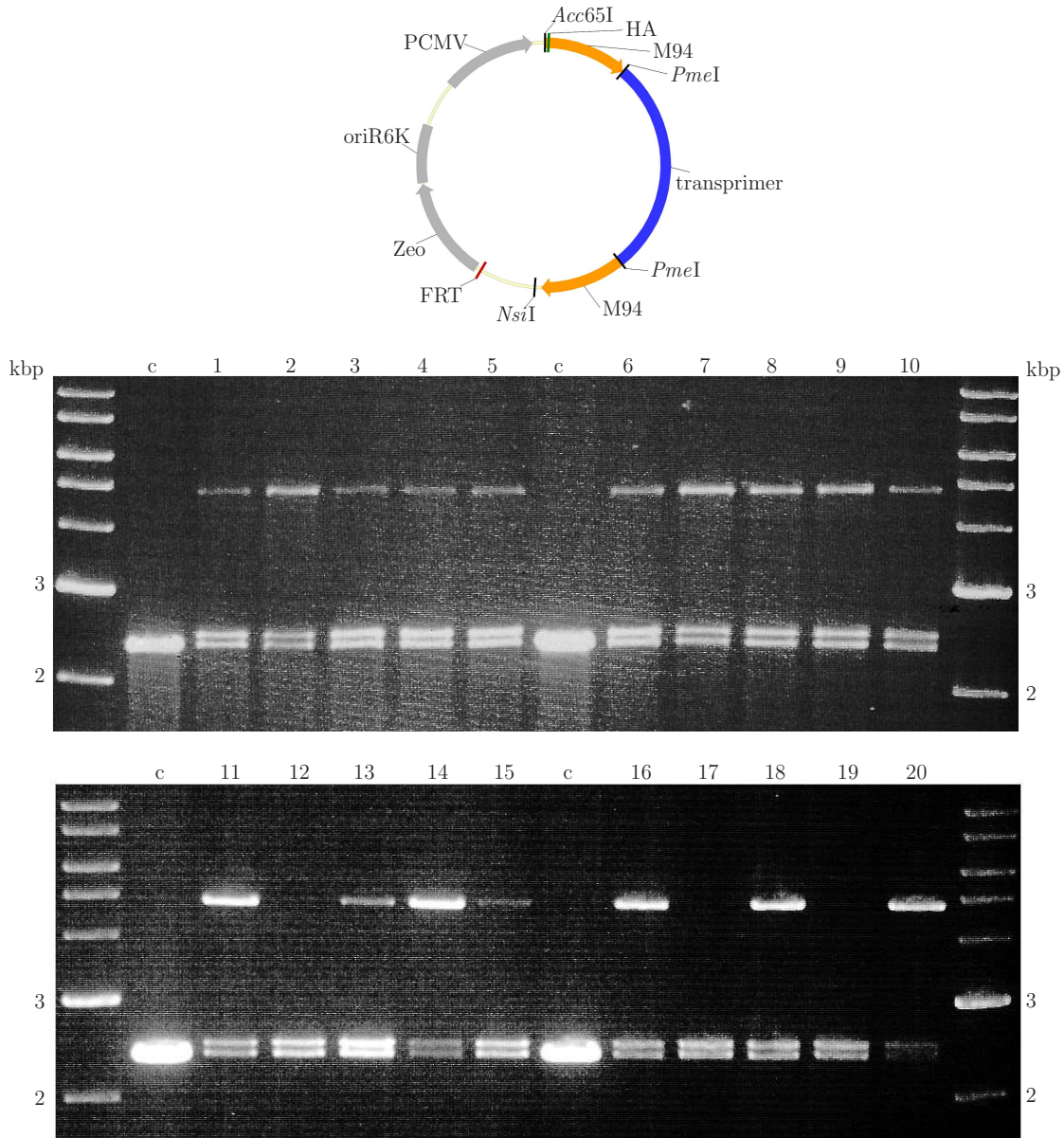


Figure 3.8: Restriction analysis of the transprimer insertions into HA-M94. DNA of 20 mutants, numbered 1 to 20 in the figure, was isolated and digested using *Acc65I* and *NsiI*. The pOriR6K-*ie* vector was digested as control (c), as HA-M94 containing the transprimer was subcloned into this vector. The digest resulted in two fragments of 2,488 bp and 2,390 bp, corresponding to HA-M94 including the transprimer and vector fragment, respectively. Both bands were present in each of the 20 tested mutants.

As in the previous analysis the 2,448 bp band indicated HA-M94 including the transprimer insertion, resulting in a vector fragment of 2,390 bp. Both bands were indeed detected in

each of the 20 analysed clones (Fig. 3.8). This demonstrated the successful elimination of undesirable transprimer insertions in the vector backbone by subcloning of the library pool. Thus the quantity of transprimer insertions in HA-M94 in the library pool increased from 4 out of 20 in the first analysis to 20 out of 20 in the second analysis.

In order to remove the transprimer from the vector, a library portion was plated (1,200,000 clones) as in the previous step and DNA was isolated from collected colonies. The digestion of this DNA pool using *PmeI* enabled the isolation of the remaining vector fragment by extraction from agarose gel and thereby the removal of the transprimer. By religation of the isolated vector, the final mutation of a 15 bp insertion was generated. The final library of M94 mutants contained 3.2×10^4 clones, which statistically corresponded to 25 mutations per base pair of the 1,120 bp of the subcloned fragment without the transprimer. Therefore the library was expected to cover the M94-ORF, given that no hot spots were present.

About 100 of the clones were analysed for their loss of chloramphenicol resistance mediated by the transprimer through parallel growth analysis on LB agar plates containing either chloramphenicol and zeocin or exclusively zeocin. All of them were chloramphenicol sensitive. Additionally 20 mutants were analysed to position the 15 bp insertion (Fig. 3.9). As the insertion maintained a *PmeI* restriction site, the position could be identified by digestion using *PmeI* and *NdeI*, the latter present as unique restriction site in the vector.

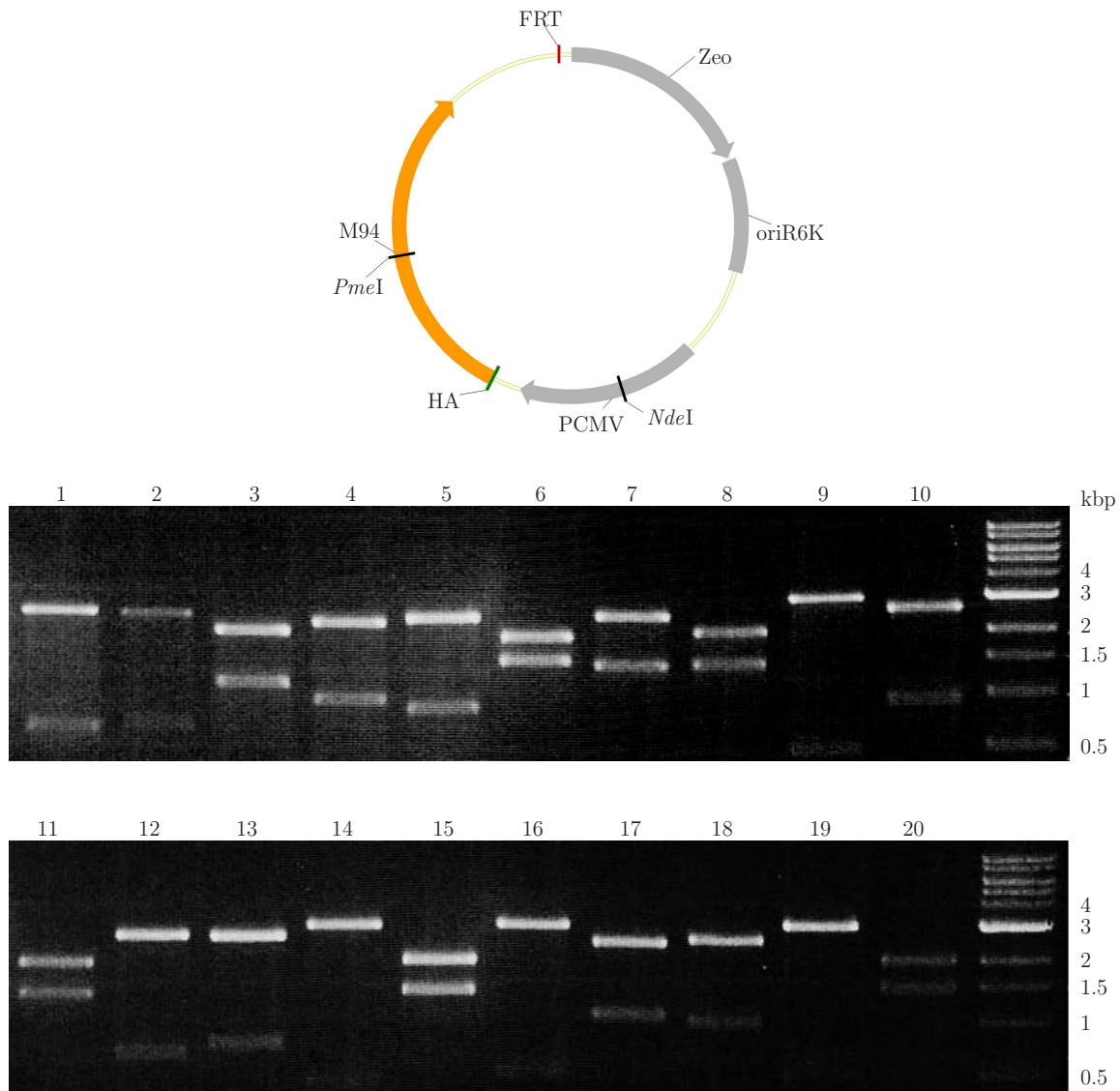


Figure 3.9: Restriction analysis for the position of the mutation in HA-M94. Again the DNA of 20 mutants was isolated, numbered 1 to 20 in the figure. The digest by *NdeI* and *PmeI* revealed the position of the mutation, due to the *PmeI* restriction site in the mutation and the fixed *NdeI* restriction site in the vector. The size of the resulting fragments depended on the *PmeI* restriction site position compared to the *NdeI* restriction site. The fragment sizes were different in most mutants, demonstrating different mutations for each.

The *PmeI*-*NdeI*-digest resulted in two fragments corresponding in size to the position of the mutation. Since the position of the *NdeI* restriction site was defined in the vector and the *PmeI* restriction site was dependent on the location of the 15 bp insertion, the distance to the *NdeI* restriction site varied. Accordingly, most fragments differed in size (Fig. 3.9), reflecting the different positions of the insertions. The screen revealed no preferred insertion

sites for the transprimer in HA-M94 suggesting a library with covering mutations.

Based on the above data, 37 clones were sequenced. The sequences revealed 23 insertion mutants and 11 stop mutants, whereas 3 mutations were outside the M94-ORF. This represented 63 % insertion mutants and 30 % stop mutants, reflecting the ratio 3:1 of insertion mutants to stop mutants as expected by the transposon mutagenesis (Fig. 3.4). The mutants also showed a random distribution over the M94-ORF, with only two stop mutations at the same position. No insertion mutants occurred at the same position, but 3 could be found in a range within 5 aa.

3.5 Analysis of the M94 library

As the library passed the quality control, an expanded analysis was performed to cover the whole M94-ORF. Therefore a larger pool was plated and single colonies were picked. The DNA from these colonies was isolated and sequenced. For sequencing two primers were used to cover the M94-ORF at least on one strand.

In total 613 mutants have been sequenced. From these 494 had a correct mutation in M94, namely one 15 bp insertion in the M94-ORF. About 10 % of the mutations were incorrect due to the transposon mutagenesis as declared by the manufacturer [7]. The remaining 10 % incorrect mutations consisted of 5 % mutations outside of the M94-ORF either in the 85 bp up- and downstream to the ORF that were kept during subcloning or in the HA-tag and further 5 % of the mutants where the sequence revealed a mixed clone. The latter ones could have been singularised and sequenced again, but as the library displayed sufficient coverage, this was not necessary.

From the 494 correct mutants, 399 mutations were unique, implying mutations in the same base pair were counted as one mutation. This clearly demonstrated that the library contained almost no preferred insertion sites for the transprimer, as the unique mutations occurred in 80 % of the correct mutations. Among the mutations which were found more than once, appeared 58 % twice, 22 % three times and 20 % four times or more.

The mutants were named corresponding to the number of the last amino acid before the

insertion, with i for insertion and s for stop mutant. From the identified mutants, 14 stop mutants equally distributed over the M94-ORF were selected to analyse dispensable parts of M94. In addition, 60 insertion mutants distributed equally were selected for the detailed analysis. The preferential distance between the insertions was 5 aa. Since the isolated samples did not reflect the total library, a few insertions were spaced up to 12 aa apart. Figure 3.10 shows the M94-ORF depicted as line and in A the insertions mutants at their positions in M94 are displayed, whereas the stop mutants are illustrated in B.

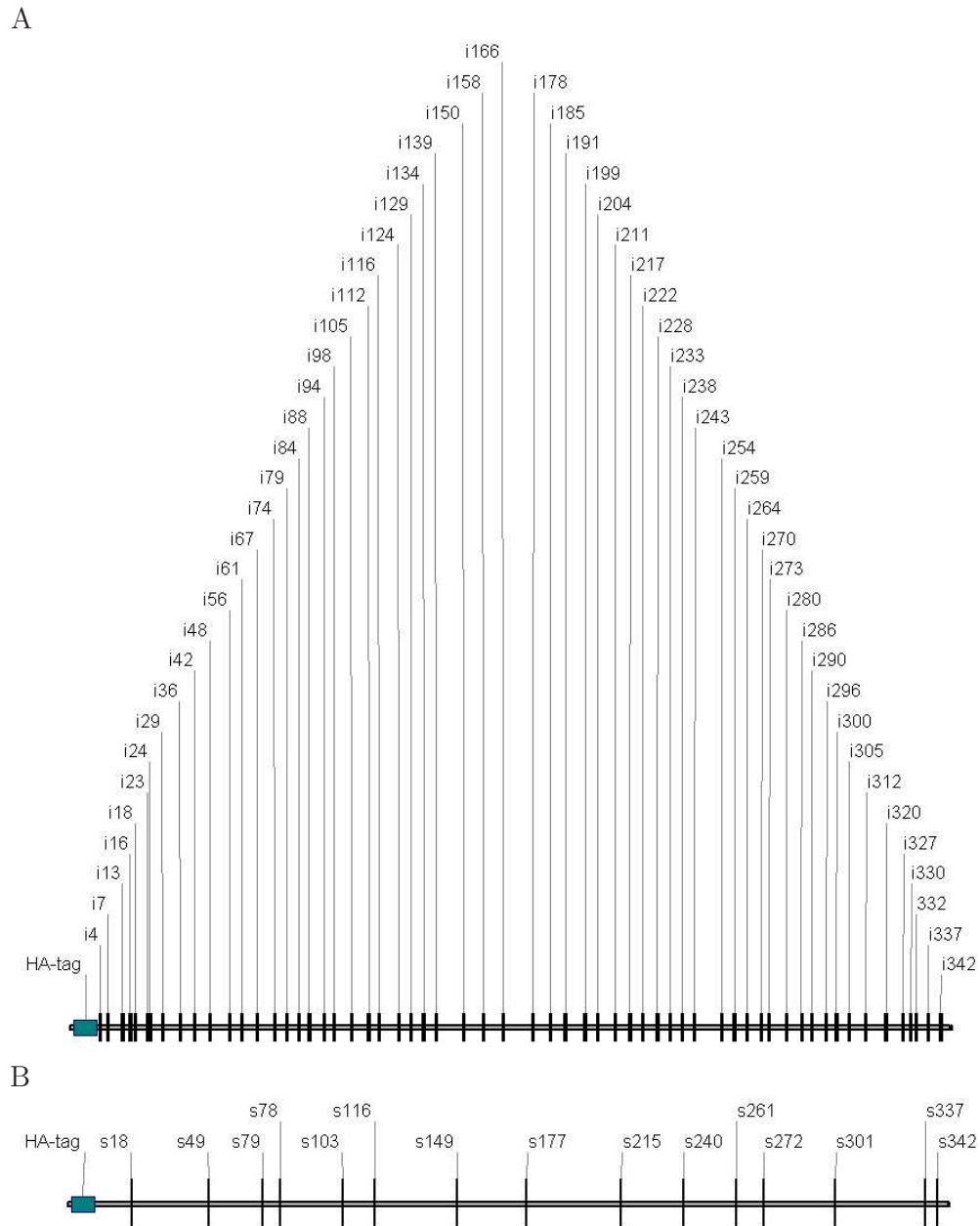


Figure 3.10: Selected insertion mutants (A) and stop mutants (B) on the HA-M94 sequence. The 60 insertion mutants and 14 stop mutants picked for analysis are indicated in the sequence of HA-M94, depicted as line. They are named with i for insertion and s for stop and the number of the aa in front of the mutation.

The influence of the mutation on the function of M94 was investigated in the viral context. So the role of M94 in the MCMV life cycle was analysed and also essential regions in M94 could be defined.

3.6 Analysis of M94 mutants in the viral context

To analyse the mutants in the viral context, mutants were individually inserted into the MCMV genome by means of the Flp-FRT system using BAC technology. The Flp recombinase was expressed from the plasmid pCP20 [15], which contains a temperature sensitive replicon. Therefore, it is unable to replicate at temperature above 37°C. The Flp recombinase recognises the FRT sites and mediates site specific recombination between the MCMV BAC containing a FRT site and the rescue plasmid harbouring the mutant M94 gene also including a FRT site (section 2.2.5.2).

Since the wt ORF successfully complemented the deletion of endogenous M94 after insertion at an ectopic position (Fig. 3.1), the BAC deleted in its endogenous M94 can also be used to test the complementation of M94 function by the mutant upon insertion. On account of this the mutant could or could not accomplish the M94 function resulting in virus rescue. Therefore the analysis was named loss-of-function screen and a scheme of the analysis is presented in figure 3.11. The mutants are individually inserted into the deletion BAC via the Flp-FRT system. The plasmid pCP20 expressing the Flp recombinase was then lost due to the temperature shift from 30°C to 43°C. Subsequently DNA from colonies was isolated and the restriction analysis revealed, whether the mutant was inserted once or repeatedly into the BAC. The latter mutants were rejected from the analysis and only single insertions were proceeded further.

A representative example for restriction analysis is shown in figure 3.12 using *Nsi*I. The successful insertion of plasmids carrying the mutant gene was indicated by the loss of the 1,930 bp band of the control as well as the appearance of an additional band of 4,771 bp in the mutant BACs. Double insertions were identified by a band 3,510 bp in size. Consequently double insertions, in this gel example the lanes 3, 4 and 7, were identified. In total 7 rearranged BACs and 58 double insertions occurred in this analysis of about 342 samples.

As shown in figure 3.11, identified single insertions were then selected and singularised.

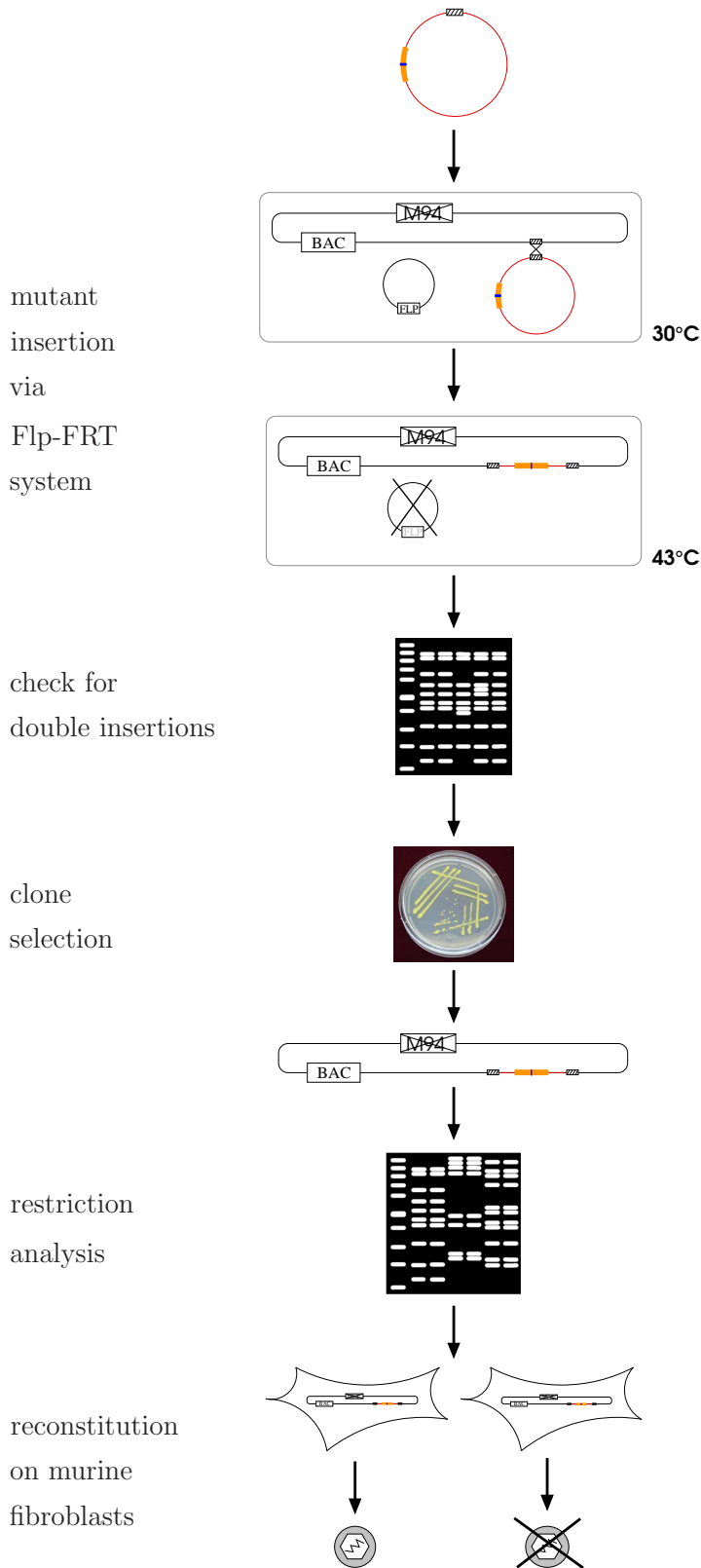


Figure 3.11: Loss-of-function screen. This figure represents a workflow of the analysis of the M94 mutants in the viral context to determine essential regions of the protein. The mutants were individually inserted into the MCMV BAC deleted in M94 via the Flp-FRT system. Constructs were checked for double insertions and clones with single insertions were selected. New DNA was isolated for restriction analysis and virus reconstitution on murine fibroblasts.

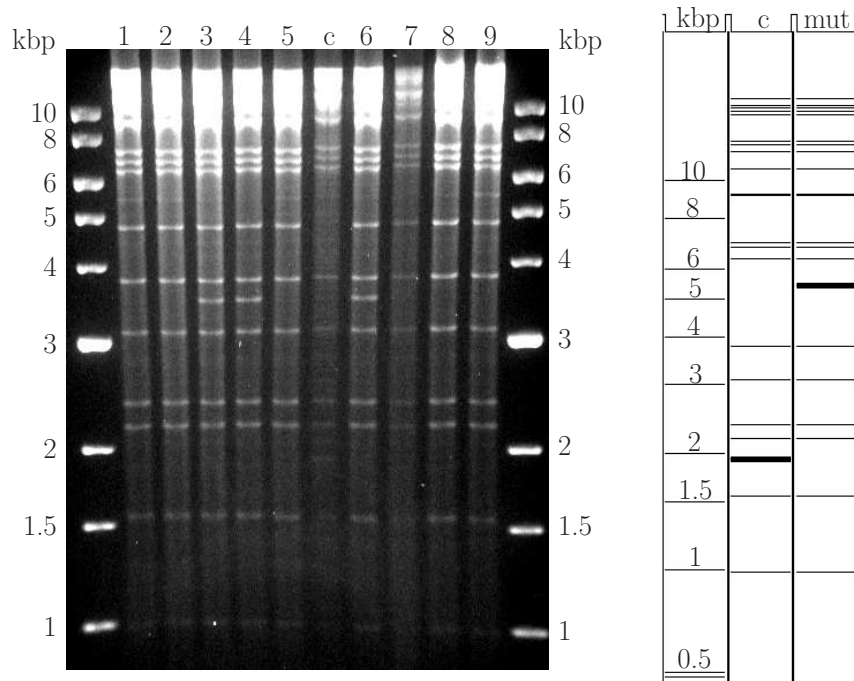


Figure 3.12: Restriction analysis for identification of double insertion. The mutant BACs (no. 1 to 9) were restricted by *NsiI* and the parental BAC with M94 deletion was added as control (c). A schematic representation of the restriction is shown on the right and vanishing and upcoming bands are marked by thick lines. The insertion of the M94 mutants was detected by the loss of the 1,930 bp band in the control and a new band at 4,771 bp in the mutant BACs. Double insertion were identified by an additional band at 3,510 bp.

Fresh DNA was isolated from single colonies and analysed by restriction analysis using 3 different enzymes, to ensure correct BACs with single insertion.

A representative example for this restriction analysis is shown in figure 3.13. The digest shown in A is equal to the digest presented in figure 3.12, with the 1,930 bp band present in the control, but lost in the mutant BAC. The mutant BACs show the additional band of 4,771 bp.

The digest by *HindIII* showed only a faint difference in the restriction pattern of the control and the mutant BAC, which could not be identified in the gel. Nevertheless the restriction was useful in detecting rearrangements in the BAC itself, as seen in BAC mutant no. 10. The *PsiI* digest finally showed two additional bands in the mutant BACs, with a size of 1,035 bp and 6,991 bp. Out of this presented BAC mutants, all were assessed correct, except no. 5 due to the failed *PsiI* digest, which was repeated (data not shown) and no. 10 as unidentified bands were detected in the *HindIII* digest for this the BAC was rejected,

appearing in 15 mutants of about 228 analysed mutants. The correct BACs were used for subsequent analysis.

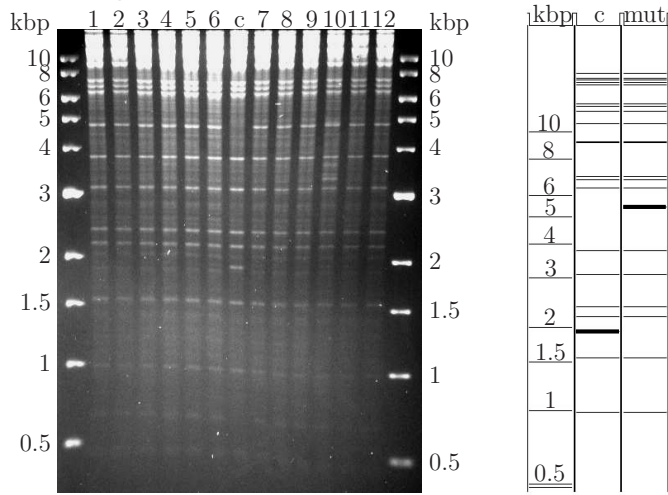
Finally BACs passing the restriction analysis were reconstituted on murine embryonic fibroblasts, along with mock control without DNA, a negative control containing a replication deficient deletion BAC, and a positive control comprising wt DNA. The reconstitution of the mutant BACs resulted in viral progeny, indicated by total cell lysis in a time frame comparable to the wild type lysis. No detectable cell lysis after six weeks was evaluated as no viral reconstitution.

The loss-of-function screen was performed for all mutants with two independent clones to ensure the observed phenotype. Conflicting results, in total 8 in all analysed mutants, were dissolved by isolation and reconstitution of two additional mutants. Viral progeny indicated the successful complementation of the missing endogenous M94 by the mutant, whereas no viral progeny demonstrated the incapability of the mutant protein of fulfilling the native M94 function.

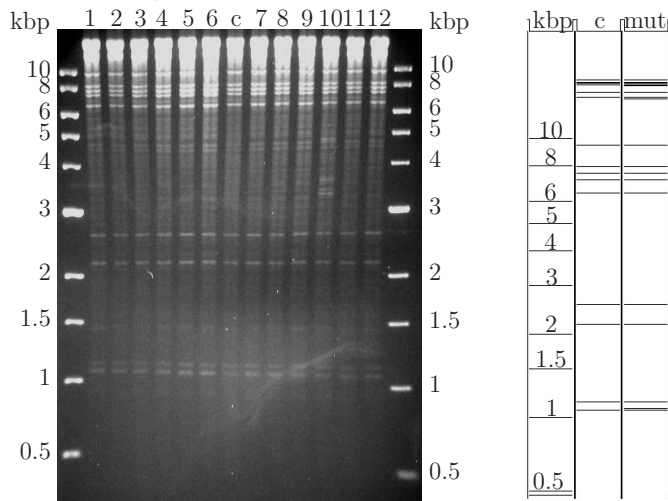
The results of the loss-of-function screen are summarised in figure 3.14. In case the mutant successfully provided the wt M94 function, viral progeny was produced. This indicated that no essential function of the protein was inhibited by the mutation. If the mutant failed to substitute wt M94, there was no viral progeny. This suggested that a sequence region corresponding to an essential function of M94 was targeted by the mutation. Thus, regions in M94 corresponding to essential functions could be successfully defined in this loss-of-function screen.

As 39 of the 60 tested insertion mutants produced viable virus, only 21 insertion mutants failed to support viral progeny. So 65 % of the insertion mutants demonstrated no effect on the M94 function, suggesting a relative insensitivity of M94 to insertions. This is reflected by the bioinformatic analysis of M94 indicating a predicted α -helix in the conserved C-terminus and only a few other small secondary structures. Apparently secondary structures were infrequently not destroyed by insertion mutations and also a potential linker sequence

A: *Nsi*I-digest



B: *Hind*III-digest



C: *Psi*I-digest

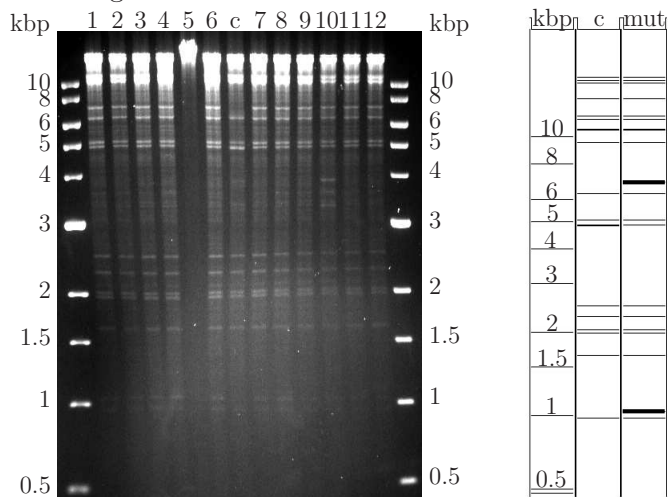


Figure 3.13: Restriction analysis of the BAC mutants in the loss-of-function screen. The mutant BACs, in the gels numbered 1 to 12 and in the scheme labelled as mut were restricted using *Nsi*I, *Hind*III, and *Psi*I with the M94 deletion BAC as control (c). The schematic gels indicate the differences in restriction patterns by thicker lines.

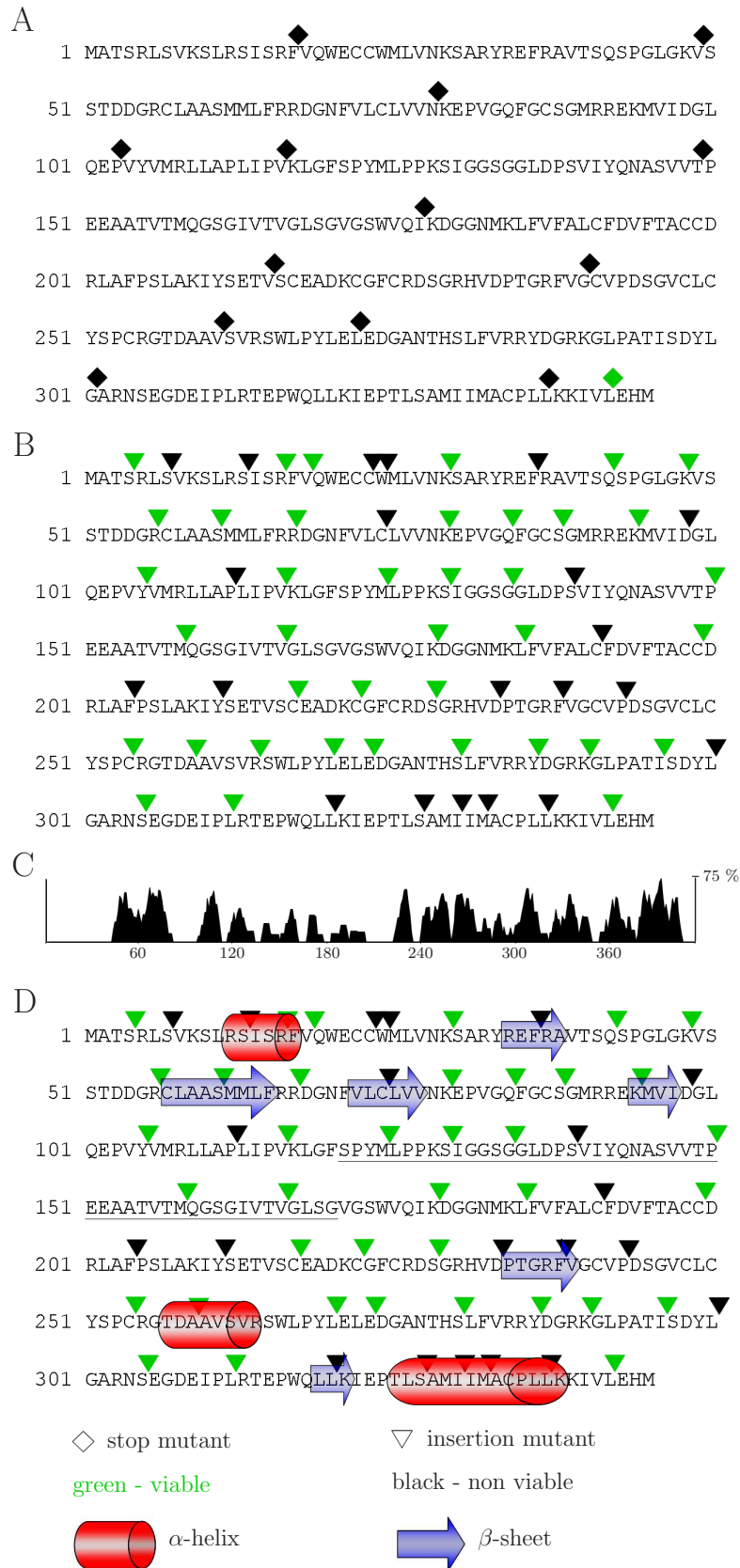


Figure 3.14: Result of the loss-of-function screen. The amino acid sequence of M94 is shown in single letter code and aa position are indicated in A, B, and D. Insertion mutants are depicted as arrowheads, stop mutants as diamonds, and both at their position on the aa sequence. Viable constructs are illustrated in green, whereas non viable mutants appear black. In C the similarity blot of 35 homologous sequences of *Herpesviridae* are presented, whereas in D the bioinformatic analysis of the protein with predicted α -helices, β -sheets, and an underlined linker are shown.

(121-170 aa) connecting two protein domains was not influenced by insertions. At the same time every stop mutant except the last one resulted in no viral progeny. This last stop mutant s342 deleted only the last three aa of M94, which were not included in the conserved part of the C-terminus, demonstrating that indeed the C-terminus is the only conserved part of the protein. Therefore, the C-terminal part of M94 is not dispensable.

3.7 Identification of inhibitory mutants

Next to the identification of essential regions in M94, further aim of this study was the identification of potential DN mutants of this protein. To do so, the mutants were analysed in the so called inhibitory screen, which utilised a different genome context.

The assay was similar to the assay illustrated in Fig. 3.11, except that the mutant M94 genes were introduced into the wt MCMV instead of the M94 deletion BAC. So the mutants were inserted ectopically in addition to the endogenous M94 (Fig. 3.15). A DN mutant would abolish the viral production by inhibition of an essential M94 function. Therefore the mutant had to interfere with the activity of the endogenous M94, which allowed the identification of a potential DN mutant as defined in section 1.2.5.

By definition a DN mutant can not complement the wt M94 function in the M94 deletion background and can not produce viral progeny in the loss-of-function screen. Therefore, all mutants having failed in virus reconstitution in the loss-of-function screen were also tested in the inhibitory screen. Additionally 8 stop mutants in the C-terminus were analysed, as the C-terminus appeared to be very sensitive to changes in the loss-of-function screen. Again two independent clones for each mutant were analysed to verify the observed phenotype.

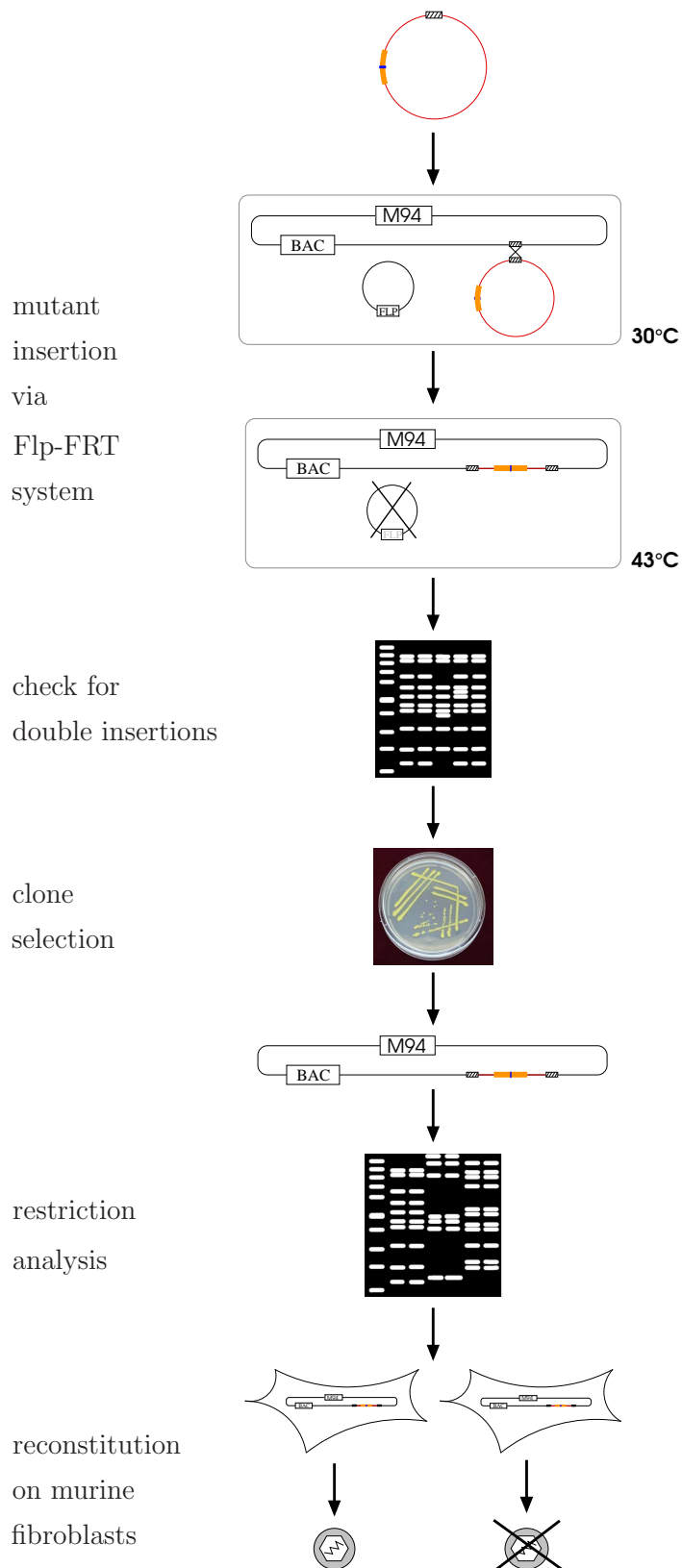


Figure 3.15: Inhibitory screen. This figure illustrates the workflow of the analysis of the M94 mutants in the viral context to identify inhibitory mutants. The screen differed to the loss-of-function screen (3.11) only in the introduction of the mutants into the wt MCMV-BAC instead of the M94 deletion BAC. So in this inhibitory screen, the mutants were inserted in the presence of the endogenous M94.

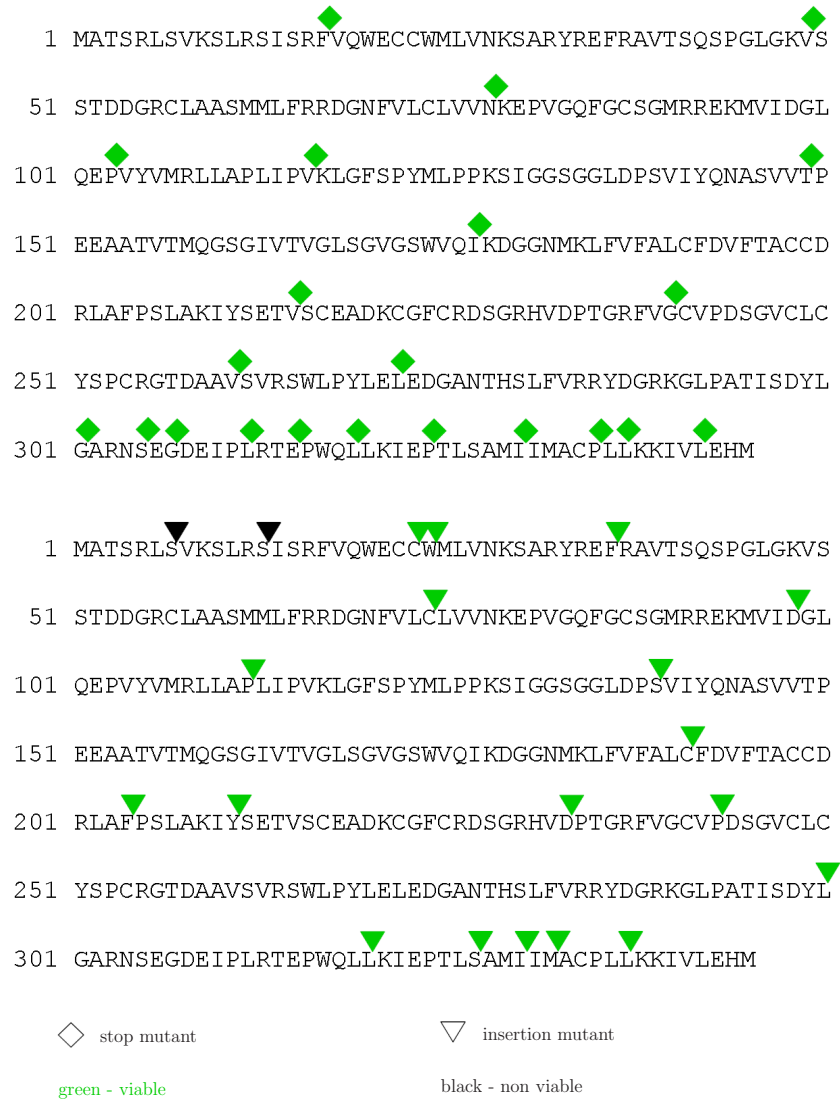


Figure 3.16: Result of the inhibitory screen. The amino acid sequence of M94 in single letter code and the aa positions are presented. Stop mutants are indicated by diamonds, insertion mutants by arrowheads, both at their position in the aa sequence. Viable mutants are illustrated in green and non viable in black.

Figure 3.16 illustrates the result of the inhibitory screen. 42 mutants analysed in this screen and 40 of them produced viral progeny like wild type and none of the stop mutants demonstrated inhibitory function. But two insertion mutants at the very N-terminus showed no viral reconstitution, the insertion mutants at the aa positions 7 and 13, named M94i7 and M94i13. Altogether, two inhibitory mutants were identified by this assay.

The analysis by the inhibitory screen only demonstrated an inhibition of the reconstitution of virus. To exclude toxicity of the mutants inhibiting viral reconstitution, these inhibitory

mutants were further analysed. In the following assay also infectious virus is analysed, which needs to pass through the complete viral life cycle.

3.8 Verification of the dominant negative mutants

To analyse the phenotype introduced by the inhibitory mutants, they have to be expressed in the viral context. This requires either delivery of the mutant expression cassette in *trans* or construction of a recombinant virus which expresses the inhibitory mutants in a conditional fashion. In the latter case the transcription unit encoding the mutant needs to be off during virus reconstitution and must be turned on when analysis of the phenotype is needed. This enables the parallel analysis of the phenotype produced by the expression of the DN and the phenotype without its expression in the same construct.

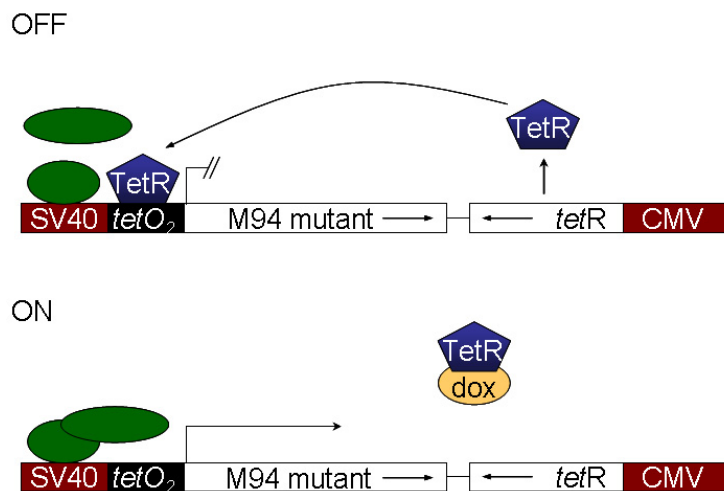


Figure 3.17: Conditional expression cassette (adapted from [77]). The constitutively expressed *tet*-repressor (*tetR*) binds to the *tet*-operator (*tetO₂*) in the promoter region of the M94 mutant, thereby preventing transcription. By addition of Dox the *tetR* binding to the operator is inhibited in binding and the mutant can be expressed.

The Dox inducible expression cassette (Fig. 3.17) which was described in Rupp et al. [77] enabled the study of mutants of dominant negative MCMV proteins. The cassette contains a *tet*-repressor (*tetR*) gene under control of the CMV promoter. The repressor protein (TetR) is therefore constitutively expressed and binds to the *tet*-operator (*tetO₂*) in the

promoter region of the mutant gene, which is expressed under control of either the SVT promoter or the CMV promoter. This TetR binding inhibits the expression of the mutant protein (OFF). Only by addition of Dox, which binds to the TetR and prevents its binding to the *tetO₂*, expression of the mutant is induced (ON).

The mutants to be analysed were cloned by PCR from the library constructs into the vectors containing the different cassettes with either the SVT or the CMV promoter by *MluI* and *PvuII* digest. These vectors were restricted by *AscI* and *HpaI* and dephosphorylated prior ligation with the digested PCR fragments, resulting in 4 constructs, verified by sequencing. These constructs were analysed for the conditional expression of the mutants.

The mutant cassettes were introduced into the BACs via the Flp-FRT system as described in Fig. 3.11. They also were analysed by restriction analysis and proper clones were selected for reconstitution. For the analysis in the viral context the mutants were introduced into two different BACs. The first pSM3fr-FRT, contains the entire MCMV genome and an FRT site between the genes m16 and m17. The second pSM3fr-FRT- Δ 1-16, lacks the genes m01 to m16 and also contains an FRT site. The genes m01 to m16 are not essential for viral growth in cell culture [18]. Integration of the cassette into pSM3fr-FRT produces an overlength genome, which is avoided when using pSM3fr-FRT- Δ 1-16 as backbone. The overlength reduces the packaging efficiency of the virus and consequently inhibits growth. By passaging the virus several times, the BAC-cassette of the cloned MCMV genome is lost and the slight growth deficiency is resolved [91]. As there are already genes deleted in pSM3fr-FRT- Δ 1-16 no overlength is produced and passaging is not necessary. Therefore the pSM3fr-FRT- Δ 1-16 MCMV genome can be used directly in cell culture experiments without extensive passaging the recombinants before analysis.

In total, 8 different constructs for the analysis of the mutants in different genome backbones and under control of different promoters were produced as recorded in table 3.2. The resulting viruses were named accordingly by replacing pSM3fr by MCMV. Meanwhile "R" in RM94i7/13 refers to the ectopic insertion of the conditional cassette containing the mutant, whereas in constructs named EHAM94 the "E" implies ectopic insertion of the pOriR6K vector, so M94 under control of the CMV promoter with constitutive expression

(Fig. 3.1).

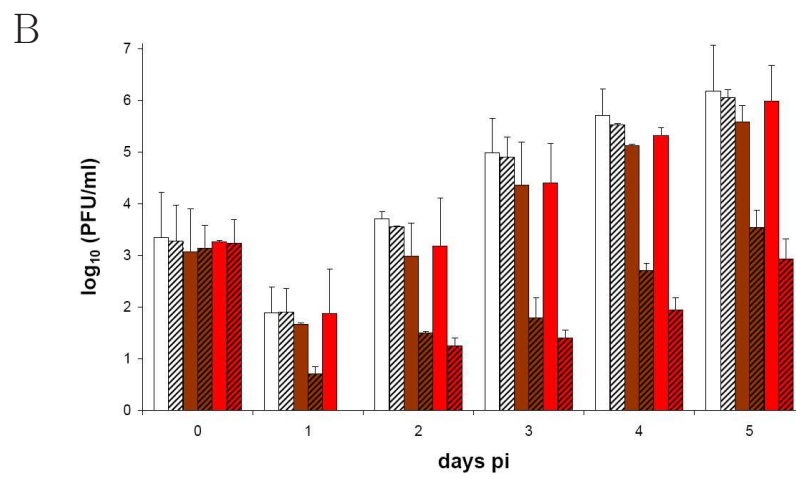
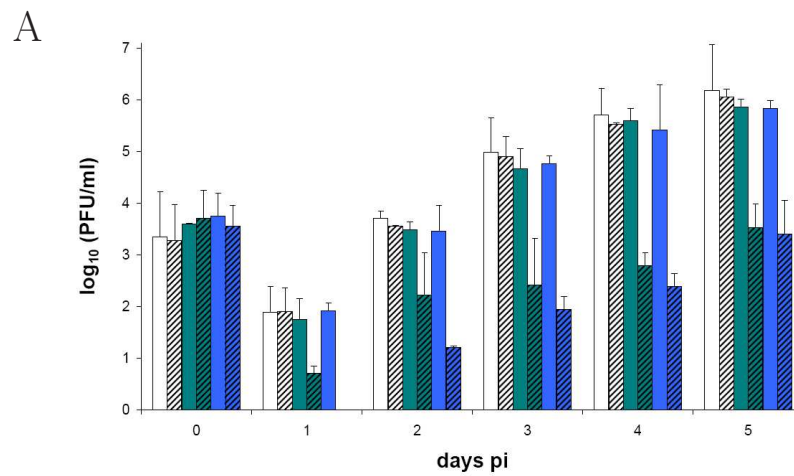
Table 3.2: Conditional expression constructs. The pSM3fr-FRT BAC contains the whole MCMV genome, whereas pSM3fr-FRT- Δ 1-16 BAC is deleted in the genes m01 to m16. The pOriR6K vectors including the inhibitory mutants M94i7 and M94i13 in the conditional expression cassette either with the CMV (pO6CMV) or the SVT (pO6SVT) promoter, were inserted into the BACs. The resulting constructs are named as shown and the resulting viruses accordingly.

parental BAC	pOriR6K vector	resulting construct	resulting virus
pSM3fr-FRT	pO6CMV-M94i7	pSM3frCMV-RM94i7	MCMV _{cmv} -RM94i7
pSM3fr-FRT	pO6CMV-M94i13	pSM3frCMV-RM94i13	MCMV _{cmv} -RM94i13
pSM3fr-FRT	pO6SVT-M94i7	pSM3frSVT-RM94i7	MCMV _{svt} -RM94i7
pSM3fr-FRT	pO6SVT-M94i13	pSM3frSVT-RM94i13	MCMV _{svt} -RM94i13
pSM3fr-FRT- Δ 1-16	pO6CMV-M94i7	pSM3fr Δ 1-16CMV-RM94i7	MCMV Δ 1-16 _{cmv} -RM94i7
pSM3fr-FRT- Δ 1-16	pO6CMV-M94i13	pSM3fr Δ 1-16CMV-RM94i13	MCMV Δ 1-16 _{cmv} -RM94i13
pSM3fr-FRT- Δ 1-16	pO6SVT-M94i7	pSM3fr Δ 1-16SVT-RM94i7	MCMV Δ 1-16 _{svt} -RM94i7
pSM3fr-FRT- Δ 1-16	pO6SVT-M94i13	pSM3fr Δ 1-16SVT-RM94i13	MCMV Δ 1-16 _{svt} -RM94i13

The viral growth characteristic of these constructs and of the parental wild type viruses were then analysed by multi-step growth curves in absence and presence of Dox, hence without and with expression of the DN mutants.

The first growth kinetics are summarised in figure 3.18. The growth of the parental virus MCMV-FRT- Δ 1-16 was not influenced by the Dox treatment (Fig. 3.18 A, B), as titres remain equal by addition of Dox. In contrast all mutant viruses were inhibited in response to Dox. The induction of mutant M94i7 inhibited the production of released viral particles by 2 logs irrespectively whether its expression was under control of the CMV promoter (MCMV- Δ 1-16_{cmv}-RM94i7, Fig. 3.18A) or the SVT promoter (MCMV Δ 1-16_{svt}-RM94i7, Fig. 3.18B). The mutant M94i13 demonstrated an slightly increased inhibitory activity (2.5 logs) under control of the CMV promoter (MCMV Δ 1-16_{cmv}-RM94i13, Fig. 3.18A) and an even higher (3 logs) under control of the SVT promoter (MCMV Δ 1-16_{svt}-RM94i13, Fig. 3.18B). Since both mutant proteins were able to inhibit viral replication upon expression, they fulfilled one characteristics of a DN mutant and they will further on be named DN mutants.

As M94i13 showed the stronger phenotype, a second clone of MCMV Δ 1-16_{cmv}-RM94i13



□ MCMV-FRT-Δ1-16

■ MCMVΔ1-16cmv-RM94i7

■ MCMVΔ1-16cmv-RM94i13

■ MCMVΔ1-16svt-RM94i7

■ MCMVΔ1-16svt-RM94i13

□ - Dox

▨ + Dox

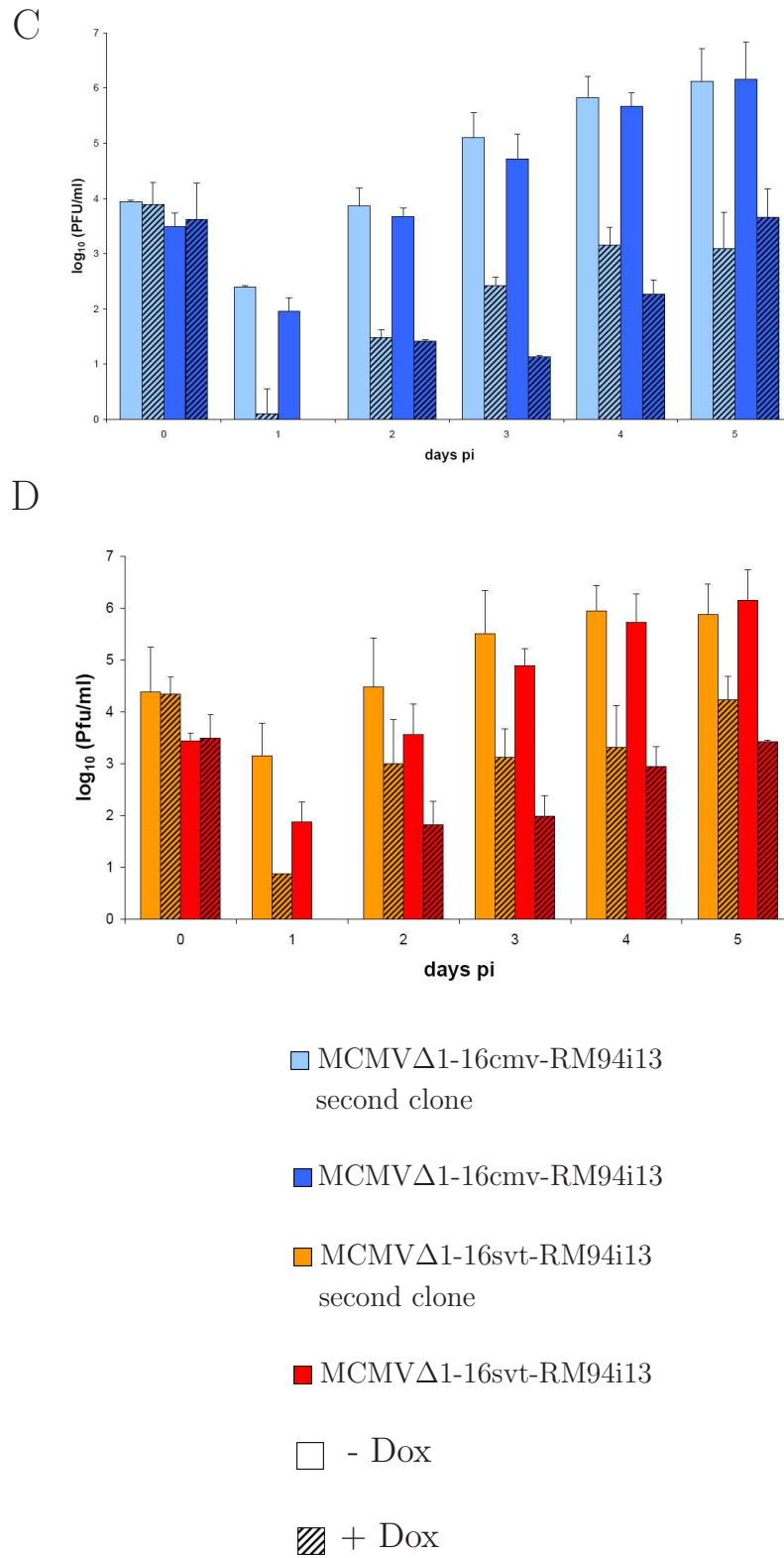


Figure 3.18: Growth kinetics of inhibitory mutants in the pSM3fr-FRT-Δ1-16 background. Addition of Dox is indicated by shaded bars. The parental virus MCMV-FRT-Δ1-16, shown in white, was not inhibited by Dox treatment (A, B). The inhibitory mutants M94i7 and M94i13 were expressed under control of either the CMV promoter (blue, A) or the SVT promoter (red, B). The inhibitory mutant M94i13 demonstrated increased inhibition, which was confirmed by second clones for both viruses (C, D).

and MCMV- Δ 1-16svt-RM94i13 were analysed in a separate growth kinetic experiments (Fig. 3.18 C, D) in comparison to the clones already assayed. Although the titres varied through the growth kinetic, the final titres showed small differences, demonstrating a clone-independent phenotype of inhibition by the DN mutant.

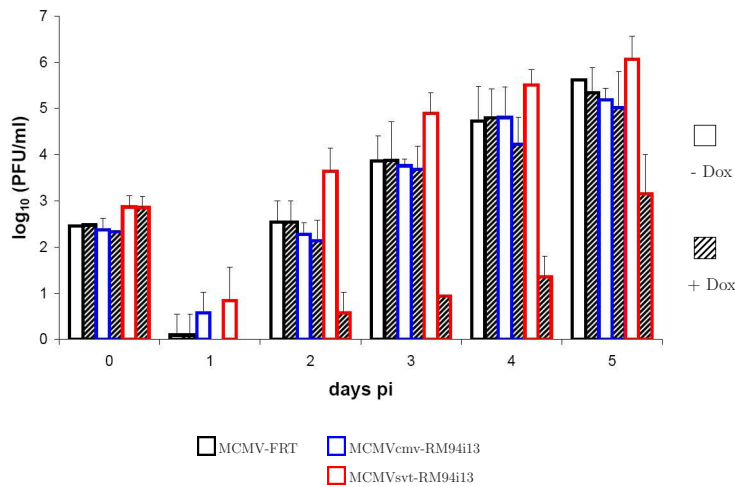


Figure 3.19: Growth kinetics of DN mutant M94i13 in the MCMV-FRT background. The addition of Dox is indicated by shaded bars. The wt virus MCMV-FRT is presented in white and was not influenced by Dox treatment. The DN mutant M94i13 under control of the CMV promoter (framed blue) did not respond to addition of Dox, whereas inhibition was detected under control of the SVT promoter (framed red).

To verify the inhibitory activity showed by the previous growth curve, the mutant function was also demonstrated in the wt MCMV backbone containing the complete genome, under control of either the SVT or the CMV promoter (Fig. 3.19). Again the wt control MCMV-FRT was not influenced by Dox in its growth characteristics.

The inhibition of the mutant M94i13 under control of the CMV promoter, MCMVcmv-RM94i13, as detected in the pSM3fr-FRT- Δ 1-16 background (Fig. 3.18), was lost in the wt context. In contrast, the inhibition upon Dox was still present under control of the SVT promoter, MCMVsvt-RM94i13, which is believed to have a lower basal expression. This difference is probably due to different basal expression strength of the promoters. In other studies the CMV promoter mediated a stronger expression than the SVT promoter. So the basal expression with the CMV promoter is higher and this resulted in an increased evolutionary pressure to neutralise the effect, driving the loss of expression the DN mutant.

Therefore, in MCMV wt background the DN phenotype was lost over time under control of the CMV promoter, but remained stable with about 3 logs inhibition in the construct containing the SVT promoter.

3.9 Protein analysis of the DN mutant

The basic principle of a DN effect is the overexpression of the mutant to inhibit the wild type function (section 1.2.5). Therefore the protein expression of the endogenous M94 and the HA-tagged DN mutant M94 were analysed.

3.9.1 Characterisation of anti-M94 serum

Anti-sera to M94 serum were produced by metabion (section 2.1.10). The two sera A and B were produced in different rabbits. In order to test the reactivity of the sera, samples from transfection and infection experiments were analysed by the sera and pre-sera for specific reaction on pM94 (Fig. 3.20).

Infections were performed with mock, MCMV Δ M94tTA, and MCMV Δ 1-16 in NIH3T3 cells, whereas the transfections in 293 cells contained either pOriR6K-ie or pOriR6K-HAM94. The calculated size of pM94 is 37.7 kDa. As former studies of the UL94 homologue in HCMV [95] revealed no size variants, the predicted size was expected. Also a blot stained against the HA-tag was utilised for verification of the protein identity.

The staining against the HA-tag revealed in one band at the predicted size of about 38 kDa. The signal could only be detected in the transfection T2 as the wt infection contained no HA-tagged M94 and the transfection T1 contained only the empty vector.

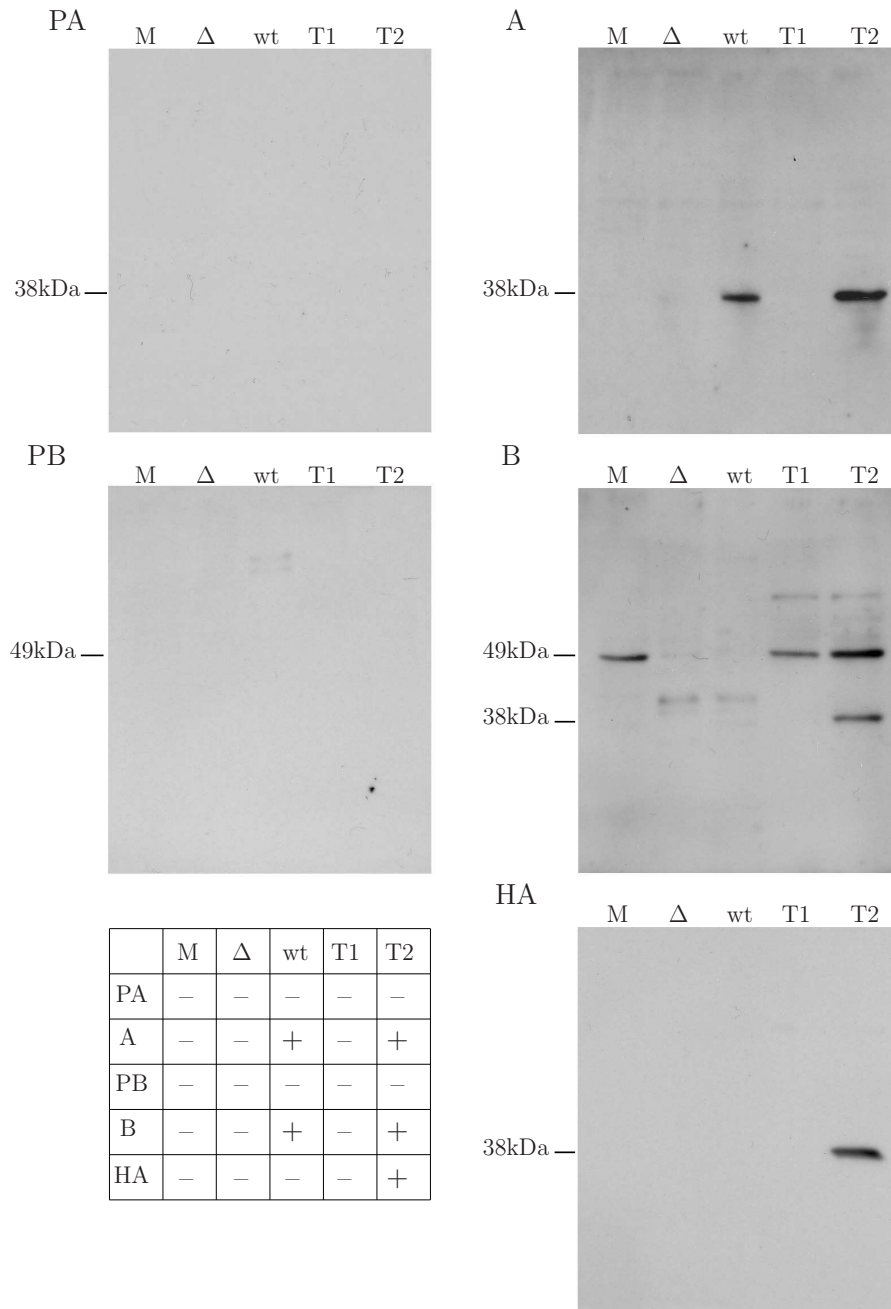


Figure 3.20: Analysis of specific binding of sera A and B for pM94 in comparison to binding of pre-sera (PA and PB). The infection samples mock (M), MCMVΔM94tTA (Δ), and MCMVΔ1-16 (wt) were analysed together with transfection samples from pOriR6K-ie (T1) and pOriR6K-HAM94 (T2). The HA staining indicates the HA-tagged M94 at 38 kDa, whereas serum B detected also an unspecific signal at 49 kDa. The table indicates the expected band pattern.

Both pre-sera showed minor staining, whereas the serum B demonstrated an unspecific reaction in transfection around 49 kDa, also present in the mock control of the infection. A band at correct size of 38 kDa was detected in the transfection of pOriR6K-HAM94, but

not in the wt infection.

The staining with serum A resulted in a unique band at the correct size. The M94 protein was detected by the serum A both in infection, as the signal appeared only in MCMV Δ 1-16 and not in the mock or M94 deletion virus MCMV Δ M94tTA infected cells, as well as after transfection, where the empty pOriR6K-ie demonstrated no signal in contrast to pOriR6K-HAM94. Serum A detected a single specific band at about 38 kDa corresponding to pM94 and could be used for further experiments. This analysis also demonstrated the antibody reaction to both, the endogenous M94 in MCMV Δ 1-16 and the HA-tagged M94 in pOriR6K-HAM94.

3.9.2 Analysis of the expression of M94 alleles

The inhibition demonstrated in the growth analysis should reflect the expression of the DN mutant. Also the potential influence of the DN expression on the viral expression cascade required investigation.

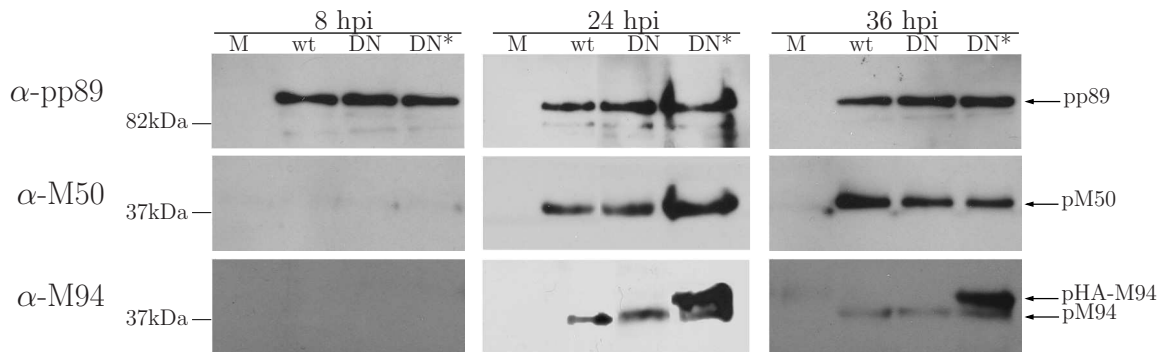


Figure 3.21: Analysis of the gene expression of mock control (M), MCMV Δ 1-16 (wt), and MCMV Δ 1-16svt-RM94i13 in absence (DN) and presence (DN*) of Dox by staining with antibodies against pp89 (α -pp89), M50 (α -M50), and M94 (α -M94) at different time points (hpi). The detected proteins are indicated by arrows.

Therefore, NIH3T3 cells were infected at MOI 0.5 with mock, MCMV Δ 1-16, and MCMV Δ 1-16svt-RM94i13 in absence and presence of Dox and protein was extracted at 8 hpi, 24 hpi, and 36 hpi (Fig. 3.21). Following separation of the proteins by SDS-PAGE and blotting on a membrane, the blots were stained for different proteins. The detection of pp89 by a

specific serum served as infective control as the immediate early protein pp89 is expressed as first viral product after infection. It is represented in figure 3.21 and its expression is detected from 8 hpi on. The loading of gels was equilibrated on the basis of the pp89 analysis. The staining of pM50 provided a comparison to the expression of a true late gene.

The separation of the two M94 forms was achieved by application of precasted gels from BioRad. The M94 anti-sera detected the endogenous pM94 as well as the pHA-M94. The staining shows the presence of the endogenous pM94 in the wt and the DN mutant in absence and presence of Dox from 24 hpi on. The HA-M94 expression is demonstrated by the additional band present from 24 hpi on in the DN mutant in presence of Dox. The slower migration of the HA-tagged protein is due to the additional aa in pHA-M94 resulting from the 5 aa insertion at position i13 and the HA-tag. Altogether, the induction of the DN mutant expression by Dox treatment and also the overexpression of the mutant compared to the wt protein could be clearly shown.

Notably, the analysis also demonstrated the stability of the endogenous pM94 which was not influenced by the expression of the DN mutant. The same is true for pp89 and pM50, both were not influenced in their amount and time point of expression by expression of the DN mutant. So the cascading viral gene expression at least for pp89 and pM50 was not influenced by the expression of the M94 DN mutant.

3.9.3 M94 is expressed by true late kinetics

The analysis of the M94 and the HA-M94 mutant expression at different time points did not allow to conclude on the true late expression of either. Therefore NIH3T3 cell were infected in absence and presence of PAA with MOI of 0.5. PAA inhibits specifically the viral polymerase and thus viral genome replication and expression of true late genes. The wt M94 is a true late gene, consequently dependent on the viral genome replication. As HA-M94 was expressed under control of a different promoter it was relevant, whether its expression kinetic was also true late.

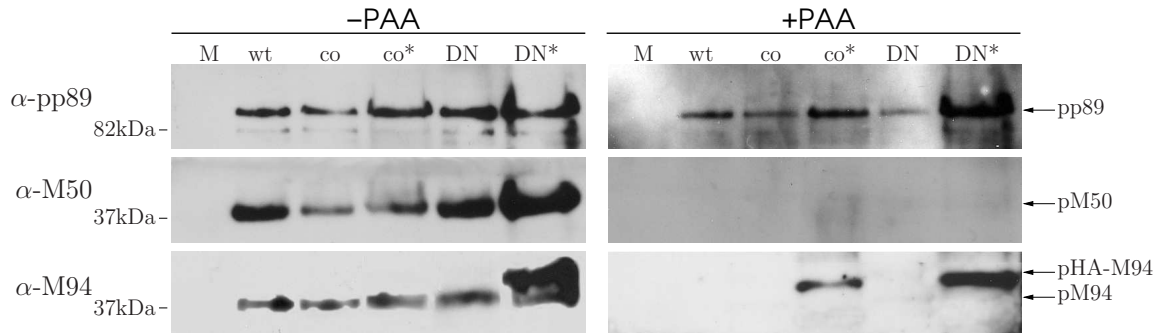


Figure 3.22: Gene expression analysis of several viruses in the absence (-PAA) and presence (+PAA) of PAA. NIH3T3 cell were infected with mock control (M), MCMV Δ 1-16 (wt), MCMV Δ 1-16SVT-RHAM94 in absence (co) and presence (co*) of Dox, and MCMV Δ 1-16svt-RM94i13 in absence (DN) and presence (DN*) of Dox. The blots were stained with antibodies against pp89 (α -pp89), M50 (α -M50), and M94 (α -M94) and detected proteins are indicated by arrows.

The western blot analysis on pp89, pM50, and pM94 shown in figure 3.22 demonstrates the mutant and wt M94 expression in absence and presence of PAA. In addition to the viruses already analysed in Fig. 3.21, MCMV Δ 1-16 and MCMV Δ 1-16svt-RM94i13 in absence and presence of Dox, a control virus was analysed. This overexpression control virus MCMV Δ 1-16SVT-RHAM94 is equal to MCMV Δ 1-16svt-RM94i13, but it contains the wt HA-M94 without mutation in the conditional expression cassette.

The loading equilibration of all samples was based on the pp89 staining and as before pM50 served as established true late gene. Accordingly, the detectable expression of M94 in all viruses disappeared by treatment with PAA. By this the true late expression of M94 was proven. This result was expected as homologues also demonstrated true late expression [63, 95].

In contrast, the expression of pHA-M94 was not influenced by the PAA treatment indicated by the bands present in MCMV Δ 1-16SVT-RHAM94 and MCMV Δ 1-16svt-RM94i13 both in presence of Dox and PAA. Thus M94 expression of the inserted gene was independent from the viral genome replication. In summary the wt M94 was expressed with true late expression, whereas the mutant HA-M94 is not dependent on viral genome replication.

3.10 M94 plays an essential role in secondary envelopment

In order to localise the inhibition in the lytic cycle by the expression of the DN mutant, transmission electron microscopy (EM) was performed. In parallel the ultra structural phenotype of the M94 deletion virus was also studied for comparison.

To this end, NIH3T3 cells were infected with a MOI of 1 and centrifugal enhancement for one hour with MCMV Δ 1-16, MCMV Δ M94tTA and MCMV Δ 1-16svt-RM94i13 in absence and presence of Dox. Afterwards cells were fixed by high-pressure freezing, freeze-substituted, plastic embedded, thin-sectioned and analysed by transmission electron microscopy [93]. Both viruses under all conditions showed a wt-like capsid distribution in the nucleus (Fig. 3.23) and also primary envelopment mainly on nuclear infoldings (Fig. 3.24). Next, the analysis demonstrated secondary envelopment namely tegumented enveloped capsids in the cytoplasm for the wt virus as well as the DN virus in absence of Dox indicated by arrows. In contrast no secondary envelopment could be detected in cells infected with the M94 deletion mutant or the M94 DN expressing virus in presence of Dox although tegumented capsid accumulations in the centre of an assembly complex-like structure were present, indicating a role of M94 in the secondary envelopment. In addition enveloped viral particles were also not observed in vesicles, which are believed to appear ahead of the secondary envelopment.

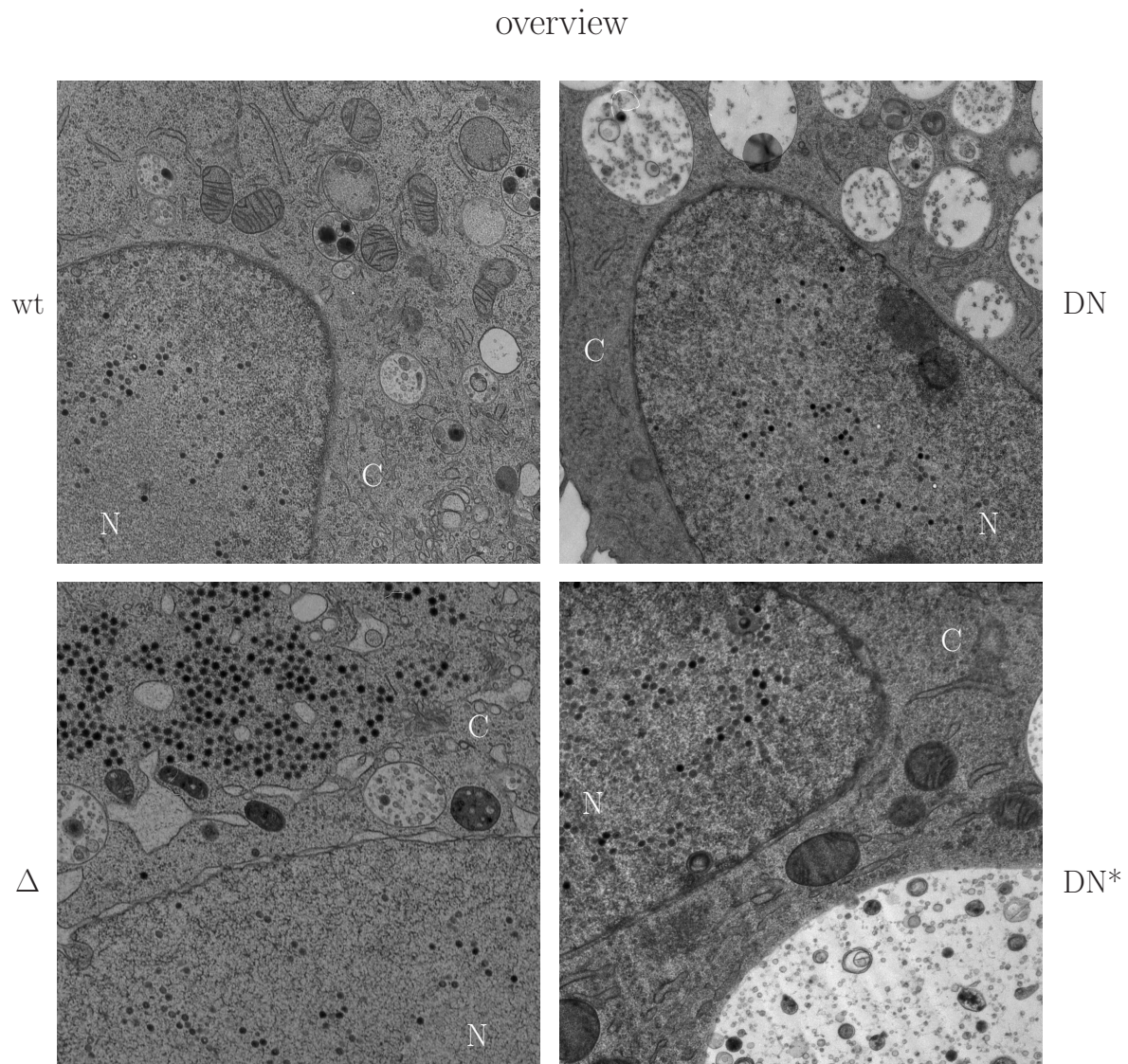


Figure 3.23: Electron microscopy analysis of cells infected by MCMV Δ 1-16 (wt), MCMV Δ M94tTA (Δ) and MCMV Δ 1-16svt-RM94i13 in absence (DN) and presence (DN*) of Dox. A representative view of the cell including nucleus (N) and cytoplasm (C) is shown.

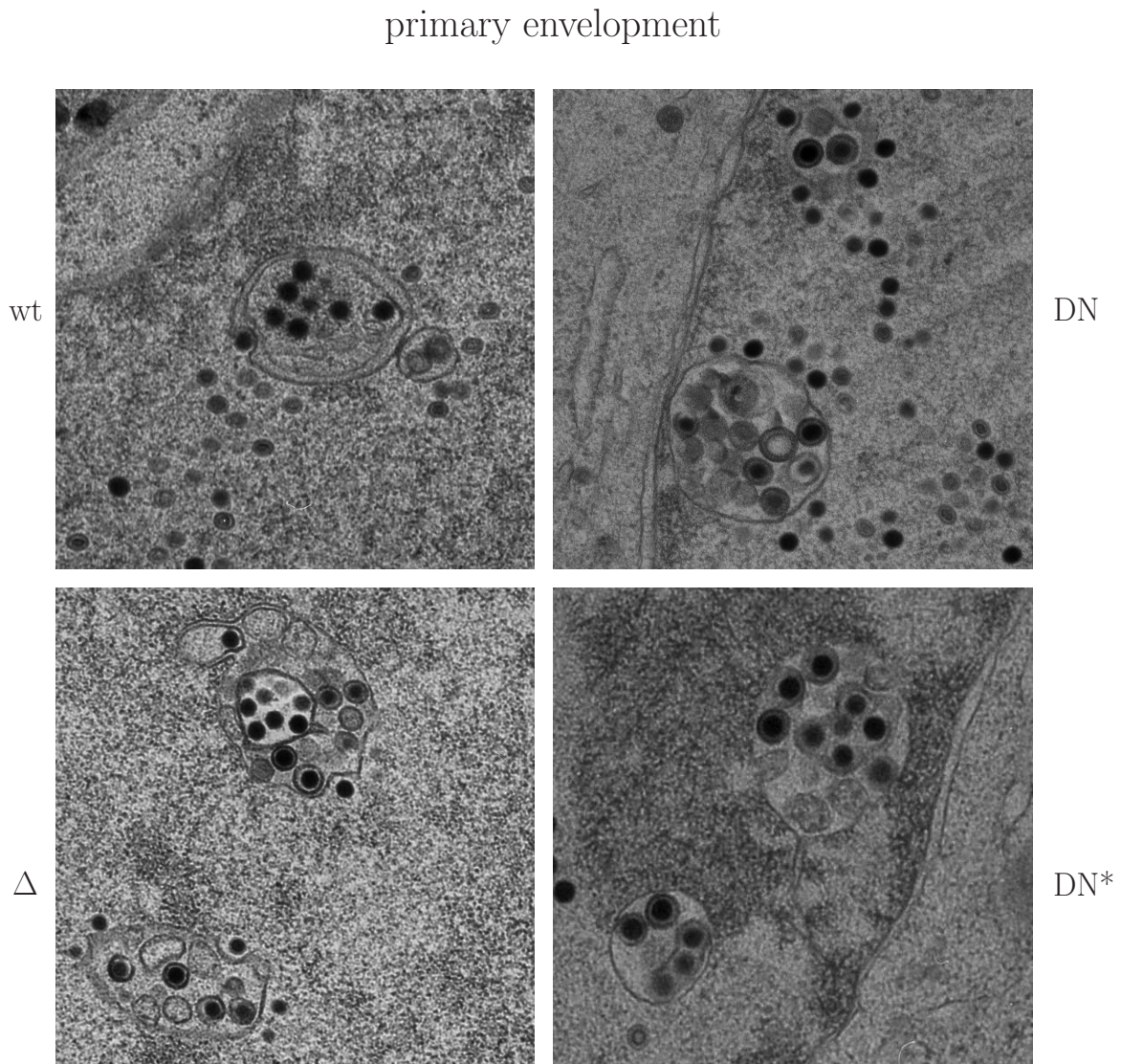


Figure 3.24: Electron microscopy analysis of the primary envelopment of MCMV Δ 1-16 (wt), MCMV Δ M94tTA (Δ) and MCMV Δ 1-16svt-RM94i13 in absence (DN) and presence (DN*) of Dox in the nucleus is presented.

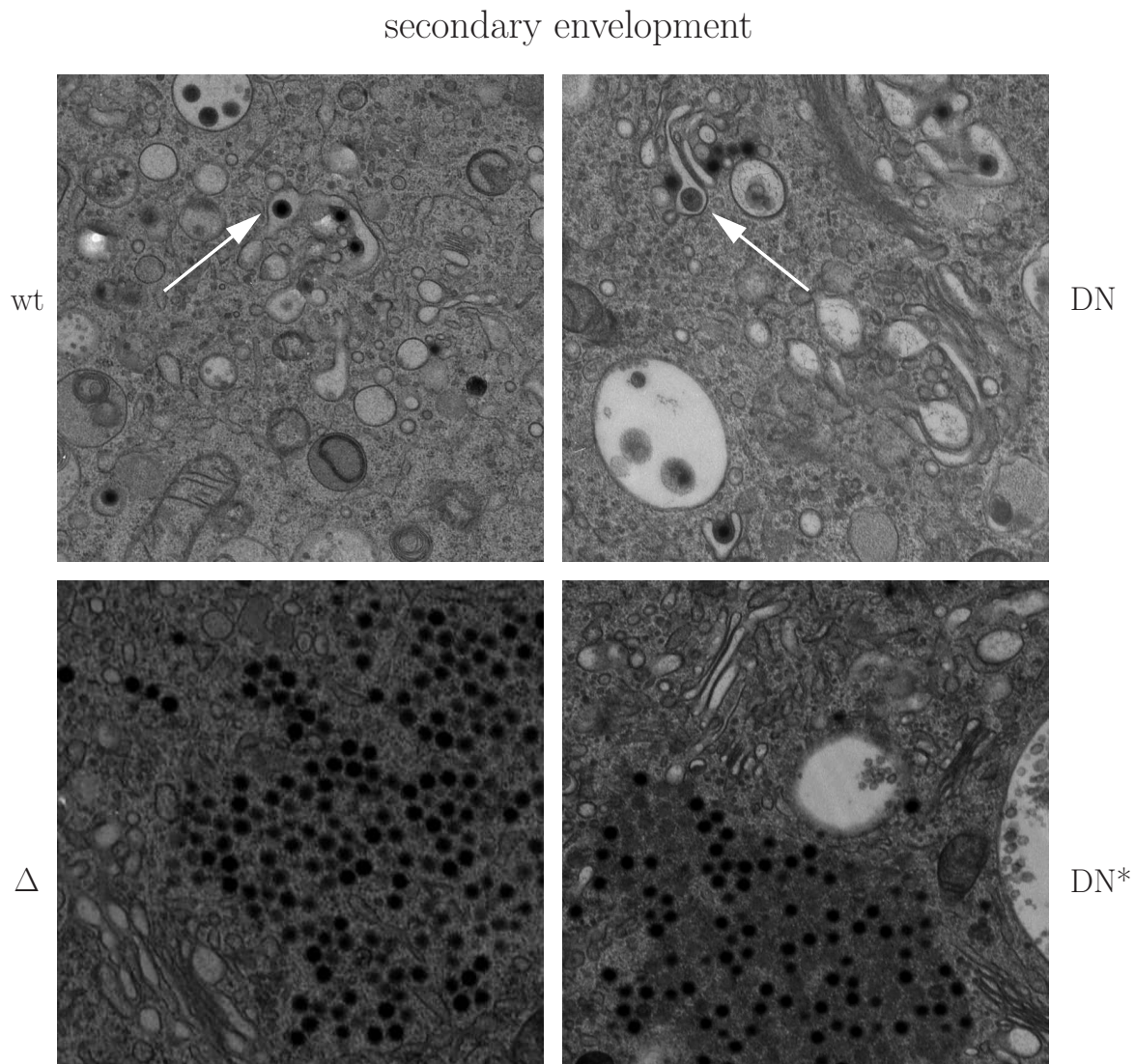


Figure 3.25: Electron microscopy analysis illustrating the secondary envelopment of MCMV Δ 1-16 (wt), MCMV Δ M94tTA (Δ) and MCMV Δ 1-16svt-RM94i13 in absence (DN) and presence (DN*) of Dox in the cytoplasm. Secondary envelopment is indicated by arrows.

3.11 Spread deficiency of MCMV lacking M94

Until now it is unclear whether secondary envelopment is required for cell-to-cell spread in β -Herpesvirinae [82]. The lack of secondary envelopment in presence of functional M94

raised the question whether this also results in a loss of cell-to-cell spread. In order to analyse the spread phenotype of the M94 deletion virus, NIH3T3 and NTM94 cells were infected with wt and M94 deletion virus. The remaining virus was removed by intensive washing and CFSE stained NIH3T3 were added. Virus spread was then permitted for 48 h. Afterwards, the culture was stained against immediate early antigen pp89, resulting in cells either pp89-positive, CFSE-positive, double positive or double negative for both stains [48].

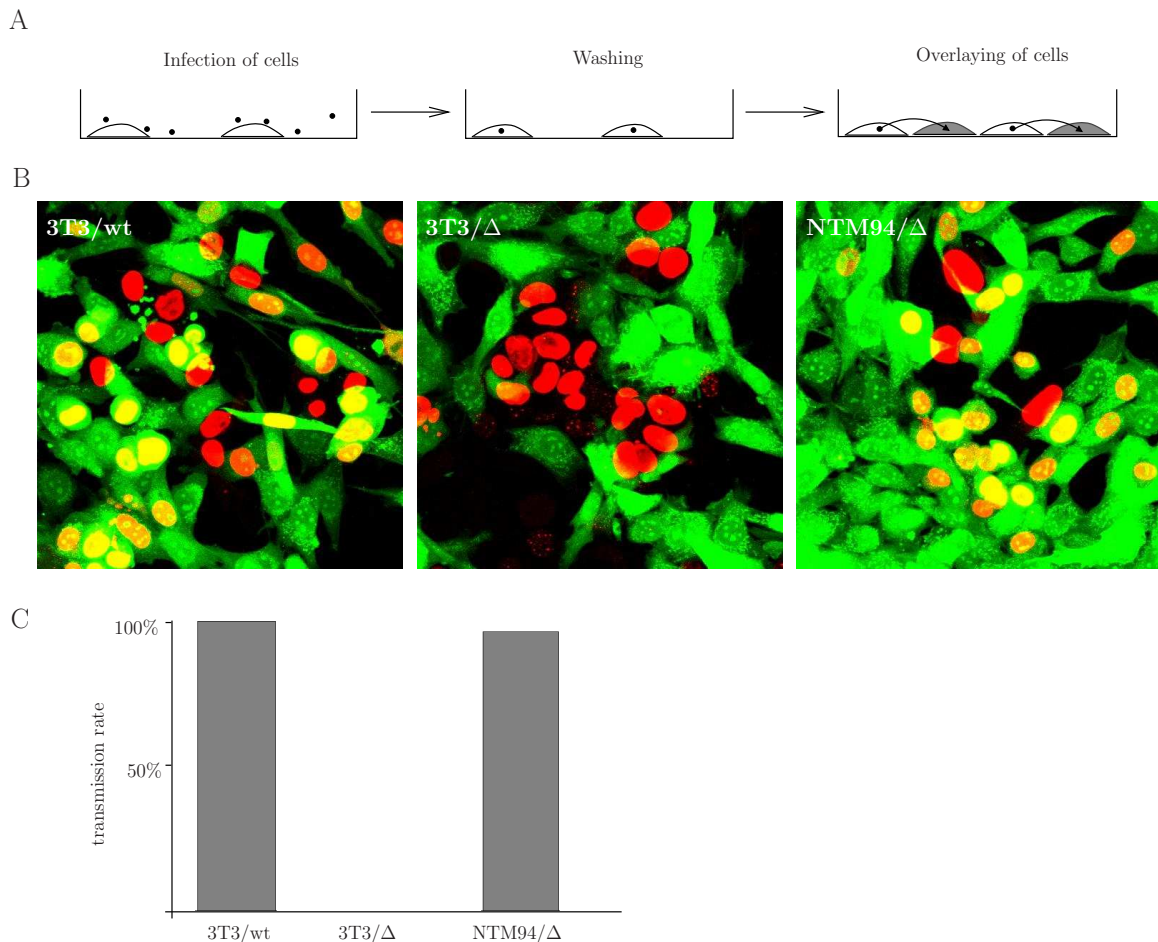


Figure 3.26: Analysis of the spread assay. A schematic diagram of the spread assay is shown in A, whereas B illustrates representative pictures of pp89 (red) and CFSE (green) stained NIH3T3 (3T3) and NTM94 (NTM94) cells infected by either MCMV Δ 1-16 (wt) or MCMV Δ M94tTA (Δ). Virus transmission was determined by calculating the ration between pp89-positive/CFSE stained cells to pp89-negative/CFSE stained cells (C).

Cells positive for both stains indicate the transmission of virus from infected CFSE negative cells to CFSE positive cells. Figure 3.26 shows a scheme of the spread assay and images by confocal microscopy. Virus transmission was determined by counting pp89- and CFSE-positive cells resulting in the depicted transmission rate by determination of the ratio between pp89-positive/CFSE stained cells to pp89-negative/CFSE stained cells. Thereby the ability of the wt virus to spread rapidly throughout the cell population was demonstrated by a transmission rate of 100 %. In contrast the M94 deletion virus was unable to infect the freshly added cells. This lack of cell-to-cell spread was restored by using the complementing cell line NTM94 in the assay resulting in a transmission rate of 97 %. This analysis demonstrated that the deletion of M94 resulted in a block of the induction of both release of infectious particles and cell-to-cell spread.

3.12 M94 is not essential for viral cleavage-packaging

Since Nalwanga et al. [63] localised pUL16, the homologue of pM94 in intranuclear assemblons and Oshima et al. [64] discovered the single strand (ss) DNA binding of pUL16 the HSV homolog of pM94, there are speculations on the involvement of M94 and its homologues in cleavage-packaging of viral genomes [45]. Our EM analysis indicated no detectable defect in the nuclear morphogenesis in absence of functional M94. Yet an accessory role of M94 in packaging could not be excluded by the EM analysis. In order to investigate cleavage-packaging, an assay for the end cleavage reaction in MCMV infection was designed. By Southern blot analysis the different genome forms present in the cleavage-packaging process could be separated.

As already mentioned in the introduction, the genomes of *Herpesviridae* are replicated as head-to-tail concatemers.

The concatemers depicted in figure 3.27(A) are cleaved into unit-length genomes by the terminase enzyme of the virus and inserted into preformed capsids (B). This process is highly conserved throughout the *Herpesviridae*. The events of genome cleavage and pack-

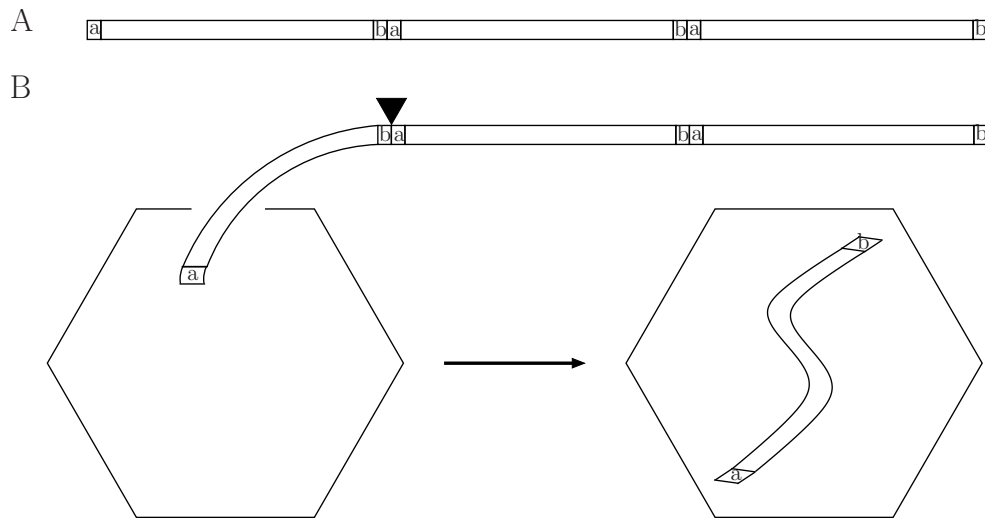


Figure 3.27: Schematic diagram of head-to-tail concatemers (A). Several MCMV genomes with terminal repeats a and b are illustrated as boxes in the head-to-tail-concatemeric form. The concatemer is cleaved by the terminase (black arrowhead) and the unit length genome is packed into the capsid (B).

aging are coupled and therefore appear simultaneously.

The viral genome replication proceeds by production of concatemers. The capsid assembles simultaneously into procapsids, in which the unit length genomes are inserted from the head-to-tail concatemers. Therefore, during encapsidation the concatemers need to be cleaved into unit length genomes by the viral terminase. Through this parallel process concatemers and unit-length genomes coexist during late stage of viral replication. To distinguish between these two forms, a digestion of viral DNA and a fragment detection by Southern blot analysis were combined.

3.12.1 Packaging assay

To analyse the viral DNA with regard to DNA cleavage-packaging, the total DNA from infected cells harvested at 48 hpi was isolated, digested by *Apa*LI, and subjected to by agarose gel electrophoresis. The two genome forms were separated by their fragment size indicated by a probe in a Southern blot analysis.

A similar assay was already established in the group by Mirela Popa [68], but this assay was not suitable for analysis of constructs based on pSM3fr-FRT- Δ 1-16 and therefore a new assay based on the same principle was established in this study to analysis pSM3fr-FRT

and pSM3fr-FRT- Δ 1-16 based constructs in parallel.

For the detection of both genome forms, a probe detecting two *Apa*LI-fragments was generated. Figure 3.28 illustrates the products derived from concatemers and cleaved genomes.

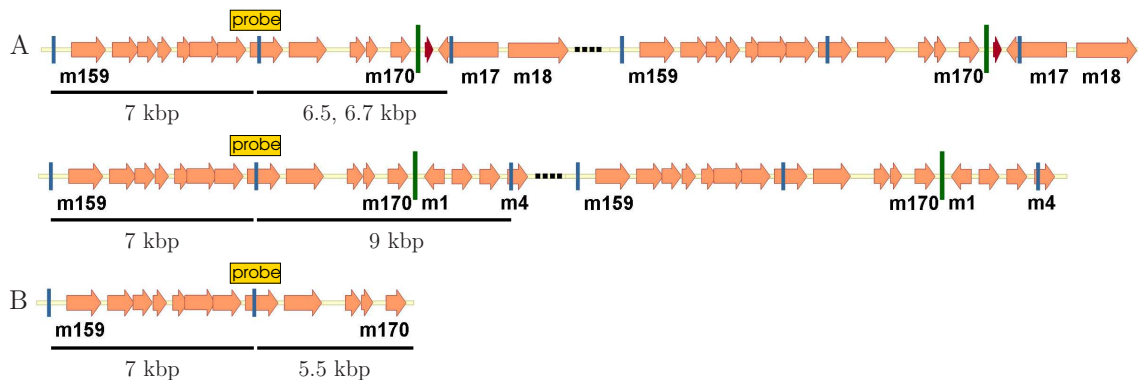


Figure 3.28: Position of the Southern probe on the concatemeric genome form (A) and cleaved genomes (B). The *Apa*LI restriction sites are displayed in blue and the green lines represent the genome termini, whereas the FRT site is indicated by a red arrow. Fragments detected by the probe are indicated with their corresponding sizes.

Two fragments were detected by the probe, irrespective whether the genome was cleaved or in its concatemeric form (Fig. 3.28). The control fragment of 7 kbp representing an internal genomic fragment was utilised for normalisation of loading of the samples. The terminal fragment representing unit-length genomes was produced by the *Apa*LI digest at the hybridisation position of the probe and the cleavage into unit-length genomes at the genome termini by the viral terminase, resulting in a 5.5 kbp fragment. The size of the fragment identifying the concatemers varied. These terminal fragments resulted from the *Apa*LI digest beyond the genome termini and had a size of 6.5 kbp in wt, 6.7 kbp in the pSM3fr-FRT- Δ 1-16 backbone and 9 kbp in the pSM3fr-FRT backbone. In pSM3fr-FRT- Δ 1-16 the ectopic insertion at the FRT site relocates the *Apa*LI restriction site generating a larger fragment than in the wt. In pSM3fr- Δ M94tTA the non deleted genes m01 to m16 prolonged the fragment.

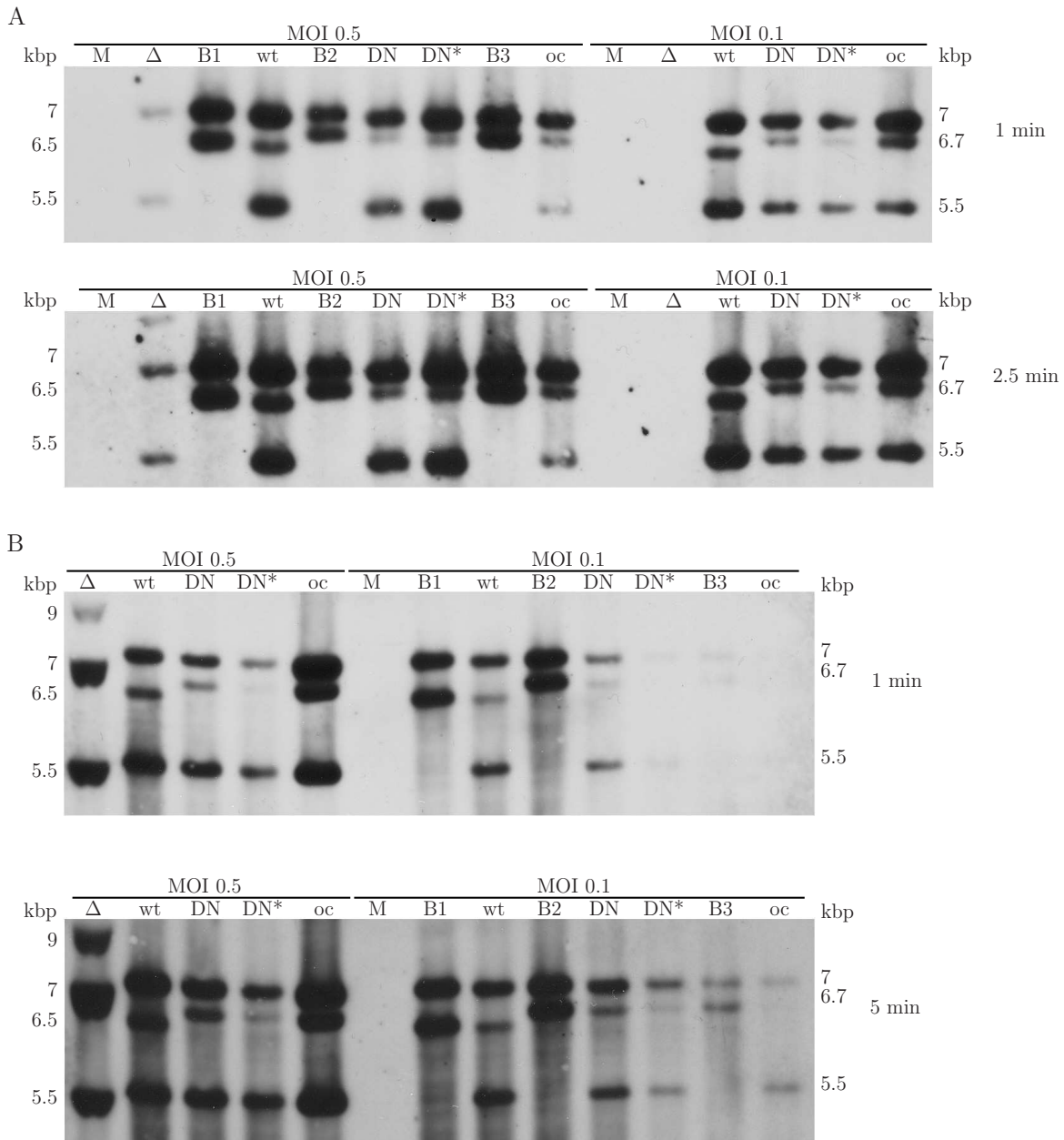


Figure 3.29: Packaging assay for mock (M), MCMV Δ M94tTA (Δ), MCMV Δ 1-16 (wt), MCMV Δ 1-16svt-RM94i13 in absence (DN) and presence (DN*) of Dox, and MCMV Δ 1-16-EHAM94 (oc) at MOI 0.5 and 0.1 for two independent analyses (A and B) at different exposure times (min). The BACs pSM3fr-FRT- Δ 1-16 (B1), pSM3fr- Δ 1-16svt-RM94i13 (B2), and pSM3fr- Δ 1-16-EHAM94 (B3) were analysed as concatemeric controls. The fragments representing the control 7 kbp, the cleaved genomes 5.5 kbp and all concatemeric fragments 9 kbp, 6.7 kbp and 6.5 kbp, are indicated.

Figure 3.29 shows the result of the packaging assay. DNA from infections with mock, M94 deletion MCMV Δ M94tTA, wt MCMV Δ 1-16, DN mutant MCMV Δ 1-16svt-RM94i13 in absence and presence of Dox and control virus MCMV Δ 1-16-EHAM94 which consti-

tutively expresses HA-M94 were analysed. Next to the infection samples the BACs for generation of the viruses were analysed. Due to the circular form of the BACs no free terminal fragments were present resulting in two bands, one for the concatemeric form and the control band.

The control fragment of 7 kbp was present in all samples, but varied in intensity due to different loading. The equilibration based on the 7 kbp fragment was required due to different amounts of viral DNA in the DNA extractions but as almost no viral DNA was produced in the spread deficient MCMV Δ M94tTA the complete extraction was utilised in one analysis. Therefore equilibration was complicated and loading differed in both analysis A and B and reduced the comparability.

The upshift of the 6.5 kbp concatemeric fragment of MCMV Δ 1-16 to the 6.7 kbp concatemeric fragment of MCMV Δ 1-16svt-RM94i13 and MCMV Δ 1-16-EHAM94 is reflected by the analysis as well as the 9 kbp concatemeric fragment of MCMV Δ M94tTA. The 5.5 kbp fragment representing the cleaved genomes was present in all samples, while the band of Δ in analysis B was shifted due to the excessive loading.

Due to divers loading a direct comparison of ration of fragments was not feasible and only the appearance of all fragments for all mutants was detected.

In order to equilibrate the differences caused by the differences in the amount of genome loads, the band intensities were compared. Therefore the chemiluminescence signal was assessed using a chemiluminescence scanner and quantified by computer analysis (Tab. 3.30).

Table 3.3: Values of the quantification of the packaging assay corresponding to figure 3.30

	Δ	wt	DN	DN*	oc
control	23,217	7392	6012	6651	135,178
concatemer	8831	4008	3257	3328	67,590
cleaved	16,280	5848	4483	5306	101,521

By plotting the relative intensities of the three bands of one sample, the ratio between

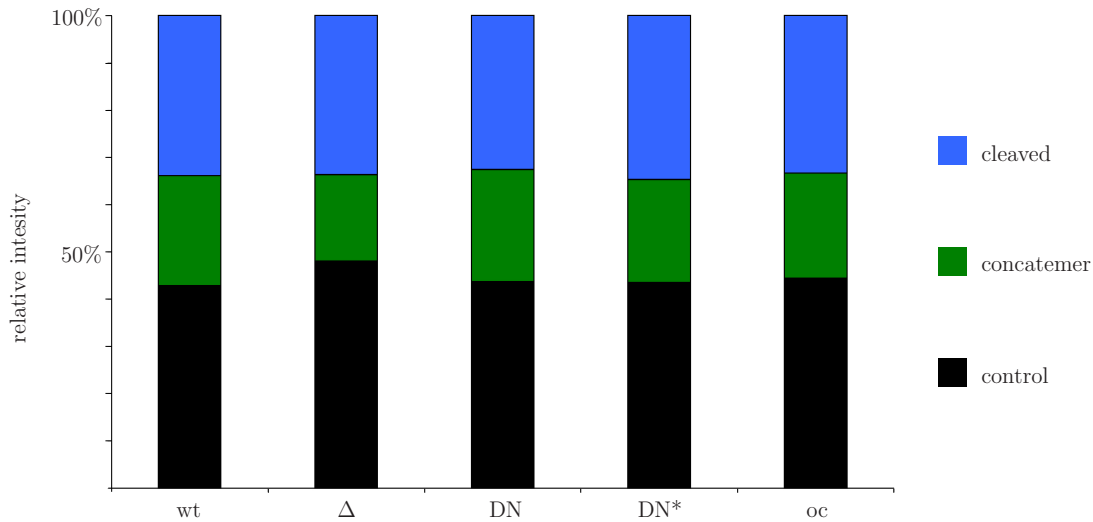


Figure 3.30: Quantification of the packaging assay. The chemiluminescence signals of the Southern analysis (Fig. 3.29) were detected and quantified. Values for each genome form of MCMV Δ M94tTA (Δ), MCMV Δ 1-16 (wt), MCMV Δ 1-16svt-RM94i13 in absence (DN) and presence (DN*) of Dox, and MCMV Δ 1-16-EHAM94 (oc) were compared to each other. The relative intensities of the control fragment (black), concatemeric fragment (green) and cleaved fragment (blue) are illustrated in percentage.

the fragments was determined (Fig. 3.30). Analyses of both assays were used, except MCMV Δ M94tTA, and mean values are depicted. The control fragment is illustrated in black and constitutes approximately 50 % of the total fragments as it was present both in the concatemers and the cleaved genomes. The percentage of the concatemeric form (green) was lower than the percentage of the cleaved genomes (blue), representing the proportion seen in the assay (Fig. 3.29).

Altogether, the analysis demonstrated a stable ratio between concatemeric and unit-length genomes for all tested viruses. Neither the deletion of M94 nor the expression of the DN mutant resulted in any influence on the ratio between concatemeric and cleaved genome form. The phenotype of both mutants was comparable to wild type. This demonstrates that M94 plays no essential role in the cleavage-packaging process of viral genomes.

Chapter 4

Discussion

The aim of this project was to investigate the essential function of the MCMV protein M94. By analysis of a library of M94 mutants generated by a Tn7 based mutagenesis in the viral context, sequences affecting essential protein functions were identified. These loss-of-function mutants were used to identify DN mutants of M94. These DN mutants were analysed in comparison to the M94 deletion mutant. This study revealed that M94 plays an essential role in secondary envelopment and also that M94 deletion is sufficient for loss of cell-to-cell spread. In addition, it could be demonstrated that M94 is not required for cleavage-packaging of the viral genome.

4.1 Generation of mutant libraries

The established transposon mutagenesis and subsequent analysis in the viral context permits the definition of essential genes. This is especially useful for genes with unclear function like M94 as by this analysis regions in the protein essential for virus replication can be located and also potential DN mutants can be identified. By further characterisation of the mutants, the step of the essential contribution of the protein function in the virus life cycle can be determined.

Our previous mutagenesis procedure used for the analysis of the protein M53 could be sig-

nificantly improved during this study. Former transposon mutageneses suffered from the presence of numerous clones including mutations in the backbone of the mutated plasmid in addition to the desired mutations in the gene of interest. These vector mutations needed to be separated from the mutations in the gene of interest. This problem was solved during M53 mutagenesis [47] by subcloning M53 including the transprimer from the target vector into an expression vector. This procedure was also performed in this study. Despite this advancement, the mutagenesis of M53 experienced several throwbacks.

First of all, the utilised donor vector in the M53 mutagenesis was constructed from pGPS4 and pST76K [46] and contained a temperature sensitive origin of replication. So that the donor vector was in subsequent steps rejected from the mutagenesis at non-permissive temperature. In contrast, pGPS4 included in the GPS[®]-LS Linker scanning system from NEB was utilised in the M94 mutagenesis. Therefore the necessity of a special donor vector which is commercially not available was omitted. This makes the procedure generally applicable.

Secondly, the first analysis of the final M53 library revealed the necessity of preselection of mutants by PCR as about 50 % of the mutants did not contain M53 for unknown reasons or were truncation mutants. Among 986 M53 mutants analysed by PCR only 498 were selected for sequencing. Thereby the labour intensive mutant analysis was increased by an additional procedure. This preselection was eliminated in the M94 mutagenesis as the first analysis of the final library demonstrated no mutations outside of the subcloned fragment (Fig. 3.9). Therefore M94 mutants from the library could be directly forwarded to sequencing.

Table 4.1: Comparison of the transposon mutagenesis of M53 and M94.

	M53 mutagenesis	M94 mutagenesis
sequenced mutants	498	613
correct mutants	389	494
unique mutants	109	399

The quantity of sequenced, correct and unique mutants for the M53 library and the M94

library are presented in table 4.1. Subsequently to preselection, 498 mutants of the M53 library have been sequenced, whereas 613 mutants of the M94 library were sequenced. In the M53 library 389 of the sequenced mutants contained a single correct mutation in the M53-ORF. This is a comparable proportion of 80 % of mutants as in the M94 library where 494 of the 613 sequenced mutants were correct. In the M94 library half of the incorrect mutants resulted from using GPS[®]-LS Linker scanning system as mentioned in the manual [7]. The remaining 10 % incorrect mutations contained 5 % mixed clones. Mutations outside the M94-ORF due to imprecise subcloning constituted the remaining 5 % of incorrect mutations. Analogue reasons caused incorrect mutations in the M53 library. The libraries are then comparable in this point, disregarding the omitted preselection of the M94 library.

However, there is a definitive enhancement of resolution in the M94 library compared to the M53 library. The M94 library contained 80 % (399 of 494) unique mutants, whereas the M53 library included only 28 % (109 of 389) unique mutants. Certainly a direct comparison is complicated as diverse methods were applied on different genes. However, we believe that the cloning bias seen in the M53 mutagenesis was eliminated in the M94 mutagenesis. This resulted in an enhanced assortment of mutants for a detailed analysis of M94.

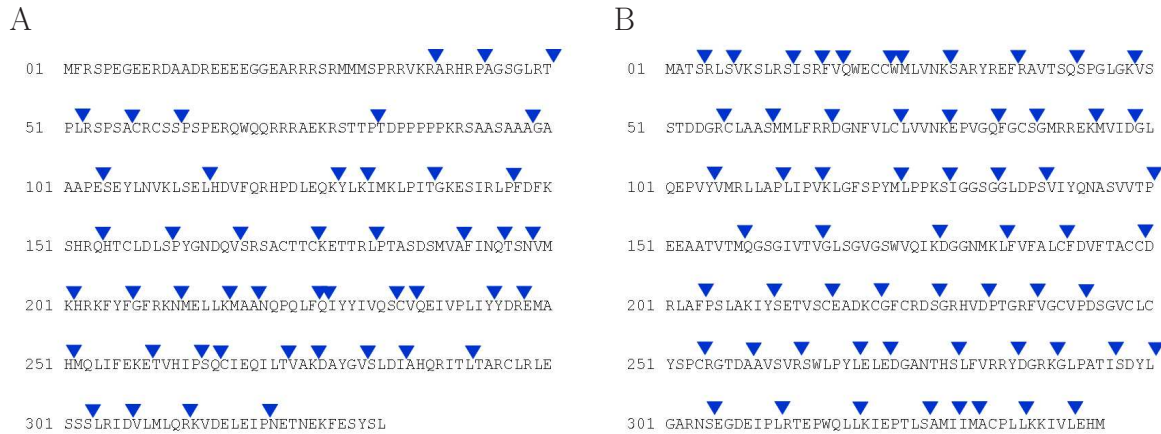


Figure 4.1: Comparison of the coverage of insertion mutants of the M53 library [46] (A) and the M94 library (B) generated in this study.

Due to the increased unique number of mutants in the M94 library, the coverage could also

be enhanced. This is demonstrated by the maximal interval of 20 aa between two insertion mutation in the M53 library and of 12 aa in the M94 library as depicted in figure 4.1 and also by the average distance of two insertion mutations of 7.2 aa (46 insertions mutations in 333 aa) in the M53 library and of 5.75 aa (60 insertion mutation in 345 aa) in the M94 library.

4.2 Analysis of M94 mutants by *cis*-complementation

The growth properties of the M94 deletion virus demonstrated first, that M94 is essential and second, that the null phenotype can be restored by *cis*-complementation at an ectopic position in the genome under control of a foreign promoter. This result was a necessary prerequisite for the systemic analysis of M94 mutants in the viral context. The read out of successful viral reconstitution from transfected BACs or failure served as a relevant but simple assay. This was important as the essential function of M94 was unknown, therefore the generated mutants could not be analysed for a specific function. Instead, any essential function of M94 in the viral life cycle was detected and located to a specific site in the M94 protein by the individual analysis of the M94 mutants.

The analysis of 14 truncation mutants revealed that only the last three aa of the C-terminus of M94 are dispensable for its essential function(s). As in the UL16/94 family the C-terminus was already described to be conserved [95] and also essential for binding of UL16 to UL11 [96], this result is consistent with the literature. Also the *in silico* analysis predicted an α -helix in the C-terminus, which overlapped with the four insertion mutants, that did not complement wt M94. Therefore this C-terminal α -helix seems to be important for the essential function of M94.

Out of the 60 tested insertion mutants 39 kept the function of M94, whereas the remaining 21 failed to complement wt M94. These non-complementing mutations are for the most part arranged in clusters in the N-terminus, the C-terminus, and between aa 234 and 244 indicating a functional site in this region. However, in the bioinformatically predicted linker region (aa 121-170) only a single insertion mutant out of 7 demonstrated a non-

complementing phenotype hence supporting the prediction. The same is probably true for the region of aa 254 to 299 even though a linker region is not predicted. Therefore the bioinformatic analysis could only partially be confirmed.

4.3 Identification and analysis of DN mutants

The identification of a DN mutant can be a difficult task, in particular, if knowledge about the protein structure is limited and therefore a targeted mutation is impossible. Hence, a random approach for identification as utilised in this study remains the only chance.

Subsequently to the analysis of the M94 mutants in the *cis*-complementation assay, the lethal mutants demonstrating no viral reconstitution in this assay and some additional stop mutants in the C-terminus were subjected to the inhibitory screen. In total 42 lethal mutants were analysed for their ability to inhibit viral reconstitution in presence of the M94 wt allele. The lethal phenotype in the *cis*-complementation assay can be due to different reasons such as incorrect folding, protein instability or aberrant localisation of the protein. The mutants identified by the inhibitory screen need to keep a wt function, namely the ability to form complexes and lose other distinct functions.

Only 2 inhibitory mutants were found. Surprisingly they were located in the N-terminus of the protein. As the C-terminus is conserved and found to carry an essential site, the inhibitory mutants were expected to be located in this region, especially as the N-terminus was not correlated with any functionality or conservation until then.

In order to verify the inhibitory phenotype of the mutants and exclude toxic effects they were subcloned into an inducible expression cassette. The growth analysis demonstrated the actual inhibition of viral growth due to Dox treatment by 3 orders of magnitude.

The following analysis of the protein expression demonstrated that the HA-tagged M94 mutant was indeed expressed upon Dox treatment. Also, the overexpression of M94i13 compared to M94 was demonstrated. As the inhibition in presence of the wt allele was related to the overexpression of the mutant in presence of Dox, this mutant was identified as a DN mutant as defined previously [36].

The analysis revealed that the stability of the wt protein was not affected by the expression of the DN mutant as the expression levels were comparable regardless of the DN expression. The analysis of the expression of a representative IE gene pp89 and a representative late gene pM50 at different time points showed no effect on the viral gene expression due to the expression of M94i13. The data indicated that viral gene expression was not influenced by the expression of the DN mutant. The analysis of M94 expression in the presence of PAA hence inhibiting the viral DNA replication showed that endogenous M94 was expressed with true late kinetics. Due to the SV40 promoter driving the M94i13 expression, this protein was not expressed with true late kinetics.

4.4 Comparative analysis of the M94 deletion and DN mutant

To identify the function in the MCMV life cycle which is inhibited by the DN mutant transmission electron microscopy was performed. A complementing cell line for the M94 deletion virus was available and it was analysed along with the DN mutant. Previous publications predicted a role for M94 in viral cleavage-packaging [63,64]. If this would be an essential function of M94 the primary envelopment, namely the envelopment of filled capsids at the inner nuclear membrane (INM) and de-envelopment at the outer nuclear membrane (ONM), should be affected or at least more unfilled capsids should be visible in the nucleus. Surprisingly, the primary envelopment seemed not to be affected in both mutants and the phenotype of the M94 deletion mutant and the M94 DN mutant was comparable to wt.

The EM demonstrated a loss of secondary envelopment as the reason for the inhibition of viral growth. Even more, there were no viral particles in vesicles present at all, although tegumented capsids were present in the cytoplasm. This phenotype of tegumented filled capsids accumulating in the cytoplasm next to the Golgi compartment demonstrates an accurate process of the virus life cycle up to this point but the incapability to proceed by

acquiring the final envelope.

Next to its role in viral cleavage-packaging, a role in secondary envelopment has also been proposed for UL16 in HSV due to its interaction with UL11 [96]. Therefore, the loss of secondary envelopment was in line with this prediction. The two genetically different and independent constructs either deletion or DN mutant protein demonstrated the identical phenotype with respect to secondary envelopment and therefore excluded artifacts in the genetic procedure or in the EM analysis.

Previous study on deletion mutants, namely the UL99 deletion virus of HCMV, demonstrated a comparable loss of secondary envelopment [82]. Despite this finding, the study revealed that the virus was still able to spread from cell to cell. Therefore the same was investigated for the M94 deletion virus in a spread assay.

The results demonstrated, in contrast to the UL99 deletion virus, a spread deficient phenotype. The deficient phenotype was reverted to almost wt by applying the complementing cell line providing pM94 in the assay. Thus the loss of cell-to-cell spread was solely due to the lack of M94. From this result we concluded that the exclusive deletion of M94 is sufficient for a total block in cell-to-cell spread.

As mentioned earlier, primary envelopment of MCMV was not affected by deletion of M94 or by expression of the M94 DN mutant. As previous publications discussed a role of M94 homologues in viral cleavage-packaging due to localisation in assemblons [63] and ssDNA binding [64] this potential role was investigated in more detail by a newly designed packaging assay. This analysis clearly demonstrated that cleavage of viral genomes was present in comparable quantities for wt, the DN mutant and the deletion mutant. As cleavage and packaging are connected and appear simultaneously, we concluded that M94 has no essential function in viral cleavage-packaging and confirmed by the packaging assay the observations of the electron microscopy. This data also demonstrated that at least for *β-Herpesvirinae* the primary and secondary envelopment are mechanistically separated.

4.5 M94 is a key player in secondary envelopment of *β -Herpesvirinae*

The complex life cycle of the different *Herpesvirinae* subfamilies involves formation of capsids in the nucleus, the encapsidation of the viral genome, transfer of the filled capsid into the cytoplasm, tegumentation, final envelopment and egress of viral particles. Although differences in the subfamilies exist, especially the processes in the nucleus are conserved and share significant homologies. The capsid assembles out of 5 capsid proteins into the procapsid. After a protease maturation step the viral genome is inserted into the capsid via the capsid portal by the viral terminase, a complex comprised of 3 conserved proteins. The concatemers derived from the rolling cycle replication of the viral genome are cleaved into unit-length genomes by the viral terminase and simultaneously encapsidated. The following pathway of transfer of the filled capsids into the cytoplasm is still under discussion.

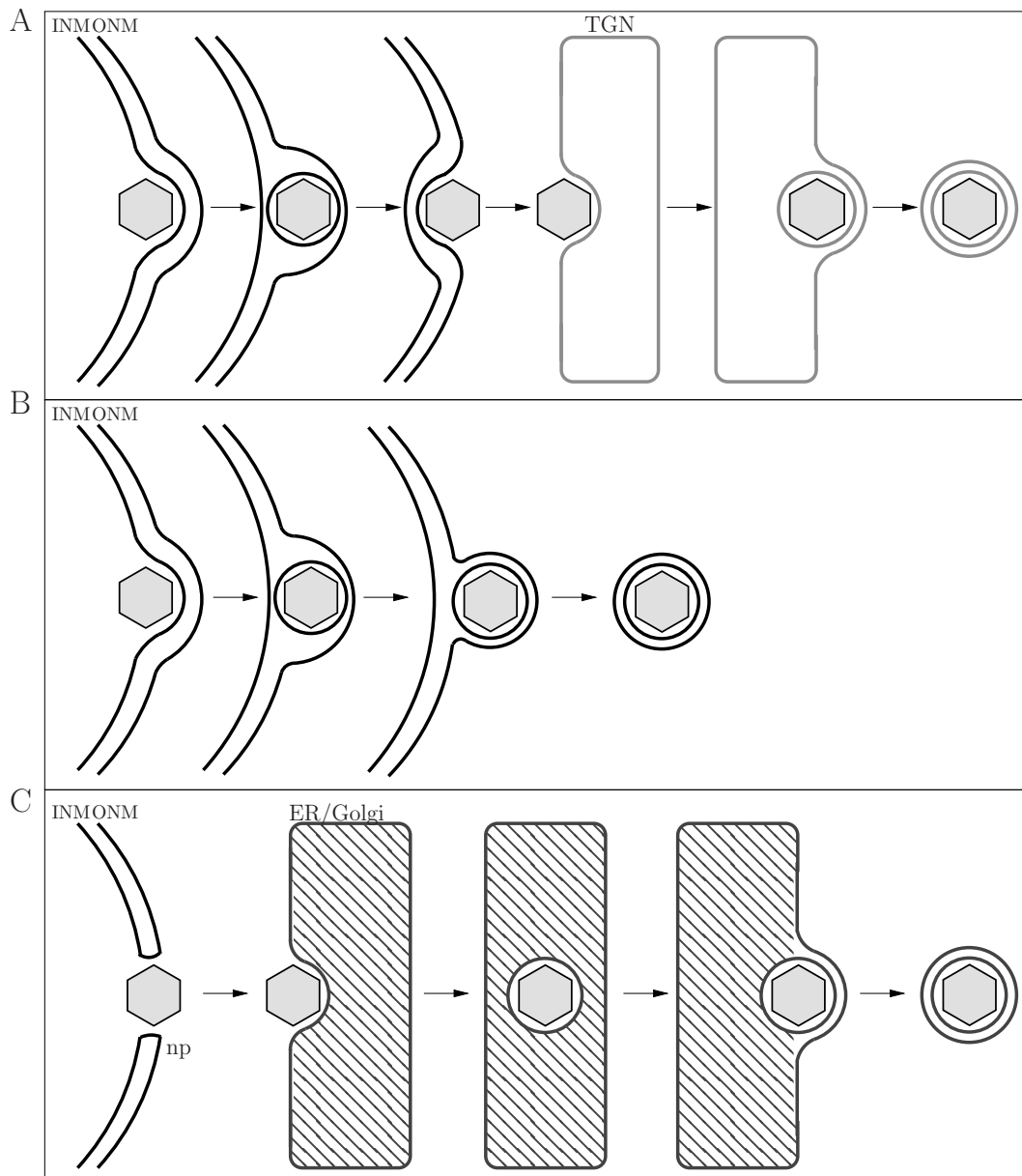


Figure 4.2: Schematic representation of models of nuclear egress of herpesvirus particles. The dual envelopment hypothesis (A) includes acquisition of a primary envelope at the INM after budding into the perinuclear space and subsequently loss of this primary envelope by fusion with the ONM. The resulting cytosolic capsids undergo a secondary envelopment at the TGN, from where they are transported in vesicles to the plasma membrane. In the single envelopment hypothesis (B) the capsid also buds into the perinuclear space acquiring its envelope and subsequently enters a transport vesicle at the ONM which directly delivers the virions to the plasma membrane. The third model (C) is characterised by egress of the nucleocapsid through an enlarged nuclear pore (np) and the only envelopment occurs at endoplasmic reticulum (ER) or Golgi followed by budding into vesicles for transport.

Three models for the nuclear egress are currently discussed (Fig. 4.2). Two of these include only a single envelopment of capsid either at the ONM or at the ER/Golgi compartment. The remaining model assumes two spatially and temporarily separated envelopment pro-

cesses, the primary envelopment at the INM and the secondary envelopment at the TGN. Studies in α -*Herpesvirinae* of different deletion mutants demonstrated blocks in primary and secondary envelopment. However, for a complete block in secondary envelopment in α -*Herpesvirinae* multiple gene deletions are required, a single deletion mutant exhibiting this phenotype was not identified so far. In this study a single deletion mutant causing a loss of secondary envelopment was identified. This proves that the primary and secondary envelopment are distinct processes as primary envelopment is not inhibited in the M94 deletion virus and the M94 DN virus. In contrast to the uninfluenced primary envelopment the secondary envelopment is lost for both mutants. The first process then proceeds like wt, whereas the second process is inhibited demonstrating the autonomy of the two processes from each other.

The identification of a M94 DN mutant leads to the conclusion of at least two essential functions inherited by M94 as one function probably binding in a complex needs to remain like wt, whereas a second function must be destroyed to generate the inhibitory phenotype. One of these functions is located in the N-terminus of M94 as mutations in this region specifically inhibited a protein function causing the DN phenotype. The second essential function might well be located in the C-terminus of M94 as this was identified as an essential region in the loss-of-function screen. Although other reasons as incorrect protein folding might have resulted in the lethal phenotype of the C-terminal mutants, the assumption of an essential region related to a distinct protein function is reasonable. A publication on the α -*Herpesvirinae* homologue UL16 demonstrated a transient binding of UL16 to the viral capsid by the conserved cysteines of UL16 family members, which are located in the C-terminus of the homologues [53]. The strict conservation of these cysteines implies a function related to these cysteines, which is also conserved and shared between α -*Herpesvirinae* and β -*Herpesvirinae*. So from the two essential functions of M94 one is located in the N-terminus and the second one probably in the C-terminus.

Another known function of UL16 family members is the interaction with UL11 family members, which was shown in HSV [45] and HCMV [43]. UL11 and its HCMV homologue UL99 are small myristylated proteins which associate with membranes via a membrane

anchor and are known to be involved in secondary envelopment [4, 83]. This binding is most likely present in MCMV not only due to the high homology of HCMV and MCMV but also as it links M94 to secondary envelopment. Preliminary studies in our lab to identify viral binding partners of M94 confirmed the binding to the UL11 family member of MCMV M99. This interaction was lost in the analysis of the M94 DN mutant (unpublished data). We therefore speculate that the binding site for the M99 interaction is located in the N-terminus of M94.

This hypothesis leads to a model for secondary envelopment involving M99, M94, and the nucleocapsid. In this model M94 binds to the capsid and by interaction with M99 connects the capsid to the TGN, where M99 acts as membrane anchor as shown in figure 4.3.

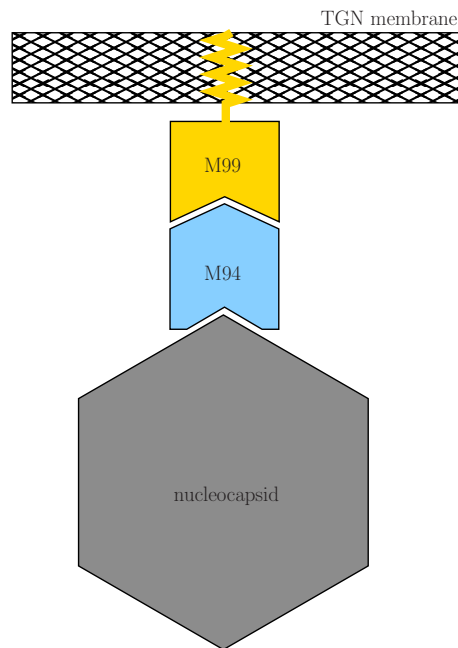


Figure 4.3: Model for secondary envelopment involving the nucleocapsid, M94 and M99 including its membrane anchor at the TGN membrane.

It is known that secondary envelopment in α -*Herpesvirinae* involves more proteins than in β -*Herpesvirinae*, for example several glycoproteins. This redundancy is also demonstrated by the dispensability of UL16 in HSV. The model for secondary envelopment presented here reveals the key function of M94 in β -*Herpesvirinae*. It is the unique protein connect-

ing the capsid to the TGN membrane. Therefore the deletion of M94 or inhibition of this bridging function results in a complete loss of secondary envelopment.

Further experiments are required to strengthen the model presented here. First, the M94-M99 interaction needs to be verified in MCMV by pull-down experiments and immunofluorescence. Subsequently the M99 binding site in M94 can be mapped by fragment complementation assay using the mutants generated in this study. In addition, isolation of capsids and identification of bound M94 will reveal the validity of this model.

Bibliography

- [1] **Adler, S. P.** 1983. Transfusion-associated cytomegalovirus infections. *Rev. Infect. Dis.* **5**:977–993.
- [2] **Adler, S. P.** 1988. Cytomegalovirus transmission among children in day care, their mothers and caretakers. *Pediatr. Infect. Dis. J.* **7**:279–285.
- [3] **Baines, J. D., and B. Roizman.** 1991. The open reading frames UL3, UL4, UL10, and UL16 are dispensable for the replication of herpes simplex virus 1 in cell culture. *J. Virol.* **65**:938–944.
- [4] **Baines, J. D., and B. Roizman.** 1992. The UL11 gene of herpes simplex virus 1 encodes a function that facilitates nucleocapsid envelopment and egress from cells. *J. Virol.* **66**:5168–5174.
- [5] **Barth, P. T., N. Datta, R. W. Hedges, and N. J. Grinter.** 1976. Transposition of a deoxyribonucleic acid sequence encoding trimethoprim and streptomycin resistances from R483 to other replicons. *J. Bacteriol.* **125**:800–810.
- [6] **Biery, M. C., F. J. Stewart, A. E. Stellwagen, E. A. Raleigh, and N. L. Craig.** 2000. A simple in vitro Tn7-based transposition system with low target site selectivity for genome and gene analysis. *Nucleic Acids Res.* **28**:1067–1077.
- [7] **Biolabs, N. E.** 2006. GPS-Linker-scanning system, Instruction manual. Catalog E7102S .

- [8] **Brown, J. C., M. A. McVoy, and F. L. Homa.** 2002. Packaging DNA into herpesvirus capsids. Structure-function relationships of human pathogenic viruses. Kluwer Academic/Plenum Publishers, New York, NY :111–153.
- [9] **Brune, W., C. Menard, U. Hobom, S. Odenbreit, M. Messerle, and U. H. Koszinowski.** 1999. Rapid identification of essential and nonessential herpesvirus genes by direct transposon mutagenesis. *Nat. Biotechnol.* **17**:360–364.
- [10] **Bubic, I., M. Wagner, A. Krmpotic, T. Saulig, S. Kim, W. M. Yokoyama, S. Jonjic, and U. H. Koszinowski.** 2004. Gain of virulence caused by loss of a gene in murine cytomegalovirus. *J. Virol.* **78**:7536–7544.
- [11] **Chandler, S. H., E. R. Alexander, and K. K. Holmes.** 1985a. Epidemiology of cytomegaloviral infection in a heterogeneous population of pregnant women. *J. Infect. Dis.* **152**:249–256.
- [12] **Chandler, S. H., K. K. Holmes, B. B. Wentworth, L. T. Gutman, P. J. Wiesner, E. R. Alexander, and H. H. Handsfield.** 1985b. The epidemiology of cytomegaloviral infection in women attending a sexually transmitted disease clinic. *J. Infect. Dis.* **152**:597–605.
- [13] **Chee, M. S., A. T. Bankier, S. Beck, R. Bohni, C. M. Brown, R. Cerny, T. Horsnell, C. A. Hutchison, T. Kouzarides, and J. A. Martignetti.** 1990. Analysis of the protein-coding content of the sequence of human cytomegalovirus strain AD169. *Curr. Top. Microbiol. Immunol.* **154**:125–169.
- [14] **Chen, D. H., H. Jiang, M. Lee, F. Liu, and Z. H. Zhou.** 1999. Three-dimensional visualization of tegument/capsid interactions in the intact human cytomegalovirus. *Virology* **260**:10–16.
- [15] **Cherepanov, P. P., and W. Wackernagel.** 1995. Gene disruption in *Escherichia coli*: TcR and KmR cassettes with the option of FIp-catalyzed excision of the antibiotic-resistance determinant. *Gene* **158**:9–14.

- [16] **Cheung, T. W., and S. A. Teich.** 1999. Cytomegalovirus infection in patients with HIV infection. *Mt. Sinai J. Med.* **66**:113–124.
- [17] **Chou, J., and B. Roizman.** 1989. Characterization of DNA sequence-common and sequence-specific proteins binding to cis-acting sites for cleavage of the terminal a sequence of the herpes simplex virus 1 genome. *J. Virol.* **63**:1059–1068.
- [18] **Cicin-Sain, L., I. Bubic, M. Schnee, Z. Ruzsics, C. Mohr, S. Jonjic, and U. H. Koszinowski.** 2007. Targeted deletion of regions rich in immune-evasive genes from the cytomegalovirus genome as a novel vaccine strategy. *J. Virol.* **81**:13825–13834.
- [19] **Coen, D. M., and P. A. Schaffer.** 2003. Antiherpesvirus drugs: a promising spectrum of new drugs and drug targets. *Nat Rev Drug Discov* **2**:278–288.
- [20] **Compton, T., D. M. Nowlin, and N. R. Cooper.** 1993. Initiation of human cytomegalovirus infection requires initial interaction with cell surface heparan sulfate. *Virology* **193**:834–841.
- [21] **Craig, N. L.** 1996. Transposon Tn7. *Curr. Top. Microbiol. Immunol.* **204**:27–48.
- [22] **Datsenko, K. A., and B. L. Wanner.** 2000. One-step inactivation of chromosomal genes in *Escherichia coli* K-12 using PCR products. *Proc. Natl. Acad. Sci. U.S.A.* **97**:6640–6645.
- [23] **Davison, A. J.** 2002. Evolution of the herpesviruses. *Vet. Microbiol.* **86**:69–88.
- [24] **Davison, A. J.** 2007. Comparative analysis of the genomes. *Human herpesviruses: biology, therapy, and immunophylaxis*, Cambridge Univ Pr, New York, NY :10–26.
- [25] **Dunn, W., C. Chou, H. Li, R. Hai, D. Patterson, V. Stolc, H. Zhu, and F. Liu.** 2003. Functional profiling of a human cytomegalovirus genome. *Proc. Natl. Acad. Sci. U.S.A.* **100**:14223–14228.

- [26] **Dworsky, M., M. Yow, S. Stagno, R. F. Pass, and C. Alford.** 1983. Cytomegalovirus infection of breast milk and transmission in infancy. *Pediatrics* **72**:295–299.
- [27] **Ebeling, A., G. M. Keil, E. Knust, and U. H. Koszinowski.** 1983. Molecular cloning and physical mapping of murine cytomegalovirus DNA. *J. Virol.* **47**:421–433.
- [28] **Eickmann, M., D. Gicklhorn, and K. Radsak.** 2006. Glycoprotein trafficking in virion morphogenesis. *Cytomegaloviruses: molecular biology and immunology*. Caister Academic Press, Norfolk, VA :245–264.
- [29] **Emery, V. C.** 1999. Viral dynamics during active cytomegalovirus infection and pathology. *Intervirology* **42**:405–411.
- [30] **Gibson, W.** 1996. Structure and assembly of the virion. *Intervirology* **39**:389–400.
- [31] **Gibson, W.** 2008. Structure and formation of the cytomegalovirus virion. *Curr. Top. Microbiol. Immunol.* **325**:187–204.
- [32] **Gor, D., C. Sabin, H. G. Prentice, N. Vyas, S. Man, P. D. Griffiths, and V. C. Emery.** 1998. Longitudinal fluctuations in cytomegalovirus load in bone marrow transplant patients: relationship between peak virus load, donor/recipient serostatus, acute GVHD and CMV disease. *Bone Marrow Transplant.* **21**:597–605.
- [33] **Greener, A., M. Callahan, and B. Jerpseth.** 1996. An efficient random mutagenesis technique using an *E. coli* mutator strain. *Methods Mol. Biol.* **57**:375–385.
- [34] **Gruter, W.** 1924. Das Herpesvirus, seine aetiologische und klinische Bedeutung. *Muench. Med. Wochenschr* **71**:1058–1060.
- [35] **Gutermann, A., A. Bubeck, M. Wagner, U. Reusch, C. Menard, and U. H. Koszinowski.** 2002. Strategies for the identification and analysis of viral immune-evasive genes—cytomegalovirus as an example. *Curr. Top. Microbiol. Immunol.* **269**:1–22.

- [36] **Herskowitz, I.** 1987. Functional inactivation of genes by dominant negative mutations. *Nature* **329**:219–222.
- [37] **Ho, M.** 1991. Observations from transplantation contributing to the understanding of pathogenesis of CMV infection. *Transplant. Proc.* **23**:104–108.
- [38] **Honess, R. W., and B. Roizman.** 1975. Regulation of herpesvirus macromolecular synthesis: sequential transition of polypeptide synthesis requires functional viral polypeptides. *Proc. Natl. Acad. Sci. U.S.A.* **72**:1276–1280.
- [39] **Hudson, J. B.** 1979. The murine cytomegalovirus as a model for the study of viral pathogenesis and persistent infections. *Arch. Virol.* **62**:1–29.
- [40] **Kadonaga, J. T., and J. R. Knowles.** 1985. A simple and efficient method for chemical mutagenesis of DNA. *Nucleic Acids Res.* **13**:1733–1745.
- [41] **Kattenhorn, L. M., R. Mills, M. Wagner, A. Lomsadze, V. Makeev, M. Borodovsky, H. L. Ploegh, and B. M. Kessler.** 2004. Identification of proteins associated with murine cytomegalovirus virions. *J. Virol.* **78**:11187–11197.
- [42] **Ling, M. M., and B. H. Robinson.** 1997. Approaches to DNA mutagenesis: an overview. *Anal. Biochem.* **254**:157–178.
- [43] **Liu, Y., Z. Cui, Z. Zhang, H. Wei, Y. Zhou, M. Wang, and X. E. Zhang.** 2009. The tegument protein UL94 of human cytomegalovirus as a binding partner for tegument protein pp28 identified by intracellular imaging. *Virology* **388**:68–77.
- [44] **Ljungman, P., P. Griffiths, and C. Paya.** 2002. Definitions of cytomegalovirus infection and disease in transplant recipients. *Clin. Infect. Dis.* **34**:1094–1097.
- [45] **Loomis, J. S., R. J. Courtney, and J. W. Wills.** 2003. Binding partners for the UL11 tegument protein of herpes simplex virus type 1. *J. Virol.* **77**:11417–11424.
- [46] **Lötzerich, M.** 2007. Analysis of the nuclear egress complex of mouse cytomegalovirus. PhD thesis .

- [47] **Lötzerich, M., Z. Ruzsics, and U. H. Koszinowski.** 2006. Functional domains of murine cytomegalovirus nuclear egress protein M53/p38. *J. Virol.* **80**:73–84.
- [48] **Maninger, S., J. B. Bosse, M. Pogoda, C. Mohr, P. Walther, U. H. Koszinowski, and Z. Ruzsics.** in preparation. A genetic analysis of M94 of murine cytomegalovirus.
- [49] **McClintock, B.** 1950. The origin and behavior of mutable loci in maize. *Proc. Natl. Acad. Sci. U.S.A.* **36**:344–355.
- [50] **McGeoch, D. J., and D. Gatherer.** 2005. Integrating reptilian herpesviruses into the family herpesviridae. *J. Virol.* **79**:725–731.
- [51] **McGeoch, D. J., F. J. Rixon, and A. J. Davison.** 2006. Topics in herpesvirus genomics and evolution. *Virus Res.* **117**:90–104.
- [52] **McVoy, M. A., and S. P. Adler.** 1994. Human cytomegalovirus DNA replicates after early circularization by concatemer formation, and inversion occurs within the concatemer. *J. Virol.* **68**:1040–1051.
- [53] **Meckes, D. G., and J. W. Wills.** 2007. Dynamic interactions of the UL16 tegument protein with the capsid of herpes simplex virus. *J. Virol.* **81**:13028–13036.
- [54] **Messerle, M., I. Crnkovic, W. Hammerschmidt, H. Ziegler, and U. H. Koszinowski.** 1997. Cloning and mutagenesis of a herpesvirus genome as an infectious bacterial artificial chromosome. *Proc. Natl. Acad. Sci. U.S.A.* **94**:14759–14763.
- [55] **Mettenleiter, T. C.** 2002. Herpesvirus assembly and egress. *J. Virol.* **76**:1537–1547.
- [56] **Mettenleiter, T. C.** 2006. Intriguing interplay between viral proteins during herpesvirus assembly or: the herpesvirus assembly puzzle. *Vet. Microbiol.* **113**:163–169.
- [57] **Miller, V. L., and J. J. Mekalanos.** 1988. A novel suicide vector and its use in construction of insertion mutations: osmoregulation of outer membrane proteins and virulence determinants in *Vibrio cholerae* requires *toxR*. *J. Bacteriol.* **170**:2575–2583.

- [58] **Mocarski, E. S., L. E. Post, and B. Roizman.** 1980. Molecular engineering of the herpes simplex virus genome: insertion of a second L-S junction into the genome causes additional genome inversions. *Cell* **22**:243–255.
- [59] **Mocarski, E. S., T. Shenk, and R. F. Pass.** 2007. Cytomegaloviruses. *Fields virology*, 5th ed. Lippincott Williams & Wilkins, Philadelphia, PA :2701–2772.
- [60] **Muller, H. J.** 1932. Further studies on the nature and causes of gene mutations. *Proc. 6th Int. Congr. Genet* :213–255.
- [61] **Muranyi, W., J. Haas, M. Wagner, G. Krohne, and U. H. Koszinowski.** 2002. Cytomegalovirus recruitment of cellular kinases to dissolve the nuclear lamina. *Science* **297**:854–857.
- [62] **Mustakangas, P., S. Sarna, P. Ämmälä, M. Muttilainen, P. Koskela, and M. Koskiniemi.** 2000. Human cytomegalovirus seroprevalence in three socioeconomically different urban areas during the first trimester: a population-based cohort study. *Int J Epidemiol* **29**:587–591.
- [63] **Nalwanga, D., S. Rempel, B. Roizman, and J. D. Baines.** 1996. The UL16 gene product of herpes simplex virus 1 is a virion protein that colocalizes with intranuclear capsid proteins. *Virology* **226**:236–242.
- [64] **Oshima, S., T. Daikoku, S. Shibata, H. Yamada, F. Goshima, and Y. Nishiyama.** 1998. Characterization of the UL16 gene product of herpes simplex virus type 2. *Arch. Virol.* **143**:863–880.
- [65] **Pass, R. F.** 1996. Immunization strategy for prevention of congenital cytomegalovirus infection. *Infect Agents Dis* **5**:240–244.
- [66] **Pellett, P., and B. Roizman.** 2007. The family Herpesviridae: a brief introduction. *Fields virology*, 5th ed. Lippincott Williams & Wilkins, Philadelphia, PA :2479–2499.

- [67] **Podlech, J., R. Holtappels, N. Wirtz, H. P. Steffens, and M. J. Reddehase.** 1998. Reconstitution of CD8 T cells is essential for the prevention of multiple-organ cytomegalovirus histopathology after bone marrow transplantation. *J. Gen. Virol.* **79** (Pt 9):2099–2104.
- [68] **Popa, M.** 2009. Genetic analysis of mouse cytomegalovirus nuclear egress complex. PhD thesis .
- [69] **Quinnan, G. V., N. Kirmani, A. H. Rook, J. F. Manischewitz, L. Jackson, G. Moreschi, G. W. Santos, R. Saral, and W. H. Burns.** 1982. Cytotoxic T cells in cytomegalovirus infection: HLA-restricted T-lymphocyte and non-T-lymphocyte cytotoxic responses correlate with recovery from cytomegalovirus infection in bone-marrow-transplant recipients. *N. Engl. J. Med.* **307**:7–13.
- [70] **Rawlinson, W. D., H. E. Farrell, and B. G. Barrell.** 1996. Analysis of the complete DNA sequence of murine cytomegalovirus. *J. Virol.* **70**:8833–8849.
- [71] **Reddehase, M. J., F. Weiland, K. Münch, S. Jonjic, A. Lüske, and U. H. Koszinowski.** 1985. Interstitial murine cytomegalovirus pneumonia after irradiation: characterization of cells that limit viral replication during established infection of the lungs. *J. Virol.* **55**:264–273.
- [72] **Reed, L., and H. Münch.** 1938. A simple method of estimating fifty percent endpoints. *Am. J. Hyg* **27** (3):493–497.
- [73] **Reschke, M.** 1994. Detailed 2nd model of HCMV. Institute of Virology, University of Marburg, Germany .
- [74] **Reynolds, D. W., S. Stagno, T. S. Hosty, M. Tiller, and C. A. Alford.** 1973. Maternal cytomegalovirus excretion and perinatal infection. *N. Engl. J. Med.* **289**:1–5.
- [75] **Rifkind, D.** 1965. Cytomegalovirus infection after renal transplantation. *Arch. Intern. Med.* **116**:554–558.

- [76] **Roizman, B., L. E. Carmichael, F. Deinhardt, G. de The, A. J. Nahmias, W. Plowright, F. Rapp, P. Sheldrick, M. Takahashi, and K. Wolf.** 1981. Herpesviridae. Definition, provisional nomenclature, and taxonomy. The Herpesvirus Study Group, the International Committee on Taxonomy of Viruses. *Intervirology* **16**:201–217.
- [77] **Rupp, B., Z. Ruzsics, T. Sacher, and U. H. Koszinowski.** 2005. Conditional cytomegalovirus replication in vitro and in vivo. *J. Virol.* **79**:486–494.
- [78] **Saigal, S., O. Lunyk, R. P. Larke, and M. A. Chernesky.** 1982. The outcome in children with congenital cytomegalovirus infection. A longitudinal follow-up study. *Am. J. Dis. Child.* **136**:896–901.
- [79] **Sanchez, V., K. D. Greis, E. Sztul, and W. J. Britt.** 2000. Accumulation of virion tegument and envelope proteins in a stable cytoplasmic compartment during human cytomegalovirus replication: characterization of a potential site of virus assembly. *J. Virol.* **74**:975–986.
- [80] **Schaffer, P. A.** 1975. Temperature-sensitive mutants of herpesviruses. *Curr. Top. Microbiol. Immunol.* **70**:51–100.
- [81] **Serrano, M., A. W. Lin, M. E. McCurrach, D. Beach, and S. W. Lowe.** 1997. Oncogenic ras provokes premature cell senescence associated with accumulation of p53 and p16INK4a. *Cell* **88**:593–602.
- [82] **Silva, M. C., J. Schroer, and T. Shenk.** 2005. Human cytomegalovirus cell-to-cell spread in the absence of an essential assembly protein. *Proc. Natl. Acad. Sci. U.S.A.* **102**:2081–2086.
- [83] **Silva, M. C., Q. C. Yu, L. Enquist, and T. Shenk.** 2003. Human cytomegalovirus UL99-encoded pp28 is required for the cytoplasmic envelopment of tegument-associated capsids. *J. Virol.* **77**:10594–10605.

- [84] **Sodeik, B., M. W. Ebersold, and A. Helenius.** 1997. Microtubule-mediated transport of incoming herpes simplex virus 1 capsids to the nucleus. *J. Cell Biol.* **136**:1007–1021.
- [85] **Spaete, R. R., and E. S. Mocarski.** 1987. Insertion and deletion mutagenesis of the human cytomegalovirus genome. *Proc. Natl. Acad. Sci. U.S.A.* **84**:7213–7217.
- [86] **Spector, S. A., K. Hsia, M. Crager, M. Pilcher, S. Cabral, and M. J. Stempien.** 1999. Cytomegalovirus (CMV) DNA load is an independent predictor of CMV disease and survival in advanced AIDS. *J. Virol.* **73**:7027–7030.
- [87] **Stagno, S., R. F. Pass, M. E. Dworsky, and C. A. Alford.** 1982. Maternal cytomegalovirus infection and perinatal transmission. *Clin Obstet Gynecol* **25**:563–576.
- [88] **Stellwagen, A. E., and N. L. Craig.** 1997a. Gain-of-function mutations in TnsC, an ATP-dependent transposition protein that activates the bacterial transposon Tn7. *Genetics* **145**:573–585.
- [89] **Stellwagen, A. E., and N. L. Craig.** 1997b. Avoiding self: two Tn7-encoded proteins mediate target immunity in Tn7 transposition. *EMBO J.* **16**:6823–6834.
- [90] **Stratton, K. R., J. Durch, and R. S. Lawrence.** 2000. Overview of Analytic Approach and Results. *Vaccines for the 21st century: a tool for decision making.* Institute of Medicine, National Academy Press, Washington, DC :53–92.
- [91] **Wagner, M., S. Jonjic, U. H. Koszinowski, and M. Messerle.** 1999. Systematic excision of vector sequences from the BAC-cloned herpesvirus genome during virus reconstitution. *J. Virol.* **73**:7056–7060.
- [92] **Wagner, M., and U. H. Koszinowski.** 2004. Mutagenesis of viral BACs with linear PCR fragments (ET recombination). *Methods Mol. Biol.* **256**:257–268.

-
- [93] **Walther, P., and A. Ziegler.** 2002. Freeze substitution of high-pressure frozen samples: the visibility of biological membranes is improved when the substitution medium contains water. *J Microsc* **208**:3–10.
- [94] **White, E. A., and D. H. Spector.** 2007. Betaherpesvirus viral genes and their function. *Human herpesviruses: biology, therapy, and immunophrophylaxis*, Cambridge Univ Pr, New York, NY :204–230.
- [95] **Wing, B. A., G. C. Lee, and E. S. Huang.** 1996. The human cytomegalovirus UL94 open reading frame encodes a conserved herpesvirus capsid/tegument-associated virion protein that is expressed with true late kinetics. *J. Virol.* **70**:3339–3345.
- [96] **Yeh, P. C., D. G. Meckes, and J. W. Wills.** 2008. Analysis of the interaction between the UL11 and UL16 tegument proteins of herpes simplex virus. *J. Virol.* **82**:10693–10700.
- [97] **Zhang, Y., F. Buchholz, J. P. Muyrers, and A. F. Stewart.** 1998. A new logic for DNA engineering using recombination in *Escherichia coli*. *Nat. Genet.* **20**:123–128.

Acknowledgements

This work was supported by DFG-Schwerpunktprogramm 1175: Dynamics of cellular membranes and their exploitation by viruses.

I would like to thank Prof. Koszinowski for the opportunity to accomplish my PhD in his research group and for providing this great environment for my analysis.

I am also grateful to Prof. Beckmann for his assistance as Fachvertreter and for enabling my PhD in the faculty of biochemistry.

I would like to thank Dr. Ruzsics for this interesting project, his support through my work, discussions and critical reading of the manuscript.

Many thanks to all my colleagues for their help in my practical work, their constructive critique on my work and my presentation and also for their helpful discussions. I specifically would like to thank Madlen Pogoda for critical reading of the manuscript and Jens Bernhard Lösing who provided the EM data in cooperation with Paul Walther.

Nicht zuletzt möchte ich Thomas für all seine Hilfe danken, für seine anhaltende Liebe, Unterstützung und Aufmunterung insbesondere in manchmal schwierigen Doktorarbeitszeiten und auch für seine Hilfe bei der Erstellung dieses Dokuments und Lösung all meiner kleinen und grösseren Probleme.

Mein Dank gilt auch nicht zuletzt meiner Familie für ihre Liebe und fortwährende Unterstützung, insbesondere meinen Eltern für Hilfe in allen Lebenslagen und einen Platz ausserhalb der Doktorarbeit und meiner Schwester, meiner besten und engsten Freundin.

Ich danke auch meinem gesamten Freundeskreis für die schönen Besuche, Abendessen, Spieletreffen, Weinfeste, Kinobesuche und vieles mehr.

Curriculum vitae

PERSONAL DATA

Name: Silke Maninger
Date of Birth: January 15, 1980
Place of Birth: Wiesbaden-Sonnenberg, Germany
Nationality: German
Marital status: Single

EDUCATION

01/2006-present Max von Pettenkofer Institute, LMU, Munich, Germany.
Doctoral thesis "Genetic analysis of M94 of murine cytomegalovirus".
Supervisors: Prof. Koszinowski, Prof. Beckmann

08/2004-05/2005 Institute of Biochemistry - Molecular Genetics, Goethe-University,
Frankfurt am Main, Germany.
Diploma thesis "Heterologous expression of the cytochrome *c* oxidase
from *Aquifex aeolicus* in *Thermus thermophilus*".
Supervisors: Prof. Ludwig, Dr. Richter

10/2001-05/2005 Johann Wolfgang Goethe-University, Frankfurt am Main, Germany.
Study of biochemistry.
Degree: certified biochemist (Diplom Biochemikerin).

10/1999-10/2001 University of Bielefeld, Bielefeld, Germany.
Study of biochemistry.

Degree: intermediate examination of biochemistry (Vordiplom Biochemie).

06/1990-06/1999 Elly-Heuss-Gymnasium, Wiesbaden, Germany.

Degree: university-entrance diploma (Abitur).

PRACTICAL TRAINING AND WORK EXPERIENCE

06/2003-09/2003 Institute for Molecular Bio Science, Goethe University, Frankfurt am Main, Germany.

Subject "Deletion of genes in *Haloferax volcanii*".

Supervisor: Prof. Soppa

03/2003-06/2003 Institute of Biochemistry - Cellular Biochemistry, Goethe University, Frankfurt am Main, Germany.

Subject "Cloning and Expression of histidin-tags in *Escherichia coli*".

Supervisors: Prof. Tampé, Dr. Jacob Piehler

10/2002-11/2002 Paul-Ehrlich-Institute, Langen, Germany.

Subject "Identification of polio-virus-vaccine-strains".

Supervisor: Dr. Löwer

PRESENTATION AND PUBLICATIONS

Poster presentations

SFB 455: Virale Funktionen und Immunmodulation, Junior Faculty Retreat
Jun 25-27, 2007; Waging, Germany
Title: Analysis of the essential herpes virus gene M94 by transposon mutagenesis

Annual Meeting of the German Society of Virology
Mar 18-21, 2009; Leipzig, Germany
Title: Construction of dominant negative mutants of essential herpesvirus genes

International Herpesvirus Workshop
Jul 25-30, 2009; Ithaka, NY, USA
Title: Genetic analysis of the MCMV egress protein M94

Presentation

International Herpesvirus Workshop
Jul 25-30, 2009; Ithaka, NY, USA
Title: Genetic analysis of the MCMV egress protein M94

Publication

Maninger, S., Bosse, J. B., Pogoda, M., Mohr, C., Walther, P., Koszinowski, U. H., Ruzsics, Z.
A genetic analysis of M94 of murine cytomegalovirus
in preparation